

PHYSIOLOGICAL AND ECOLOGICAL INVESTIGATIONS OF *CLOSTRIDIUM DIFFICILE*

By

Catherine D. Robinson

A DISSERTATION

Submitted to
Michigan State University
in partial fulfillment of the requirements
for the degree of

Microbiology and Molecular Genetics- Doctor of Philosophy

2014

ABSTRACT

PHYSIOLOGICAL AND ECOLOGICAL INVESTIGATIONS OF *CLOSTRIDIUM DIFFICILE*

By

Catherine D. Robinson

Disease caused by *Clostridium difficile* is currently the most prevalent nosocomial infection and leading cause of antibiotic-associated diarrhea. It is clear that the intestinal microbiota plays a role in preventing *C. difficile* infection in the absence of antibiotics; however, the mechanisms involved in this protective function are poorly understood. Since antibiotic administration is an inducing factor of *C. difficile* infection, treatment employing antibiotics often results in recurrent disease, yet it is still the primary line of treatment. Therefore, a central goal of research in this area is to better define the role of the intestinal microbiota in suppression of disease, and ultimately develop alternative ways to prevent and treat *C. difficile* infection.

In this thesis, I present a novel *in vitro* model that was developed to study complex fecal communities. This *in vitro* model is a continuous-culture system that utilizes arrays of small-volume reactors; it is unique in its simple set-up and high replication. We adapted this model to operate as a *C. difficile* infection model, where *in vivo* *C. difficile* invasion dynamics are replicated in that the fecal communities established in the reactors are resistant to *C. difficile* growth unless disrupted by antibiotic administration. We then go on to use this model to show that newly emerged, epidemic strains of *C. difficile* have a competitive fitness advantage when competed against non-epidemic strains. We also show this competitive advantage *in*

vivo, using a mouse infection model. This result is exciting, as it suggests that physiological attributes of these strains, aside from classical virulence factors, contribute to their epidemic phenotype. Finally, the metabolic potential of *C. difficile* in regards to carbon source utilization is explored, and reveals that epidemic strains are able to grow more efficiently on trehalose, a disaccharide sugar. Moreover, preliminary *in vivo* mouse studies suggest that trehalose utilization plays a role in colonization. Therefore, the growth advantage conferred by this increased ability to utilize trehalose may contribute to the ecological fitness of these strains *in vivo*.

The *in vitro* model developed and presented in this thesis could be used to study many aspects of *C. difficile*-microbiota interactions and has the potential to elucidate mechanisms that are important for *in vivo* resistance to establishment of disease. In addition, the metabolic investigations described provide insight into understanding the physiology of not only *C. difficile* as a whole, but also physiological attributes unique to epidemic strains. Ultimately, these types of ecological and physiological investigations will bring us closer to finding better ways to treat and prevent disease caused by *C. difficile*.

ACKNOWLEDGMENTS

First of all I would like to thank my advisor Rob Britton for helping to make my experience as a doctoral student so successful and positive. Having had one child coming into graduate school and then two babies during my PhD, I had many extra challenges and responsibilities in addition to those of a graduate student. Dr. Britton was amazingly supportive of my family obligations and understanding about the difficulties that having children brings. Above that, his encouragement, support, and mentorship from an academic standpoint was exceptional. I also want to thank the other members of my graduate committee, Dr. Gemma Reguera, Dr. Chris Waters, Dr. Terry Marsh, and Dr. Vince Young for their insight and guidance.

I would also like to thank all of the Britton lab members, both past and present. It was a genuine pleasure working with all of them. I couldn't have asked for a more collaborative and pleasant lab to be a part of. I want to especially thank Jenny Auchtung for being such a great colleague and friend. She was like a second mentor to me and always had helpful advice, drawn from her abundant experiences in different areas of research as a graduate student and postdoc. She was always willing to lend an ear for venting about both research and child-rearing frustrations and offered invaluable support and encouragement.

I can't adequately express how much the support of my parents has meant to me over the years. They deserve all of the credit for making me the successful person I am today. I am thankful that they instilled in me the work ethic and sense of self-pride and dedication required to persevere through this process. The encouraging

and reassuring words from them really helped me along the way and they never fail to express how proud they are of me.

Finally, I want to thank my family- my husband, Dan, and my three girls, Alex, Lana, and Veda. They are my real motivation. I truly don't think a better, more supportive husband and father exists. He's my rock and my biggest fan and always encourages me when I question my abilities. I want to thank him for believing in me and giving me the confidence to believe in myself. I want my daughter Alex to know how much having her by my side has meant to me, not only for all of her help with the little ones, but how she supports and encourages me in her own way. I hope that I am setting a good example for all of my girls and that they will see that they can accomplish anything they set their minds to.

TABLE OF CONTENTS

LIST OF TABLES	x
LIST OF FIGURES	xi
CHAPTER 1: Overview of <i>Clostridium difficile</i> Disease and Physiology	1
Antibiotic-Associated Diarrhea.....	1
<i>C. difficile</i> : the Bacterium and the Disease.....	2
<i>C. difficile</i> infection cycle.....	2
Epidemiology, disease, and virulence factors.....	6
Molecular typing schemes.....	8
Emergence of Epidemic <i>C. difficile</i> Strains.....	9
Current impact on the health care system.....	11
Understanding Disease Development: Colonization Resistance.....	11
Bile acids and germination.....	12
Competitive exclusion.....	13
Direct antagonism.....	14
Understanding <i>C. difficile</i> Physiology: Metabolism.....	16
Early Characterization of <i>C. difficile</i> physiology.....	18
Studies of <i>C. difficile</i> -microbiota nutrient competition.....	19
Hydrolytic enzymes.....	22
Proteolysis, amino acids, and stickland fermentation.....	23
“Omics” approaches to investigating metabolism.....	27
Genomics.....	27
Transcriptomics and proteomics.....	28
Metabolomics.....	30
Autotrophy.....	31
Summary.....	31
REFERENCES.....	34
CHAPTER 2: Development of Single Chamber Human Gut Microbiota Mini-bioreactor Arrays (MBRA).....	46
Abstract.....	47
Introduction.....	48
Materials and Methods.....	50
Design of mini-bioreactor arrays (MBRA).....	50
Collection of fecal samples.....	51
Preparation of fecal samples.....	51
Media.....	52
MBRA operating conditions and sampling.....	53
HPLC of SCFA.....	54
SCFA Analysis.....	54
DNA extraction.....	55

Preparation of 16S rRNA amplicons for sequencing.....	55
Analysis of amplicon data.....	56
Comparison of cultures grown in BRMW, BRMW ₁₀ and BRMG to the fecal slurry.....	57
Analysis of variation in cultures grown in BRMW ₁₀ and comparison to the starting fecal inoculum.....	59
Results.....	59
Mini-bioreactor design.....	59
MBRA operation.....	61
Short chain fatty acid profiles of cultures grown in each medium revealed that BRMW ₁₀ communities were highly stable and most similar to the fecal inoculum.....	62
Comparison of MBRA microbial composition and structure demonstrates that communities cultured in BRMW ₁₀ are most similar to the fecal inoculum.....	67
Comparison of class-level differences among reactor communities revealed the extent of reorganization of the microbial community during culture.....	70
Examining the microbial community structure in BRMW ₁₀ communities at more frequent time intervals revealed how communities diverge from day-to-day and reactor-to-reactor.....	71
Discussion.....	75
Comparison of community ecology in BRMW ₁₀ reactors to previously published models reveals similar trends among the <i>in vitro</i> models....	78
Conclusions.....	80
Acknowledgements.....	80
APPENDIX.....	81
REFERENCES.....	87

CHAPTER 3: Epidemic <i>Clostridium difficile</i> strains demonstrate increased competitive fitness over non-epidemic isolates.....	93
Abstract.....	94
Introduction.....	95
Materials and Methods.....	97
Mini-bioreactor array (MBRA) design and operation.....	97
Strains, media, and growth conditions.....	97
Collection and preparation of fecal samples for fecal MBRA experiments.....	98
<i>C. difficile</i> invasion and competition growth studies in fecal community MBRA.....	99
Quantitative PCR of <i>tcdA</i> gene to quantify <i>C. difficile</i> invasion.....	101
Preparation of 16S rRNA amplicon sequencing.....	102
Processing and analysis of Sequencing Data.....	103
Quantitative PCR Analysis of Competition Cultures and Calculations of Competitive Index.....	104

<i>C. difficile</i> competition experiments in humanized microbiota mice (h ^m mice)	106
Results.....	108
Fecal mini-bioreactors (MBRA) provide an <i>in vitro</i> model to study <i>C.</i> <i>difficile</i> invasion in complex microbial communities.....	108
MBRAs support complex fecal microbial communities.....	112
Bioreactor community composition changes in response to Clindamycin treatment.....	114
Ribotype 027 strains exhibit a competitive advantage over non-027 strains in the presence of a complex microbiota.....	116
Ribotype 027 strains display a competitive advantage <i>in vivo</i>	121
Discussion.....	123
Fecal MBRA as a model for <i>C. difficile</i> invasion.....	127
Conclusions.....	129
Acknowledgements.....	130
APPENDIX.....	131
REFERENCES.....	142

CHAPTER 4: Differential Metabolism of Trehalose by Epidemic Ribotypes of <i>Clostridium difficile</i>	149
Introduction.....	149
Materials and Methods.....	154
<i>C. difficile</i> strains used in this study and growth conditions.....	154
Identifying nutritional compounds that increase growth of <i>Clostridium</i> <i>difficile</i>	155
Growth experiments further investigating <i>C. difficile</i> utilization of compounds identified in Phenotype MicroArray plates.....	157
Trehalose growth experiments.....	157
RT-qPCR analysis of <i>treA</i> expression.....	158
Cultures.....	158
RNA extractions.....	158
Reverse Transcription.....	159
Real-Time PCR reactions.....	159
Alignments of TreA amino acid sequences from <i>C. difficile</i> clinical isolates and other Gram-positive bacteria.....	162
Construction of a <i>treA</i> knockout mutant in the <i>C. difficile</i> parent strain, CD630Δerm.....	162
Colonization and competition of CD630Δerm wild-type and <i>treA</i> mutant strains in a mouse model of <i>C. difficile</i> infection.....	163
Quantitative PCR Analysis of Competitions and Calculations of Competitive Index.....	164
Results and Discussion.....	166
Identification of carbon sources that <i>C. difficile</i> is able to use for growth.....	166
Compounds identified in Phenotype MicroArray plates increase growth yield of several <i>C. difficile</i> strains.....	168

Characterization of growth phenotypes of <i>C. difficile</i> strains grown on trehalose.....	170
Construction of a <i>treA</i> mutant and analysis of the growth phenotype.....	172
Alignments of <i>treR</i> , the repressor of trehalase (<i>treA</i>), reveal a conserved leucine residue that is substituted with isoleucine in RT 027 strains.....	174
RT 027 strains have increased <i>treA</i> expression.....	179
A <i>treA</i> knockout mutant of <i>C. difficile</i> displays a decrease in colonization levels in a mouse model of <i>C. difficile</i> infection and a decrease in competitive fitness compared to the wild type strain.....	181
Summary and Future Directions.....	187
Acknowledgements.....	189
APPENDIX.....	190
REFERENCES.....	193
 CHAPTER 5: Discussion and Conclusions.....	 198
Discussion.....	198
Conclusions.....	203
REFERENCES.....	204

LIST OF TABLES

Table 1.1. <i>C. difficile</i> metabolic functions related to growth.....	17
Table 2.1. SCFA profiles for fecal inoculum and MBRA cultures.....	67
Table 3.1. Characterization of Strains Used in this Study.....	98
Table S3.1. Competitive indices of ribotype 027 strains at selected time points after <i>C. difficile</i> inoculation as determined by quantitative PCR.....	134
Table S3.2. Primers used for qPCR.....	135
Table 4.1. Characterization of strains used in this study.....	154
Table 4.2. Defined medium ingredients and concentrations.....	156
Table 4.3. Primers used in this study.....	161
Table 4.4. Compounds that conferred at least a 1.5-fold growth yield advantage in Biolog PM1 and PM2 plates.....	167
Table S4.1. Compounds that conferred at least a 1.5-fold growth yield advantage (relative to unsupplemented medium control) for either one or both strains in the Biolog PM3-8.....	191

LIST OF FIGURES

Figure 1.1. <i>Clostridium difficile</i> infection cycle.....	4
Figure 2.1. Schematic of MBRA design and set-up.....	61
Figure 2.2. Short Chain Fatty Acid analysis of bioreactor cultures.....	64
Figure 2.3. Pearson Product Moment Correlation Coefficient of the SCFA composition in bioreactor cultures.....	65
Figure 2.4. Microbial ecology of bioreactors compared to the fecal inoculum.....	69
Figure 2.5. Comparison of the class-level distribution of microbes in bioreactors and the fecal inoculum.....	71
Figure 2.6. Analysis of changes in community structure across time in replicate reactors.....	73
Figure 2.7. Pairwise analyses of changes in community structure across time between reactors.....	74
Figure S2.1. SCFA concentrations in bioreactor cultures.....	82
Figure S2.2. Pearson Product Moment Correlation Coefficient of the SCFA profiles.....	83
Figure S2.3. Shared community structure of bioreactor cultures.....	84
Figure S2.4. Class-level community analysis of replicate reactors in different media.	85
Figure 3.1. An example of a minibioreactor array (MBRA) used for cultivation of fecal microbial communities.....	109
Figure 3.2. Fecal bioreactor communities prevent invasion by <i>C. difficile</i> unless disrupted by treatment with clindamycin.....	110
Figure 3.3. <i>C. difficile</i> proliferation was assayed in fecal bioreactors with different levels of inoculum and in pure culture under the continuous-culture conditions used for bioreactors.....	111
Figure 3.4. Comparison of the community structure between fecal samples, mock-treated and clindamycin-treated reactors.....	113

Figure 3.5. Community structure changes in response to clindamycin-treatment.....	116
Figure 3.6. Competitive indices of ribotype 027 strains relative to non-027 strains in the presence of MBRA fecal communities.....	119
Figure 3.7. Competitive indices of ribotype 027 strains relative to non-027 strains in a mouse model of <i>C. difficile</i> infection.....	122
Figure S3.1. Bacterial abundance does not change significantly in clindamycin-treated reactors.....	136
Figure S3.2. PCR screen of DNA samples from 88 strains of <i>C. difficile</i> for detection of insert containing <i>thyA</i> or the uninterrupted <i>thyX</i>	137
Figure S3.3. Ratios of ribotype 027:non-027 <i>C. difficile</i> strains over time in MBRA competitions.....	138
Figure S3.4. Comparison of the community structure on day 7 from clindamycin-treated reactors used for <i>C. difficile</i> competition experiments to triplicate mock-treated and clindamycin-treated reactors infected with CD2015.....	139
Figure S3.5. Similar community structure changes were observed in response to clindamycin-treatment in competition bioreactor communities.....	140
Figure S3.6. Levels of <i>C. difficile</i> strains across time in mouse model of infection as determined by plating from fecal pellets.....	141
Figure S3.7. Competitive indices (CI) of two competition pairs of ribotype 027 and non-027 <i>C. difficile</i> strains in the MBRA (circles) and Mouse (triangles) models.....	141
Figure 4.1. Results of growth yield experiments using compounds selected from Phenotype MicroArray plates.....	170
Figure 4.2. Maximum growth yield of <i>C. difficile</i> strains grown in the presence of a range of trehalose concentrations in defined medium.....	171
Figure 4.3. Growth yield of <i>C. difficile</i> strains belonging to several ribotype Groups.....	172
Figure 4.4. Growth yields of CD630 wild-type (WT) and <i>treA</i> knock-out mutant in defined medium (DM) supplemented with glucose and glucose disaccharide sugars (25mM).....	174

Figure 4.5. Trehalose utilization genes located on the *C. difficile* chromosome.....174

Figure 4.6. Alignments of TreR amino acid sequences for several *C. difficile* strains of various ribotypes.....175

Figure 4.7. Alignments of TreR amino acid sequences from several Gram-positive bacterial organisms showing conservation of the leucine residue.....176

Figure 4.8. Ribbon diagram of the C-terminal (effector-binding domain) of TreR from *Bacillus subtilis* showing the locations of the predicted trehalose-6-phosphate binding pocket and conserved leucine residue (Leu-169).....177

Figure 4.9. Expression of *treA* in several *C. difficile* strains grown in DM+25mM trehalose as determined by RT-qPCR.....181

Figure 4.10. CFU/g feces of wild-type and *treA* mutant *C. difficile* infected Mice.....183

Figure 4.11. Competitive indices of wild-type CD630 Δ *erm* when competed against the *treA* knockout mutant in a conventional mouse model of *C. difficile* infection.....186

Figure 4.12. Total CFU/g feces of *C. difficile* in each group of mice.....186

CHAPTER 1

Overview of *Clostridium difficile* Disease and Physiology

Antibiotic-Associated Diarrhea

The advent of the antibiotics era in the 1940's is one of the most notable milestones in medical science history. It enabled the treatment of numerous bacterial infections that were previously fatal. Unfortunately, the use of antibiotics brought along with it several unforeseen complications. Perhaps the most significant of these is the development of antibiotic resistance (1). Not far behind it, however, is the common side effect of antibiotic administration, antibiotic-associated diarrhea (AAD). Often the cause of AAD is unknown, but may be due to several different etiologies. The antibiotic compound itself can induce allergic or toxic interactions with the intestinal mucosa, or general physiological effects on gut motility (2, 3). Even more significant, however, are the implications of the impacts that antimicrobials have on the intestinal microbiota.

The human gastrointestinal tract is home to trillions of bacteria, which can be classified into hundreds of different species (4). This large consortium of organisms plays a fundamental role in many different aspects of our health and physiology, more and more of which are being elucidated all the time (reviewed in (5)). One important function of the intestinal microbiota is to protect us from intestinal pathogens, which occurs by many different mechanisms including modulation of the host immune response, production of inhibitory compounds, and competition for limited nutrients

or binding sites, also known as colonization resistance (6). Antibiotics, particularly broad-spectrum antibiotics, not only target the desired pathogen but also inflict collateral damage to the intestinal microbiota, thereby compromising these protective functions and allowing growth of pathogenic strains (7). Several pathogens have been implicated in AAD, including *Salmonella* spp., *Clostridium perfringens*, *Staphylococcus aureus*, *Klebsiella oxytoca*, *Clostridium difficile*, and *Candida albicans* (2, 8). The most common of these is *C. difficile*, being the causative agent in as many as 25% of AAD cases (9). Moreover, *C. difficile* is responsible for ~90% of cases of pseudomembranous colitis, a more severe malady of antibiotic-associated disease (10).

***C. difficile*: the Bacterium and the Disease**

C. difficile is a Gram-positive, spore forming, anaerobic, motile rod. Hall and O'Toole first isolated and described this bacterium in 1935 while characterizing bacterial intestinal colonization of healthy new-born infants (11). While there is a high carriage rate of *C. difficile* in infants, as the intestinal microbiota matures, *C. difficile* is quickly replaced by other strains (12). This process of ecological succession has been demonstrated in both mice and humans (13-16). Consequently, asymptomatic carriage of *C. difficile* in adults is very low (17).

***C. difficile* infection cycle.** The cycle of infection for *C. difficile* is unique compared to other intestinal pathogens due to its obligate anaerobic physiology and complex interactions with the host microbiota. A simplified overview is presented in Figure

1.1. In general, a perturbation of the intestinal microbiota is required for disease development, usually by administration of broad-spectrum antibiotics. Therefore, the intestinal microbiota provides resistance to infection in healthy individuals; functions of an unperturbed intestinal microbiota that provide resistance to *C. difficile* infection will be reviewed below. Since *C. difficile* is an anaerobic organism, it can only pass from host to host in the spore form. Therefore, germination and outgrowth are required for toxin production and establishment of disease. However, it is poorly understood which of these key steps, germination or outgrowth, are most important for initiation of *C. difficile* expansion in the gastrointestinal tract. Once vegetative growth ensues, exotoxins are produced and cause damage to the intestinal epithelium, eliciting an inflammatory response and establishment of disease. Spores are produced during the course of infection, although it is also unknown what the inducing factors are for sporulation. Nonetheless, formation of spores is essential for host transmission, since it requires passage through the aerobic environment. Spores are shed through fecal material, facilitated by the development of diarrhea. They can survive in the environment for very long time periods due to their inherent resistance to environmental conditions such as desiccation, UV-light damage, chemicals, and extreme temperatures. In healthcare settings, environmental contamination of spores is a major issue related to *C. difficile* infection control. Spores present on patient bedding resist removal during laundering, are recalcitrant to alcohol-based hand sanitizers, and have been shown to spread through airborne dissemination (18-20). Moreover, spores are often transferred from patient to patient on the hands of

healthcare workers (21). Ingestion of spores by another patient with reduced intestinal resistance continues the cycle.

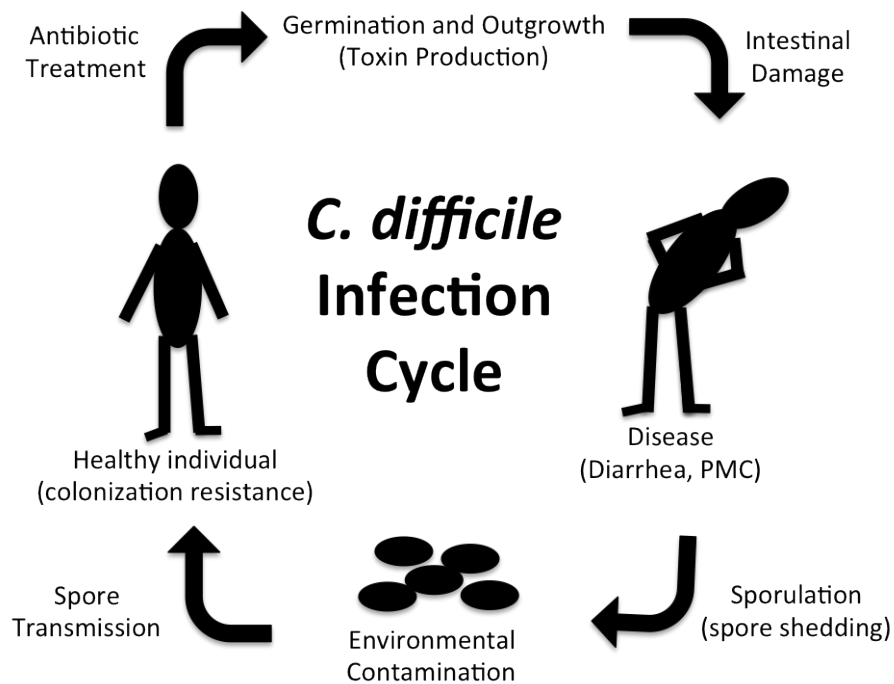


Figure 1.1. *Clostridium difficile* infection cycle. Changes to the intestinal environment induced by antibiotic treatment present conditions that allow *C. difficile* spores to germinate and outgrow. Production of toxins incites intestinal damage and development of disease. Undefined factors induce sporulation; spores are shed from the host, contaminating the environment. Spores are transmitted to new hosts, and the cycle continues. PMC= pseudomembranous colitis.

While CDI is primarily a nosocomial infection, the recent increases in community-acquired infections offer the possibility of an alternative reservoir of *C. difficile*. Several potential sources of community-acquired *C. difficile* transmission have been proposed. Recent work has shown both animals and food as potential reservoirs in the community (22). Another report suggests that the high rate of

carriage in infants is a contributor to *C. difficile* community-acquired infections (23). In addition, a recent study surveyed 30 houses in an urban city, and showed a high degree of environmental contamination within the households (24). These are all valid models for reservoirs of *C. difficile* outside of health-care environments, and it is likely that there are multiple contributors to community-acquired spread of *C. difficile*. Nonetheless, the basis for the recent increases in community-acquired CDI is undoubtedly multifactorial, and more work needs to be done in this area to find ways of preventing these infections.

A major complication of CDI is the high rate of recurrent disease. As many as 20% of patients will have a recurrent infection, and 45% of patients who have had a second infection will have subsequent infections (25). Some patients have multiple recurrent infections over several months or even years. The paradigm for recurrent disease is based on failure of the intestinal microbiota to reestablish appropriately and restore resistance to *C. difficile*. Recurrence is the result of either relapse due to reinfection of the initial infecting strain, or infection by a newly acquired strain (26, 27). Multiple studies have shown that the structure and diversity of the intestinal microbiota of patients with recurrent disease is significantly different from those who do not (17, 28). Indeed, we know that antibiotic treatment can have both short and long-term impacts on the intestinal microbiome (29-32). Since antibiotics are typically the first line of treatment for CDI, this can serve to only exacerbate the problem by further perturbing intestinal communities, thereby increasing the risk of recurrent disease. Therefore, much work is being done to try to find new ways of treating CDI in order to circumvent this problem and reduce recurrence.

Epidemiology, disease, and virulence factors. The association between *C. difficile* and antibiotic-associated disease was not elucidated until 1978, when Bartlett *et al.* showed that it is the primary causative agent of pseudomembranous colitis (33). Since then, much work has been done to investigate the epidemiology and pathogenesis of this organism. The three major risk factors for disease caused by *C. difficile* infection (CDI), are antibiotic treatment, advanced age (>65) and exposure to a hospital setting (34). Any broad-spectrum antibiotic has the potential to initiate CDI; however, some have higher rates of triggering CDI than others. Clindamycin was the major contributing antibiotic initially, followed several years later by those in the cephalosporin group (10). Most recently, fluoroquinolones have been added to this list, due to the emergence of fluoroquinolone-resistant hypervirulent strains (35). In addition to the elderly, high risk groups also include immuno-compromised individuals, patients who have had gastrointestinal surgery, and persons taking gastrointestinal medications including antiperistaltic drugs and proton pump inhibitors (36). Although community-acquired cases are rare, the incidence of these infections have increased in recent years (37).

The symptoms of CDI range from mild, self-limiting diarrhea to severe colonic inflammation and death. In severe cases, CDI is accompanied by the formation of pseudomembranes, termed pseudomembranous colitis (PMC). Pseudomembranes are characterized as regions of the mucosa that become inflamed and covered in yellowish plaques, composed of cellular debris (dead leukocytes and mucosal cells), fibrin, and mucin (38). About 10% of patients with CDAD will develop PMC (39).

Toxic megacolon, a condition in which complete loss of colonic function can occur, has associated mortality rates as high as 80% (9).

The primary virulence factors recognized in this organism are toxins, TcdA and TcdB. Not all *C. difficile* strains are toxigenic; however, only toxin-producing strains cause disease. The genes *tcdA*, *tcdB*, and associated regulatory genes are located on a 19.6 kb pathogenicity locus (PaLoc) on the chromosome of *C. difficile* (40). Additional genes include *tcdR* (a positive regulator; sigma factor), *tcdC* (a negative regulator) and *tcdE* (a holin-like protein). These large toxin proteins (308 kDa and 270 kDa, respectively) are glucosyltransferases; they inactivate members of the Ras superfamily of small GTPases. This inactivation has a cytotoxic effect on target cells by disrupting intracellular signaling pathways involved in interactions of the actin cytoskeleton and initiation of apoptosis, and induces inflammation (41). Some strains produce an additional binary toxin, CDT. Although its role and significance in CDI is not fully understood, there is evidence that it may be associated with increased mortality (42).

Several non-toxin virulence factors of *C. difficile* have been studied. Adhesins are bacterial cell-surface molecules that facilitate binding to host tissues, which in the case of *C. difficile* are primarily mucosal surfaces. These include proteins involved in intestinal adherence by binding to fibronectin, collagen, fibrinogen, and other components of mucin or intestinal epithelia. In a recent review by Vendantam *et al.*, a literature search resulted in a substantial list of *C. difficile* proteins that have either experimentally-demonstrated or putative roles in intestinal adherence (43). Several of these are cell wall proteins (CWPs) and surface layer proteins (SLPs).

Flagella also play an important role in bacterial pathogenesis. Not only are they essential for motility, but can also aid in adherence. Motility has several important functions for pathogen survival. Being able to navigate toward sources of nutrients as well as away from detrimental chemicals is advantageous for self-evident reasons. Moreover, the intestinal epithelium is continually pumping out and turning over viscous mucin; being able to better traverse this landscape aids in intestinal colonization. Experimental evidence suggesting the importance of flagella to *C. difficile* in both colonization and adherence has been reported (44).

Molecular typing schemes. In epidemiological studies, molecular typing of pathogens is used to determine genetic relatedness between clinical isolates. This information helps determine routes of transmission and sources of outbreaks. Moreover, it can help to elucidate the spread of clonal lineages among populations at several levels of resolution; within a small hospital population, regionally, nationally, or even globally. There are several different typing schemes used for *C. difficile*, including Restriction Endonuclease Analysis (REA), North American Pulsed-Field Gel Electrophoresis (NAP), PCR Ribotyping (RT), Multilocus Sequence Typing (MLST), among others (45). Each method utilizes the genetic differences between strains to classify them into different groups, or types. There are regional preferences in terms of which typing techniques are used; for example, in North America *C. difficile* is commonly typed by NAP group. Likewise, REA and RT strain designations are common in Europe. These typing methods, particularly ribotyping, are becoming more common in North America as well. Although a recent publication showed a

strong correlation among typing methods used to classify a set of 100 international isolates, a common protocol for typing isolates would be advantageous for tracking *C. difficile*, and facilitate epidemiological studies (46).

Emergence of Epidemic *C. difficile* Strains

An increase in cases of CDI, marked by significantly higher morbidity and mortality rates, has been largely attributed to the recent emergence of epidemic strains. Several outbreaks were first reported in Quebec, Canada in 2002, and several others in the United States between 2000 and 2003 (35, 47). Analysis of isolates from these outbreaks revealed a specific strain lineage of *C. difficile* was associated with the majority of these cases, typed as NAP1 (North American Pulsed-field 1), RT 027 (PCR ribotype), and BI (restriction endonuclease analysis). In addition, several attributes of these strains were identified, including production of binary toxin (CDT), resistance to fluoroquinolones, and a deletion within the *tcdC* gene, encoding the negative regulator of TcdA and TcdB (35). Epidemiological studies have reported that RT 027/NAP1 strains are associated with up to 10-fold higher morbidity rates, increased cases of severe disease leading to toxic megacolon, and necessity for colectomy (48). Furthermore, mortality rates have been reported as high as 16.7%; a near 10-fold increase from reports previous to the emergence of this strain (48). The rapid spread of RT 027/NAP1 strains since these initial outbreaks is remarkable. In just a few years following, it was reported that 57% of 478 *C. difficile* clinical isolates from 88 hospitals in Quebec, Canada were NAP1 strains (49). Moreover, RT 027 strains have been shown to be prevalent in many other hospitals and regions (50-53).

In less than a decade, this strain has spread globally and been associated with several more outbreaks, namely in Europe (54, 55). He *et al.* recently published an extensive phylogenetic study of RT 027 *C. difficile*, using whole genome sequences of a global set of 151 isolates (56). Their analyses revealed the global spread patterns of two distinct lineages within this clade of strains, both originating from North America, with one undergoing much wider global dissemination.

Initial reports regarding the emergence of RT 027/NAP1 strains designated them as hypervirulent due to associations with increased morbidity and mortality rates. It has recently come into question, however, if these strains really are hypervirulent. While several studies have shown increased rates of disease due to these strains, other reports have demonstrated a lack of correlation between ribotype and disease severity (57-59). It is possible that outbreak-associated RT 027 strains are not representative of the lineage as a whole. Nonetheless, the global spread and prevalence of this group still warrant investigation. Regardless of the ability of these strains to cause more severe disease within individuals, this observation suggests that they have increased transmission rates. In ecological terms, this implies that they have an increased ecological fitness compared to strains of other, less prevalent, ribotypes (60). Therefore, it remains to be determined if strain characteristics aside from archetypical virulence factors contribute to the pervasiveness of the RT 027 strains. A significant portion of the work presented in this thesis aims to address this specific question.

Current impact on the health care system. According to a recent report from the Centers for Disease Control and Prevention (CDC), *C. difficile* infection has surpassed MRSA and is now the most common hospital-acquired infection in the United States (61). Based on current surveillance data, *C. difficile* causes an appalling 250,000 infections per year. Moreover, the CDC reported a 400% increase in related deaths between years 2000 and 2007, with a current estimate of 14,000 deaths per year. In addition, estimated annual hospital costs associated with CDI are in excess of \$3 billion (62). The significance of *C. difficile* disease is clear, as is the need to better understand the pathogenesis of this organism. Finding better ways of preventing and treating this disease is a growing area of current investigation.

Understanding Disease Development: Colonization Resistance.

Soon after the advent of clinical antibiotic use, it was observed that antibiotic treatment often resulted in increased susceptibility to enteric pathogens. This led to the theory that the intestinal microbiota provides a protective function, termed 'colonization resistance', by inhibiting growth of pathogens and development of disease. Research in this area has revealed several different mechanisms at play, including ones that involve not only microbiota-pathogen interactions, but also indirect inhibition mediated through microbiota-host interactions (reviewed in (6)). The intricacies and dynamics involved in colonization resistance are inherently complex and multi-factorial. Moreover, the key interactions providing resistance are likely different for different pathogens. Therefore, while there have been some developments in our understanding of colonization resistance in the case of *C. difficile*

infection, much more work is needed to be done. There are several mechanisms proposed to be involved in colonization resistance against *C. difficile*, and these are briefly outlined below.

Bile acids and germination. The capacity of *C. difficile* to colonize and establish infection is dependent on the ability of spores to germinate and outgrow. *In vivo*, these processes are affected by bile acids; specific primary and secondary bile acids have been shown to act as germinants, anti-germinants, and growth inhibitors (63-65). Primary bile acids, both amino acid-conjugated and unconjugated, are secreted from the gall bladder and function in fat and cholesterol absorption. Some members of the microbiota can enzymatically deconjugate or convert these primary bile acids into secondary bile acids. As such, the intestinal track contains a complex mixture of primary and secondary, conjugated and deconjugated bile acids, and the proportions of each component within this mixture are affected by the microbiota that are present. Giel et al. recently demonstrated this using a mouse infection model to show that the balance of bile acids under normal conditions is such that germination is inhibited, yet following antibiotic treatment changes to the microbiota results in a shift in bile acids to a state which allows spore germination and outgrowth (66). To further support the role of bile acids in colonization resistance and demonstrate that this mechanism can be exploited as a way to prevent infection, Howerton et al. showed that a bile acid analog, CamSA, could prevent spore germination and therefore colonization and development of disease in mice (67). Future work in this

area is needed to better define the role of bile acids in colonization resistance and has the potential to lead to novel ways of preventing CDI.

Competitive exclusion. A central mechanism of colonization resistance that can be applied to many intestinal pathogens involves direct out-competition by the microbiota for nutrient sources and intestinal binding sites, also referred to as competitive exclusion or niche exclusion. Indeed, examples for both of these exist in the case of *C. difficile* inhibition. Initial evidence that competition occurs between intestinal microbiota and *C. difficile* was demonstrated in both an *in vitro* chemostat model and an *in vivo* mouse model (68). Further investigation by Wilson and Perini identified several compounds for which the microbiota of hamsters can outcompete *C. difficile in vitro* (69). These findings were only recently directly tested in an *in vivo* mouse model to show that *C. difficile* metabolism of sialic acids plays a role in gut colonization (70). Few studies directly testing competition for specific nutrients exist; however, the general metabolic capabilities of *C. difficile* will be extensively reviewed in the next section.

In addition to nutrient availability, another important element of an organism's niche is spatial availability. Regarding intestinal colonization, this encompasses the ability to bind to mucosal components, such as fibronectin, collagen, and fibrinogen (71). Several cell surface molecules of *C. difficile* have been implicated to be involved attachment, including fibronectin-binding proteins, cell wall proteins, and surface layer proteins (reviewed in (43)). The majority of these studies were conducted using *in vitro* conditions and therefore the contribution of these adhesins

to *in vivo* colonization has not been directly tested, nor have the specific competing members of the microbiota been identified.

This concept of niche exclusion led to the hypothesis that non-toxigenic *C. difficile* could be used to treat or prevent CDI. The premise is that they will either occupy the specific niche and therefore exclude toxigenic *C. difficile*, or outcompete already colonized toxigenic *C. difficile*, therefore displacing and eliminating them. Borriello et al. presented evidence supporting this hypothesis when they showed that pre-colonization of non-toxigenic *C. difficile* prevented disease development in a hamster infection model (72). A few years later this was tested in two hospital patients with recurrent CDI, both of which had no additional bouts of relapsing disease following administration of the non-toxigenic *C. difficile* (73). More recently, additional work investigating non-toxigenic *C. difficile* prevention of disease has been conducted in hamsters (74, 75). This work supports the theory of niche exclusion in the intestinal environment and future work to identify specific members of the microbiota, which compete with *C. difficile* for its required niche, will contribute to our understanding of the role of colonization resistance in CDI.

Direct antagonism. Additional mechanisms of colonization resistance include ones where there is direct antagonism of *C. difficile* by production of inhibitory compounds by the microbiota; these include short chain fatty acids (SCFAs), lactate, and bacteriocins. Several studies have investigated the effects of SCFAs on *C. difficile* colonization in both *in vivo* and *in vitro* models (76-78). Much of the work supports that SCFAs suppress *C. difficile* colonization, however, some of these results are

conflicting. For example, Su et al. did not see a difference in colonization levels of *C. difficile* in mono-associated mice when administered physiologically relevant concentrations of SCFAs (77). The ability of lactate, another organic acid, to suppress *C. difficile* colonization has also been shown (79). In this work, lactate produced by a potential probiotic strain, *Streptococcus thermophilis*, was demonstrated to ameliorate CDI in a mouse infection model. It is known that intestinal microbiota also produce lactic acid, and therefore, this work supports the potential role of lactic acid in colonization resistance. Lastly, Rea et al. discovered that a human fecal isolate, *Bacillus theringiensis*, produces a bacteriocin with narrow-spectrum activity against *C. difficile* (80). To date, this is the only example of a *C. difficile*-specific bacteriocin produced by the intestinal microbiota, however, it shows that there are specific antagonistic mechanisms employed by intestinal microbiota against *C. difficile* and future work in this area may contribute additional insight.

In summary, several mechanisms utilized by the intestinal microbiota to either directly or indirectly suppress *C. difficile* have been implicated to contribute to colonization resistance. While some mechanisms have been directly tested in *in vivo* models, most have not. Moreover, the specific member/s of the intestinal microbiota that are responsible for these inhibitory functions have generally not been identified. Considering the variability in microbial communities among individuals, it is likely that different strains perform these activities in different people. Therefore, there is still much to be done in this area to understand colonization resistance and be able to exploit these mechanisms for prevention or treatment of CDI.

Understanding *C. difficile* Physiology: Metabolism

The genus *Clostridium* is very diverse, comprised of both medically and biotechnologically important members. The metabolic capabilities of many of these species have been investigated; perhaps the most well known is the industrially relevant solventogenic clostridia. In contrast to some of these other clostridial species, little is known about the nutritional requirements and nutrient utilization capabilities of *C. difficile*. Since the discovery of CDI, a large portion of research has been focused on the epidemiology and pathology of *C. difficile* rather than its physiology. That approach is changing, however, with the growing body of evidence supporting that CDI is a microbiome-mediated disease. More attention is being focused now on the colonization strategies of *C. difficile* and aspects of its general biology and physiology, including metabolism, sporulation, and germination.

It is clear that the intestinal microbiota plays a role in resistance to *C. difficile* colonization and disease establishment. As reviewed above, a primary mechanism at play is likely competition for limited nutrients within the gastrointestinal tract. Understanding better the metabolic strategies that *C. difficile* employs to grow in the highly competitive intestinal environment could help to elucidate novel ways to prevent or control disease development. In the following pages I will review what is known about *C. difficile*'s metabolic capabilities based on published literature, with a focus on nutrients contributing to vegetative growth. The metabolic functions, associated compounds, experimental approaches used, and relevant references identified in the literature and included in this review are listed in Table. 1.1.

Table 1.1. *C. difficile* metabolic functions related to growth.

Metabolic Function	Compounds Metabolized	Experimental Approach	References
Sugar fermentation	Glucose, fructose, mannitol, salicin, xylose, galactose, maltose, sucrose, lactose, raffinose, inulin, glycerol	In vitro – batch culture	(81, 82)
	Mannose, melezitose, sorbitol, ribose, cellobiose, trehalose	In vitro – batch culture	(82, 83)
	raffinose, stachyose	In vitro – batch culture	(82)
	Glucose, N-acetylglucosamine	In vitro gut model	(84)
Stickland fermentation	Amino acids	In vitro – batch culture	(85-87)
		Proteomics	(88)
Hydrolysis of host tissue components	Hyaluronic acid	In vitro - biochemical assay	(89-92)
	Chondroitin-4-sulfate, heparin, collagen	In vitro - biochemical assay	(91, 92)
	Gelatin	In vitro – batch culture	(83)
Metabolism of mucin components	Sialic acids (N-acetylneuraminic acid)	In vitro gut model	(84)
		In vivo - mouse model	(70)
Amino acid utilization	Essential amino acids: cysteine, isoleucine, leucine, proline, tryptophan, valine	Defined medium development	(93)
Ethanolamine utilization	Ethanolamine	Structural and biochemical analysis of <i>eut</i> operon	(94)
Autotrophy	Carbon fixation (CO ₂ + H ₂)	In vitro – batch culture	(95)
General metabolism (<i>In silico</i> analysis)		Whole genome sequencing and annotation	(96)
General metabolism (transcriptomics)		In vitro vs in vivo (pig ileal-ligated loop model)	(97)
		In vitro vs in vivo (monoassociated mice)	(98)
General metabolism (proteomics)		In vitro vs in vivo (pig ileal-ligated loop model)	(88)
General metabolism (metabolomics)	Intestinal environment metabolites	Analytical chemical analysis of in vivo (mouse) samples	(82)

The nutritional landscape of the gut is remarkably complex, dependent on factors of the host's genetics and diet, as well as the intestinal microbial community, which has been shown to be highly variable from person to person (99). Potential nutrient sources in the gut come from the host diet, host tissues and secreted compounds, components of microbial cells, and metabolites of the host and microbiota. While it is

sometimes assumed that the intestinal environment is nutrient-rich, it is in fact a very nutrient-poor environment, especially in the large intestine. Most nutrients are depleted from the intestinal contents in transit through the small intestine by the microbes in this upper region and by host degradation and nutrient uptake. Moreover, the niche-adapted commensal microbiota present a highly competitive environment for enteropathogens to obtain the limited nutrients that are available. The nutrient utilization and competitive strategies of a few enteropathogens, such as *Salmonella enterica* and *Escherichia coli*, have been extensively studied (reviewed in (100)). Some of the key nutritional resources exploited by these pathogens include oligopeptides, mucus-derived sugars and proteins, ethanolamine, and 1,2-propanediol. While the strategies used by *C. difficile* are poorly defined to date, it is likely that it utilizes some of the same resources, and the growing body of literature in this area is helping to paint an ever-clearer picture of its intestinal niche.

Early Characterization of *C. difficile* physiology. In the original paper describing *C. difficile* (then named *Bacillus difficilis*), a classical battery of microbiological tests was conducted to characterize this newly discovered intestinal bacterium (11). They noted a difficulty in growing this organism and interpreting the employed assays, mainly due to the strictly anaerobic conditions required, hence the name “*difficilis*”. Nonetheless, a short list of nutrients utilized by *C. difficile* was reported including dextrose, fructose, mannitol, salicin, xylose and to a lesser extent galactose, maltose, sucrose, lactose, raffinose, inulin, and glycerol (Table 1.1). Their preliminary experiments were focused more on characterization of this bacterium in order to

differentiate it from other intestinal isolates and not as an extensive investigation into its metabolic capabilities.

Over four decades after this initial description of *C. difficile*, its association with antibiotic-associated disease, primarily pseudomembranous colitis, was published (33). At a time when genomic-based diagnostic assays were not available, there was a need to further develop microbiological assays for clinical identification of this pathogen. Some additional primary characterization was conducted by Hafiz et al. in 1977, but soon after simplified protocols that were more practical for clinical application were developed by Nakamura et al. (83, 101). In both studies, the carbohydrate-fermentation properties of large strain sets (30 and 82, respectively) were investigated. Nakamura et al. tested for fermentation of 28 different carbohydrates, reporting positive results for 11 of them, many of which overlapped with the previously published results of Hall and O'Toole. This added mannose, melezitose, sorbitol, ribose, cellobiose, and trehalose to the list of fermentable carbohydrates. They also noted that all 82 strains liquefied 2% gelatin, and that the additional ability to ferment mannitol was a unique characteristic, allowing it to be distinguished from other subterminally sporulating clostridia (83).

Studies of *C. difficile*-microbiota nutrient competition. The observation that antibiotic treatment was required for development of CDI sparked much interest into understanding the role of the intestinal microbiota in resistance to disease. Initial work replicating this observation in both hamster and mouse models showed that the intestinal microbiota repressed *C. difficile* growth since it was only able to colonize

the intestinal tracts of gnotobiotic or antibiotic-treated animals (102, 103). Wilson and Perini went on to further investigate the mechanism of this protective function, hypothesizing that competition between the intestinal microbiota and *C. difficile* for specific limited nutrients was important. A foundation for these studies was previously established by Freter et al. who studied the interactions and colonization dynamics between intestinal microbiota and *Escherichia coli*, and had developed a continuous-flow culture model of the mouse large intestine (104-107). Indeed, they had already shown that the intestinal microbiota could displace or inhibit growth of *C. difficile* in their *in vitro* model (68). The fact that these dynamics could be replicated in the continuous-flow culture system supported the idea that competition for growth-limiting nutrients was occurring. Wilson and Perini first showed that *C. difficile* grew slower than the dilution rate of the *in vitro* system in spent filtrates of the model, which had been seeded with mouse microbiota (84). This suggested that important nutrients had been depleted by the mouse microbiota in the medium, which was prepared from cecal contents of germ-free mice. Analysis of the carbohydrates in fresh and spent medium revealed several components that were significantly depleted in the spent medium. Individually adding these back to the *C. difficile* spent medium cultures increased the growth rate of *C. difficile*, but only for three of the components tested; glucose, N-acetylglucosamine, and N-acetylneuraminic acid. It is interesting to note that the latter two of these three are constituents of mucin. This was the first time that specific nutrients important for *C. difficile* growth in the context of the intestinal environment were identified. Another interesting finding of this work was that *C. difficile* can only utilize these nutrients in

their free form, since it lacks the ability to cleave them from mucin directly (84). Therefore, it still requires the degradative functions of other members of the intestinal microbiota to be able to utilize these compounds *in vivo*, further supporting the complexity of these competitive interactions.

Only recently was utilization of mucin-derived nutrients further investigated *in vivo*. Ng et al. used a mouse model of *C. difficile* invasion to show that sialic acids (specifically, N-acetylneuraminic acid) impact the levels of *C. difficile* colonization in the mouse large intestine (70). Moreover, their work demonstrated that members of the microbiota (in these experiments, *Bacteroides thetaiotaomicron*) that can hydrolyze sialic acids from the mucosa are required for *C. difficile* to be able to utilize them, as suggested in the work by Wilson and Perini. *C. difficile* expansion was lower in mice when it was co-colonized with a sialidase-deficient strain of *B. thetaiotaomicron* rather than the wild-type strain. Furthermore, this decrease in colonization levels was restored when the mice were fed free sialic acid. Additional support for the importance of sialic acid availability was demonstrated by showing a 4-fold decrease in colonization between wild-type *C. difficile* and a mutant unable to metabolize N-acetylneuraminic acid. However, it is clear that additional nutrients are important for *C. difficile* colonization *in vivo*, since the mutant was still able to reach relatively high levels (7×10^7 CFU/ml feces). Nonetheless, this work is important for understanding the metabolic functions of *C. difficile* playing a role in intestinal invasion; hopefully, more *in vivo* work similar to this will be done to provide insight in this area.

Hydrolytic enzymes. Hydrolytic enzymes comprise a class of virulence factors common to bacterial pathogens (108). More specifically, these refer to enzymes that can hydrolyze different components of host tissues. Some classic examples include neuraminidase, hyaluronidase, collagenase, gelatinase, and heparinase. These are important to pathogens for two main reasons. One, they are integral in pathogenesis because they incite tissue damage, stimulating inflammatory responses and allowing access to underlying tissues. Secondly, the products of the hydrolysis reactions can be used as nutrient sources. Furthermore, the activity of hydrolytic enzymes has been demonstrated for several isolates of the human fecal microbiota, particularly in reference to the break down of host mucin, supporting that these compounds are an important source of nutrients for organisms that inhabit the intestinal tract (109).

The hydrolytic activities of *C. difficile* have not been extensively studied. The studies that have been done generally include poorly characterized strains, often not specifying the virulence or toxigenicity of the strains. Drawing conclusions from these studies is even more difficult in light of the conflicting and inconsistent results. For example, Hafiz et al. screened 21 isolates for hyaluronidase activity and reported them all to be positive, while Popoff and Dodin then screened 25 isolates finding them all hyaluronidase negative (89, 90). Later, a study was published by Borriello et al. that screened three groups of strains of varying virulence for the activity of four different hydrolytic enzymes; hyaluronidase, chondroitin-4-sulfatase, heparinase, and collagenase (91). They reported nine of the eleven strains to have positive (or weak) hyaluronidase and chondroitin-4-sulfatase activity, all eleven have positive (or weak) heparinase activity, and only 6 to have collagenase activity (of which 5 were weak).

While there were no strong correlations with virulence, there was a trend of more hydrolytic activity in the more virulent strains. The same group also published a larger study of 30 strains of known virulence or toxin production where they again screened for the same hydrolytic activities (92). Again, they concluded that there were no direct correlations between enzymatic activity and virulence or toxigenic status; however, the most virulent strains in their analyses had the most positive results, whereas many of the lesser virulent strains had more negative results. It is unclear whether the hydrolytic capabilities of *C. difficile* play more of a direct role in virulence by damaging host tissues and breaking down the mucosal barrier as a means of allowing the toxins access to the underlying epithelia, or if they serve to play a more indirect role by providing nutrients for growth and expansion in the intestinal environment. In essence, these two functions are difficult to separate for *C. difficile* since its ability to compete with the intestinal microbiota and colonize is such an integral part of its pathogenesis. Nonetheless, more investigation in this area is warranted and would provide much needed insight into important metabolic strategies of *C. difficile*.

Proteolysis, amino acids, and stickland fermentation. In 1989, Seddon and Borriello developed the first chemically defined medium specifically for growth of *C. difficile* (110). Components included 9 amino acids, N-acetylglucosamine, and a mix of vitamins and minerals. They tested 10 different strains in this medium, and growth was adequate, yet poorer than growth in the standard, rich medium typically used for *C. difficile*, Brain Heart Infusion (BHI) medium. Several years later,

Karasawa et al. more thoroughly characterized the in vitro growth requirements of *C. difficile* by identifying the essential amino acids and vitamins needed for optimum growth (93). Essential amino acids included cysteine, isoleucine, leucine, proline, tryptophan, and valine; only three vitamins were found to be essential: biotin, pantothenate, and pyridoxine. Their optimized defined medium resulted in growth comparable to that in BHI medium, and was a better alternative for physiological studies.

Seddon and Borriello observed that *C. difficile* growth was stimulated when provided a source of peptides, such as proteose peptone or casein hydrolysate, hypothesizing that it may prefer to grow on short peptides rather than free amino acids. To further investigate the proteolytic capabilities of *C. difficile*, they screened 10 strains using various proteolytic assays (111). They used plate assays as well as a variety of biochemical assays using both whole cell suspensions and supernatant to separate cell-associated and extracellular enzymatic activity. In agreement with their previous work investigating the hydrolytic activities of these strains, they found variable proteolytic activity among the strains with no direct correlation to toxigenic or virulence status; however, they again observed a trend of the most virulent strains having the most proteolytic activity. Furthermore, they confirmed the collagenase activity previously reported, that there was no albuminase activity, and no chymotrypsin activity. They did observe the presence of an enzyme with trypsin-like activity and further biochemical characterization of the partially purified enzyme suggested it was similar to the known proteolytic virulence factor, clostripain, of *C. histolyticum*, another Clostridial pathogen. Finally, the authors proposed that *C.*

difficile's proteolytic activity allows for generation of amino acid sources for metabolism and growth and therefore may contribute to the virulence of this organism. For example, ATP generation through fermentation of amino acids has been demonstrated and will be discussed next.

First discovered in 1935, Stickland observed that extracts from *Clostridium sporogenes* were able to ferment amino acids in a pair-wise fashion in which one amino acid (Stickland donor) was oxidized while another amino acid (Stickland acceptor) was reduced (112). Subsequent work has shown these reactions to be utilized by other proteolytic Clostridia. Building upon the previous work showing *C. difficile*'s proteolytic activity and ability to utilize free amino acids, Jackson et al. investigated whether *C. difficile* was able to also utilize Stickland reactions for growth (85). Indeed, they showed that *C. difficile* growth was increased when cells were grown in minimal medium supplemented with Stickland pairs of amino acids. Furthermore, this metabolic activity was dependent on the presence of selenium in the medium. Using the newly sequenced and annotated genome data from the *C. difficile* type strain, CD630 (96), they identified two selenoenzymes likely to be involved in these reactions, glycine reductase, and D-proline reductase. Expression analysis showed both of these enzymes were expressed in the presence of the appropriate Stickland donor amino acids (glycine, proline, or hydroxyproline). They were also able to purify and further characterize D-proline reductase, observing that the biochemistry of this enzyme is slightly different from other known proline reductases since it does not require divalent cations and is inhibited by zinc. This was the first demonstration that Stickland amino acid fermentation is important for

growth of *C. difficile* and the identification of two enzymes that may play critical roles in this metabolic function. Moreover, if Stickland fermentations are critical for optimum growth in the intestinal environment, it suggests that the availability of selenium could be an important growth factor. More recent work has gone on to investigate the transcriptional regulation of the glycine reductase and D-proline reductase gene clusters and has identified that it is proline-dependent and mediated by the protein PrdR (86).

Based on the evidence suggesting the importance of Stickland fermentation for *C. difficile* metabolism and that the organisms utilizing this metabolic strategy are limited, Wu et al. hypothesized that the enzymes involved could be potential narrow-spectrum drug targets for development of novel *C. difficile* treatment (87).

Furthermore, recent transcriptomic and proteomic studies have demonstrated that these enzymes are expressed in *in vivo* models (88, 98). The activity of D-proline reductase requires the conversion of L-proline to D-proline, a function carried out PrdF, D-proline racemase. An insertional knock-out mutant of PrdF showed no significant reduction in growth rate in early log phase; however, mid and late-log phase growth was reduced resulting in significantly lower final growth yield of the mutant. No affect on virulence was reported as there was no difference in survival time of hamsters infected with the wild type or mutant strains and there was no significant difference in toxin expression *in vitro* (87). The generation of knock-out mutants of several genes in the Stickland fermentation pathways in this and the Bouillaut et al. study (86) show that these are not essential for growth *in vitro*.

Additionally, lack of affect of the PrdF knock-out on virulence suggests that Stickland

fermentation is not essential *in vivo* either. However, more *in vivo* work in this area investigating the role of this and other Stickland pathway enzymes on colonization levels is warranted to determine if Stickland metabolism is important for *C. difficile* growth and competition in the intestinal environment.

“Omics” approaches to investigating metabolism.

Genomics. The first *C. difficile* whole genome sequence and analysis was published by Sebaihia et al. in 2006 for strain CD630, a virulent strain isolated from a patient with severe pseudomembranous colitis in Switzerland in 1982 (96). CD630 has a 4.3 Mbp chromosome (and also a 7.9 kbp plasmid), with an unusually high (11%) percentage of mobile elements and a low G+C content (29%). In terms of energy metabolism, genome annotation identified a large amount of genes involved in carbohydrate transport and metabolism as well as genes involved in degradation of ethanolamine, a bacterial carbon and nitrogen source. Ethanolamine is a component of the phosphatidylethanolamine, a common phospholipid of biological membranes, and hence is abundant in the gastrointestinal environment due to the multitude of microbes present as well as the sloughing off of host mucosal epithelia (113). The ability of several gut-associated bacteria to degrade ethanolamine has been reported (114), as has its role in virulence and colonization for several pathogens (115). Recently, a structural and biochemical study of the proteins encoded in the *C. difficile* ethanolamine gene cluster and microcompartment formation was reported (94). However, the direct role of ethanolamine utilization in *C. difficile* colonization or virulence has not been investigated.

Transcriptomics and proteomics. The availability of whole genome sequence data, especially through web-based microbial genomics sources such as IMG (Integrated Microbial Genomes) and NCBI (National Center for Biotechnology Information), has facilitated utilization of “omics” approaches to investigate *C. difficile* colonization. Several studies have applied transcriptomics and proteomics to determine which genes or proteins are differentially expressed under *in vivo* vs *in vitro* conditions (88, 97, 98, 116, 117). The focus of many of these studies is on identifying genes related more directly to virulence (toxin expression) and stress tolerance, yet some data has emerged providing information about the metabolic strategies employed *in vivo*.

In an effort to further understand *C. difficile* adaptation to the host environment, Scaria et al. developed a pig ileal-ligated loop model and used it to determine the transcriptional profile of *C. difficile* 4, 8, and 12 hours post-infection (97). Comparison of microarray data between *in vivo* (pig ligated loop model) and *in vitro* (BHI medium) conditions revealed upregulation of several pathways involved in transport and metabolism of amino acids and various carbohydrates, anaerobic respiration, and lipid degradation. In particular, the data suggested metabolism of xylose, mannose, and glycogen to be important *in vivo*. This study was one of the first transcriptional profiling studies of *C. difficile* gene expression in an *in vivo* model.

The same group then used a proteomics approach to look at *C. difficile* protein expression in a similar pig ligated loop model (88). Again, they compared samples from *in vitro* and *in vivo* conditions 4, 8, and 12 hours post infection; of the 705 quantifiable proteins identified, 109 were differentially expressed. Many proteins

involved in metabolism and energy production were identified, including those important for amino acid metabolism, carbohydrate metabolism, and Stickland fermentation. Many of the pathways upregulated in this study overlap with their previous transcriptomic study; however, some did not and this is probably a reflection of the differences in the technical challenges of these two techniques, and inherent differences in the targets of the analyses. Regardless, these studies provide useful data suggesting important metabolic adaptations of *C. difficile* to its host environment and can be mined for potential functions to more directly test through genetic manipulation and *in vivo* colonization and virulence experiments.

Another *in vivo* transcriptomic study recently published by Janoir et al. used this comprehensive approach by first identifying genes upregulated *in vivo* and then testing knock-out mutants of those genes for defects in colonization (98). They compared temporal gene expression *in vitro* (TY medium) vs *in vivo*, using *C. difficile*-monoassociated mice; 549 differentially expressed genes were identified, 20% of which were ascribed to metabolic pathways. Like the other *in vivo* transcriptomic and proteomic studies in the pig ileal-ligated loop model, the pathways included lipid and carbohydrate transport and metabolism, and fermentation of carbohydrates and amino acids. In addition, genes involved in glycogen synthesis and degradation of polysaccharides were upregulated *in vivo*. Evidence for a preference for the leucine/proline Stickland fermentation pair was also apparent in the data. Interestingly, one-sixth of the upregulated genes were of unknown function, two of which were selected for further investigation. Genetic knock-out mutants of these two genes were tested against the wild type strain for decreased colonization fitness.

One of them, CD1581, had significantly lower colonization in the co-infection experiment, providing direct evidence for the importance of the product of this gene for colonization *in vivo*. The observation that the other hypothetical protein mutant did not show a colonization defect even though the gene was differentially expressed supports that colonization factors identified in these initial genetic studies must be directly tested in follow-up experiments.

Metabolomics. Yet another approach to understanding the metabolic strategies used by *C. difficile* for colonization was recently published by Theriot et al. (82). They used metabolomics to first identify changes in the available nutrients between caecal contents of *C. difficile* resistant and susceptible (antibiotic-treated) mice, identifying significant changes in levels of some amino acids, carbohydrates, lipids, peptides and xenobiotics. *In vitro* growth experiments confirmed the ability of *C. difficile* to utilize some of the carbohydrates shown to increase in the *C. difficile*-susceptible metabolic environment, namely glucose, fructose, mannitol, sorbitol, raffinose, and stachyose. Additionally, they identified two different *C. difficile*-resistant states, one before antibiotic treatment, and one six weeks after antibiotic treatment. Interestingly, the bacterial communities between these states were very different, however, their metabolomic profiles were strikingly similar, especially with regard to compounds found to be important for *C. difficile* germination and growth. This supports that the functions of the intestinal microbiota, which shape the metabolic environment, rather than the specific community member are more important for resistance to *C. difficile*. This study took a novel approach to understanding *C. difficile* colonization by first

characterizing the nutrients available to *C. difficile*, then testing its ability to utilize these compounds. In contrast, previous studies first identified *C. difficile* compound utilization by genomic and phenotypic analyses, then tested if these affected colonization. Additional studies combining data from these two complementary approaches will undoubtedly provide even more insight into understanding *C. difficile* intestinal colonization and bring us closer to development of novel ways to prevent and treat CDI.

Autotrophy. A completely novel growth strategy used by *C. difficile* was recently discovered by Kopke et al. (95). This was an exciting discovery as it was the first time a bacterial pathogen was demonstrated to be able to grow autotrophically. Metabolic byproducts of the microbial breakdown of some intestinal saccharide and protein sources include carbon dioxide and hydrogen gases. *C. difficile* can in turn fix the CO₂ and form acetate by way of the Wood-Ljungdahl pathway; several genes belonging to this pathway are conserved among *C. difficile* isolates. Indeed, it was demonstrated that *C. difficile* can grow on CO₂ and H₂ as the sole source of carbon and energy in a defined medium (95). Experiments designed to directly test the contribution of autotrophic growth to *in vivo* colonization are needed; however, the ability of *C. difficile* to grow autotrophically adds another growth strategy to *C. difficile's* metabolic repertoire.

Summary

Disease caused by *C. difficile* is a common complication in antibiotic treatment. Until recently, it was not considered a significant nosocomial threat. However, increases in

disease prevalence and severity have generated an urgency to understand the epidemiology and etiology of this disease. A likely contributing factor to the increased disease incidence is the emergence of epidemic strains that appear to spread more readily and potentially cause more severe disease. *C. difficile* infection is distinctive in that there is a clear role of the intestinal microbiota in the development of disease. However, the specific mechanisms that govern outgrowth of *C. difficile* in the colon are poorly understood. One hypothesis regarding inhibition of *C. difficile* in the absence of antibiotic treatment suggests that members of the microbiota outcompete *C. difficile* for key nutrient sources. Several studies have been published providing evidence that supports this hypothesis. There is some understanding of the general metabolic capabilities of *C. difficile*, however, which specific nutrients are key players in colonization resistance and how much of an impact they have on the ability of *C. difficile* to outgrow in the colon is poorly understood. Understanding all of the strategies *C. difficile* uses to compete for the limited resources available in the gastrointestinal tract could provide insight into how the microbiota impacts disease progression, and ultimately lead to new infection control strategies. Furthermore, it is unclear if characteristics of the newly emerged epidemic strains related to colonization and competitive dynamics within the intestinal environment contribute to their increased prevalence and ability to cause disease. The work presented in this thesis aims to address some of these issues. Chapter 2 presents the development of an *in vitro* model to study fecal bacterial communities, which was adapted in chapter 3 as a *C. difficile* infection model. We used the *in vitro C. difficile* infection model to show that in the presence of complex fecal microbiota, epidemic ribotype

027 strains outcompete strains of other ribotypes. Also presented are *in vivo* data supporting this competitive advantage of the RT 027 strains in a mouse infection model. Chapter 4 focuses on the growth metabolism of *C. difficile* and shows that epidemic strains are able to grow more efficiently on the disaccharide trehalose. This metabolic characteristic of epidemic strains may contribute to the competitive advantage we observed in our *in vitro* and *in vivo* models. Moreover, if the importance of trehalose metabolism translates into the human intestinal environment, this work provides insight into defining the intestinal niche of *C. difficile*, and understanding the evolution and emergence of epidemic strains.

REFERENCES

REFERENCES

1. **Aminov RI.** 2010. A brief history of the antibiotic era: lessons learned and challenges for the future. *Front Microbiol* **1**:134.
2. **Bartlett JG.** 2002. Antibiotic-associated diarrhea. *New England Journal of Medicine* **346**:334–339.
3. **Högenauer C, Hammer HF, Krejs GJ, Reisinger C.** 1998. Mechanisms and management of antibiotic-associated diarrhea. *Clin. Infect. Dis.* **27**:702–710.
4. **Qin J, Li R, Raes J, Arumugam M, Burgdorf KS, Manichanh C, Nielsen T, Pons N, Levenez F, Yamada T, Mende DR, Li J, Xu J, Li S, Li D, Cao J, Wang B, Liang H, Zheng H, Xie Y, Tap J, Lepage P, Bertalan M, Batto J-M, Hansen T, Le Paslier D, Linneberg A, Nielsen HB, Pelletier E, Renault P, Sicheritz-Ponten T, Turner K, Zhu H, Yu C, Li S, Jian M, Zhou Y, Li Y, Zhang X, Li S, Qin N, Yang H, Wang J, Brunak S, Doré J, Guarner F, Kristiansen K, Pedersen O, Parkhill J, Weissenbach J, MetaHIT Consortium, Bork P, Ehrlich SD, Wang J.** 2010. A human gut microbial gene catalogue established by metagenomic sequencing. *Nature* **464**:59–65.
5. **de Vos WM, de Vos EA.** 2012. Role of the intestinal microbiome in health and disease: from correlation to causation. *Nutrition Reviews* **70**:S45–S56.
6. **Stecher B, Hardt W-D.** 2008. The role of microbiota in infectious disease. *Trends in Microbiology* **16**:107–114.
7. **Paterson DL.** 2004. “Collateral Damage” from Cephalosporin or Quinolone Antibiotic Therapy. *CLIN INFECT DIS* **38**:S341–S345.
8. **Ayyagari A, Agarwal J, Garg A.** 2003. Antibiotic associated diarrhoea: infectious causes. *Indian J Med Microbiol* **21**:6–11.
9. **Yassin SF, Young-Fadok TM, Zein NN, Pardi DS.** 2001. Clostridium difficile-associated diarrhea and colitis. *Mayo Clin. Proc.* **76**:725–730.
10. **Kelly CP, Pothoulakis C, LaMont JT.** 1994. Clostridium difficile Colitis. *N. Engl. J. Med.* **330**:257–262.
11. **HALL IC.** 1935. Intestinal flora in new-born infants. *Am J Dis Child* **49**:390–402.
12. **Wilson KH.** 1993. The microecology of Clostridium difficile. *Clin. Infect. Dis.* **16 Suppl 4**:S214–8.

13. **Rotimi VO, Duerden BI.** 1981. The development of the bacterial flora in normal neonates. *Journal of Medical Microbiology* **14**:51–62.
14. **SCHAEDLER RW, DUBOS R, COSTELLO R.** 1965. The Development Of The Bacterial Flora In The Gastrointestinal Tract Of Mice. *J. Exp. Med.* **122**:59–66.
15. **Favier CF, Vaughan EE, de Vos WM, Akkermans ADL.** 2002. Molecular monitoring of succession of bacterial communities in human neonates. *Appl Microbiol* **68**:219–226.
16. **Koenig JE, Spor A, Scalfone N, Fricker AD, Stombaugh J, Knight R, Angenent LT, Ley RE.** 2011. Succession of microbial consortia in the developing infant gut microbiome. *Proceedings of the National Academy of Sciences* **108 Suppl 1**:4578–4585.
17. **Rea MC, O'Sullivan O, Shanahan F, O'Toole PW, Stanton C, Ross RP, Hill C.** 2012. Clostridium difficile Carriage in Elderly Subjects and Associated Changes in the Intestinal Microbiota. *Journal of Clinical Microbiology* **50**:867–875.
18. **Roberts K, Smith CF, Snelling AM, Kerr KG, Banfield KR, Sleigh PA, Beggs CB.** 2008. Aerial Dissemination of Clostridium difficile spores. *BMC Infect Dis* **8**:7.
19. **Hellickson LA, Owens KL.** 2007. Cross-Contamination of Clostridium difficile Spores on Bed Linen During Laundering. *American Journal of Infection Control* **35**:E32–E33.
20. **Jabbar U , BA, Leischner J , MD, Kasper D , MD, Gerber R , MD, Sambol SP , BS, MT(A, Parada JP , MD, MPH, Johnson S , MD, Gerding DN , MD.** 2010. Effectiveness of Alcohol-Based Hand Rubs for Removal of Clostridium difficile Spores from Hands. *Infection Control and Hospital Epidemiology* **31**:565–570.
21. **Gerding DN, Muto CA, Owens RC Jr.** 2008. Measures to Control and Prevent Clostridium difficile Infection. *Clin Infect Dis* **46**:S43–S49.
22. **Rupnik M.** 2007. Is Clostridium difficile-associated infection a potentially zoonotic and foodborne disease? *Clin Microbiol Infect* **13**:457–459.
23. **Rousseau C, Poilane I, De Pontual L, Maherault A-C, Le Monnier A, Collignon A.** 2012. Clostridium difficile carriage in healthy infants in the community: a potential reservoir for pathogenic strains. *Clin Infect Dis* **55**:1209–1215.
24. **Alam MJ, Anu A, Walk ST, Garey KW.** 2014. Investigation of potentially pathogenic Clostridium difficile contamination in household environs.

- Anaerobe **27C**:31–33.
25. **Johnson S.** 2009. Recurrent *Clostridium difficile* infection: A review of risk factors, treatments, and outcomes. *Journal of Infection* **58**:403–410.
 26. **Wilcox MH, Fawley WN, Settle CD, Davidson A.** 1998. Recurrence of symptoms in *Clostridium difficile* infection—relapse or reinfection? *Journal of Hospital Infection* **38**:93–100.
 27. **Figueroa I, Johnson S, Sambol SP, Goldstein EJ, Citron DM, Gerding DN.** 2012. Relapse versus reinfection: recurrent *Clostridium difficile* infection following treatment with fidaxomicin or vancomycin. *Clin. Infect. Dis.* **55**:S104–S109.
 28. **Chang JY, Antonopoulos DA, Kalra A, Tonelli A, Khalife WT, Schmidt TM, Young VB.** 2008. Decreased Diversity of the Fecal Microbiome in Recurrent *Clostridium difficile*-Associated Diarrhea. *J Infect Dis* **197**:435–438.
 29. **Peterfreund GL, Vandivier LE, Sinha R, Marozsan AJ, Olson WC, Zhu J, Bushman FD.** 2012. Succession in the gut microbiome following antibiotic and antibody therapies for *Clostridium difficile*. *PLoS One* **7**:e46966.
 30. **Jakobsson HE, Jernberg C, Andersson AF, Sjölund-Karlsson M, Jansson JK, Engstrand L.** 2010. Short-term antibiotic treatment has differing long-term impacts on the human throat and gut microbiome. *PLoS One* **5**:e9836.
 31. **Schubert AM, Rogers MAM, Ring C, Mogle J, Petrosino JP, Young VB, Aronoff DM, Schloss PD.** 2014. Microbiome Data Distinguish Patients with *Clostridium difficile* Infection and Non-*C. difficile*-Associated Diarrhea from Healthy Controls. *MBio* **5**:e01021–14–e01021–14.
 32. **Jernberg C, Löfmark S, Edlund C, Jansson JK.** 2007. Long-term ecological impacts of antibiotic administration on the human intestinal microbiota. *ISME J* **1**:56–66.
 33. **Bartlett JG, Chang TW, Gurwith M, Gorbach SL, Onderdonk AB.** 1978. Antibiotic-associated pseudomembranous colitis due to toxin-producing clostridia. *N. Engl. J. Med.* **298**:531–534.
 34. **McDonald LC, Owings M, Jernigan DB.** 2006. *Clostridium difficile* infection in patients discharged from US short-stay hospitals, 1996–2003. *Emerg. Infect. Dis.* **12**:409.
 35. **Loo VG, Poirier L, Miller MA, Oughton M, Libman MD, Michaud S, Bourgault A-M, Nguyen T, Frenette C, Kelly M, Vibien A, Brassard P, Fenn S, Dewar K, Hudson TJ, Horn R, René P, Monczak Y, Dascal A.** 2005. A predominantly clonal multi-institutional outbreak of *Clostridium difficile*-

- associated diarrhea with high morbidity and mortality. *N. Engl. J. Med.* **353**:2442–2449.
36. **Barbut F, Petit JC.** 2001. Epidemiology of *Clostridium difficile*-associated infections. *Clin Microbiol Infect* **7**:405–410.
 37. **Kuijper EJ, Barbut F, Brazier JS, Kleinkauf N, Eckmanns T, Lambert ML, Drudy D, Fitzpatrick F, Wiuff C, Brown DJ, Coia JE, Pituch H, Reichert P, Even J, Mossong J, Widmer AF, Olsen KE, Allerberger F, Notermans DW, Delmee M, Coignard B, Wilcox M, Patel B, Frei R, Nagy E, Bouza E, Marin M, Akerlund T, Virolainen-Julkunen A, Lyytikäinen O, Kotila S, Ingebretsen A, Smyth B, Rooney P, Poxton IR, Monnet DL.** 2008. Update of *Clostridium difficile* infection due to PCR ribotype 027 in Europe, 2008. *Euro Surveill.* **13**.
 38. **Poutanen SM.** 2004. *Clostridium difficile*-associated diarrhea in adults. *Canadian Medical Association Journal* **171**:51–58.
 39. **McFarland LV.** 1998. Epidemiology, Risk Factors and Treatments for Antibiotic-Associated Diarrhea. *Dig Dis* **16**:292–307.
 40. **Voth DE, Ballard JD.** 2005. *Clostridium difficile* toxins: mechanism of action and role in disease. *Clin. Microbiol. Rev.* **18**:247–263.
 41. **Shen A.** 2012. *Clostridium difficile* toxins: mediators of inflammation. *J Innate Immun* **4**:149–158.
 42. **Gerding DN, Johnson S, Rupnik M, Aktories K.** 2013. *Clostridium difficile* binary toxin CDT: Mechanism, epidemiology, and potential clinical importance. *gutmicrobes* **5**:6–18.
 43. **Vedantam G, Clark A, Chu M, McQuade R, Mallozzi M, Viswanathan VK.** 2012. *Clostridium difficile* infection: toxins and non-toxin virulence factors, and their contributions to disease establishment and host response. *gutmicrobes* **3**:121–134.
 44. **Tasteyre A, Barc MC, Collignon A, Boureau H, Karjalainen T.** 2001. Role of FliC and FliD flagellar proteins of *Clostridium difficile* in adherence and gut colonization. *Infection and Immunity* **69**:7937–7940.
 45. **Killgore G, Thompson A, Johnson S, Brazier J, Kuijper E, Pepin J, Frost EH, Savelkoul P, Nicholson B, van den Berg RJ, KATO H, Sambol SP, Zukowski W, Woods C, Limbago B, Gerding DN, McDonald LC.** 2008. Comparison of Seven Techniques for Typing International Epidemic Strains of *Clostridium difficile*: Restriction Endonuclease Analysis, Pulsed-Field Gel Electrophoresis, PCR-Ribotyping, Multilocus Sequence Typing, Multilocus Variable-Number Tandem-Repeat Analysis, Amplified Fragment Length Polymorphism, and

- Surface Layer Protein A Gene Sequence Typing. *Journal of Clinical Microbiology* **46**:431–437.
46. **Manzo CE, Merrigan MM, Johnson S, Gerding DN, Riley TV, Silva J, Brazier JS, the International Clostridium difficile Study Group.** 2014. International typing study of *Clostridium difficile*. *Anaerobe* **28C**:4–7.
 47. **McDonald LC, Killgore GE, Thompson A, Owens RC, Kazakova SV, Sambol SP, Johnson S, Gerding DN.** 2005. An epidemic, toxin gene-variant strain of *Clostridium difficile*. *N. Engl. J. Med.* **353**:2433–2441.
 48. **Bartlett JG.** 2006. Narrative review: the new epidemic of *Clostridium difficile*-associated enteric disease. *Ann. Intern. Med.* **145**:758–764.
 49. **Hubert B, Loo VG, Bourgault A-M, Poirier L, Dascal A, Fortin E, Dionne M, Lorange M.** 2007. A portrait of the geographic dissemination of the *Clostridium difficile* North American pulsed-field type 1 strain and the epidemiology of *C. difficile*-associated disease in Québec. *Clin Infect Dis* **44**:238–244.
 50. **Waslawski S, Lo ES, Ewing SA, Young VB, Aronoff DM, Sharp SE, Novak-Weekley SM, Crist AE, Dunne WM, Hoppe-Bauer J, Johnson M, Brecher SM, Newton DW, Walk ST.** 2013. *Clostridium difficile* ribotype diversity at six health care institutions in the United States. *Journal of Clinical Microbiology* **51**:1938–1941.
 51. **Goorhuis A, Van der Kooi T, Vaessen N, Dekker FW, Van den Berg R, Harmanus C, van den Hof S, Notermans DW, Kuijper EJ.** 2007. Spread and Epidemiology of *Clostridium difficile* Polymerase Chain Reaction Ribotype 027/Toxinotype III in The Netherlands. *CLIN INFECT DIS* **45**:695–703.
 52. **Wilcox MH, Shetty N, Fawley WN, Shemko M, Coen P, Birtles A, Cairns M, Curran MD, Dodgson KJ, Green SM, Hardy KJ, Hawkey PM, Magee JG, Sails AD, Wren MWD.** 2012. Changing epidemiology of *Clostridium difficile* infection following the introduction of a national ribotyping-based surveillance scheme in England. *CLIN INFECT DIS* **55**:1056–1063.
 53. **Wultańska D, Młynarczyk G, Harmanus C.** 2014. Occurrence of *Clostridium difficile* PCR-ribotype 027 and it's closely related PCR-ribotype 176 in hospitals in Poland in 2008-2010. *Anaerobe*.
 54. **Kuijper EJ, van Dissel JT.** 2008. Spectrum of *Clostridium difficile* infections outside health care facilities. *Canadian Medical Association Journal* **179**:747–748.
 55. **Gerding DN , MD.** 2010. Global Epidemiology of *Clostridium difficile* Infection in 2010. *Infection Control and Hospital Epidemiology* **31**:S32–S34.

56. **He M, Miyajima F, Roberts P, Ellison L, Pickard DJ, Martin MJ, Connor TR, Harris SR, Fairley D, Bamford KB, D'Arc S, Brazier J, Brown D, Coia JE, Douce G, Gerding D, Kim HJ, Koh TH, Kato H, Senoh M, Louie T, Michell S, Butt E, Peacock SJ, Brown NM, Riley T, Songer G, Wilcox M, Pirmohamed M, Kuijper E, Hawkey P, Wren BW, Dougan G, Parkhill J, Lawley TD.** 2013. Emergence and global spread of epidemic healthcare-associated *Clostridium difficile*. *Nat Genet* **45**:109–113.
57. **Sirard S, Valiquette L, Fortier LC.** 2011. Lack of Association between Clinical Outcome of *Clostridium difficile* Infections, Strain Type, and Virulence-Associated Phenotypes. *Journal of Clinical Microbiology* **49**:4040–4046.
58. **Carlson PE, Walk ST, Bourgis AET, Liu MW, Koplaku F, Lo E, Young VB, Aronoff DM, Hanna PC.** 2013. The relationship between phenotype, ribotype, and clinical disease in human *Clostridium difficile* isolates. *Anaerobe* **24**:109–116.
59. **Walk ST, Micic D, Jain R, Lo ES, Trivedi I, Liu EW, Almassalha LM, Ewing SA, Ring C, Galecki AT.** 2012. *Clostridium difficile* ribotype does not predict severe infection. *Clin. Infect. Dis.* **55**:1661–1668.
60. **Smits WK.** 2013. Hype or hypervirulence: a reflection on problematic *C. difficile* strains. *Virulence* **4**:592–596.
61. **US CFDCAP.** 2013. Antibiotic resistance threats in the United States, 2013.
62. **Dubberke E.** 2012. *Clostridium difficile* infection: The scope of the problem. *J. Hosp. Med.* **7**:S1–S4.
63. **Sorg JA, Sonenshein AL.** 2008. Bile Salts and Glycine as Cogerminants for *Clostridium difficile* Spores. *Journal of Bacteriology* **190**:2505–2512.
64. **Sorg JA, Sonenshein AL.** 2009. Chenodeoxycholate is an inhibitor of *Clostridium difficile* spore germination. *Journal of Bacteriology* **191**:1115–1117.
65. **Wilson KH.** 1983. Efficiency of various bile salt preparations for stimulation of *Clostridium difficile* spore germination. *Journal of Clinical Microbiology* **18**:1017–1019.
66. **Giel JL, Sorg JA, Sonenshein AL, Zhu J.** 2010. Metabolism of Bile Salts in Mice Influences Spore Germination in *Clostridium difficile*. *PLoS ONE* **5**:e8740.
67. **Howerton A, Patra M, Abel-Santos E.** 2013. A new strategy for the prevention of *Clostridium difficile* infection. *J Infect Dis* **207**:1498–1504.
68. **Wilson KH, Freter R.** 1986. Interaction of *Clostridium difficile* and

- Escherichia coli with microfloras in continuous-flow cultures and gnotobiotic mice. *Infection and Immunity* **54**:354–358.
69. **Wilson KH, Perini F.** 1988. Role of competition for nutrients in suppression of *Clostridium difficile* by the colonic microflora. *Infection and Immunity* **56**:2610–2614.
70. **Ng KM, Ferreyra JA, Higginbottom SK, Lynch JB, Kashyap PC, Gopinath S, Naidu N, Choudhury B, Weimer BC, Monack DM, Sonnenburg JL.** 2013. Microbiota-liberated host sugars facilitate post-antibiotic expansion of enteric pathogens. *Nature* **502**:96–99.
71. **Vengadesan K, Narayana SVL.** 2011. Structural biology of Gram-positive bacterial adhesins. *Protein Sci.* **20**:759–772.
72. **Borriello SP, BARCLAY FE.** 1985. Protection of hamsters against *Clostridium difficile* ileocaecitis by prior colonisation with non-pathogenic strains. *Journal of Medical Microbiology* **19**:339–350.
73. **Seal D, Borriello SP, Barclay F, Welch A, Piper M, Bonnycastle M.** 1987. Treatment of relapsing *Clostridium difficile* diarrhoea by administration of a non-toxicogenic strain. *Eur. J. Clin. Microbiol.* **6**:51–53.
74. **Merrigan MM, Sambol SP, Johnson S, Gerding DN.** 2009. New approach to the management of *Clostridium difficile* infection: colonisation with non-toxicogenic *C. difficile* during daily ampicillin or ceftriaxone administration. *Int. J. Antimicrob. Agents* **33**:S46–S50.
75. **Nagaro KJ, Phillips ST, Cheknis AK, Sambol SP, Zukowski WE, Johnson S, Gerding DN.** 2013. Nontoxicogenic *Clostridium difficile* protects hamsters against challenge with historic and epidemic strains of toxicogenic BI/NAP1/027 *C. difficile*. *Antimicrobial Agents and Chemotherapy* **57**:5266–5270.
76. **Rolfe RD.** 1984. Role of volatile fatty acids in colonization resistance to *Clostridium difficile*. *Infection and Immunity* **45**:185–191.
77. **Su WJ, Waechter MJ, Bourlioux P, Dolegeal M, Fourniat J, Mahuzier G.** 1987. Role of volatile fatty acids in colonization resistance to *Clostridium difficile* in gnotobiotic mice. *Infection and Immunity* **55**:1686–1691.
78. **May T, Mackie RI, Fahey GC, Cremin JC, Garleb KA.** 1994. Effect of fiber source on short-chain fatty acid production and on the growth and toxin production by *Clostridium difficile*. *Scand J Gastroenterol* **29**:916–922.
79. **Kolling GL, Wu M, Warren CA, Durmaz E, Klaenhammer TR, Guerrant RL.** 2012. Lactic acid production by *Streptococcus thermophilus* alters

- Clostridium difficile infection and in vitro Toxin A production. *gutmicrobes* **3**:0–6.
80. **Rea MC, Sit CS, Clayton E, O'Connor PM, Whittal RM, Zheng J, Vederas JC, Ross RP, Hill C.** 2010. Thuricin CD, a posttranslationally modified bacteriocin with a narrow spectrum of activity against *Clostridium difficile*. *Proceedings of the National Academy of Sciences* **107**:9352–9357.
 81. **HALL IC, O'TOOLE E.** 1935. Intestinal flora in new-born infants with a description of a new pathogenic anaerobe, *Bacillus difficilis*. *Am J Dis Child* **49**:390–402.
 82. **Theriot CM, Koenigsnecht MJ, Carlson PE, Hatton GE, Nelson AM, Li B, Huffnagle GB, Li JZ, Young VB.** 2014. ncomms4114. *Nature Communications* **5**:1–10.
 83. **Nakamura S, Nakashio S, Yamakawa K, Tanabe N, Nishida S.** 2013. Carbohydrate Fermentation by *Clostridium difficile*. *Microbiol. Immunol.* **26**:107–111.
 84. **Wilson KH, Perini F.** 1988. Role of competition for nutrients in suppression of *Clostridium difficile* by the colonic microflora. *Infection and Immunity* **56**:2610–2614.
 85. **Jackson S, Calos M, Myers A, Self WT.** 2006. Analysis of Proline Reduction in the Nosocomial Pathogen *Clostridium difficile*. *Journal of Bacteriology* **188**:8487–8495.
 86. **Bouillaut L, Self WT, Sonenshein AL.** 2013. Proline-Dependent Regulation of *Clostridium difficile* Stickland Metabolism. *Journal of Bacteriology* **195**:844–854.
 87. **Wu X, Hurdle JG.** 2014. The *Clostridium difficile* proline racemase is not essential for early logarithmic growth and infection. *Can. J. Microbiol.* **60**:251–254.
 88. **Janvilisri T, Scaria J, Teng C-H, McDonough SP, Gleed RD, Fubini SL, Zhang S, Akey B, Chang Y-F.** 2012. Temporal differential proteomes of *Clostridium difficile* in the pig ileal-ligated loop model. *PLoS ONE* **7**:e45608.
 89. **Hafiz S.** 1974. *Clostridium difficile* and its toxins.
 90. **Popoff MR, Dodin A.** 1985. Survey of neuraminidase production by *Clostridium butyricum*, *Clostridium beijerinckii*, and *Clostridium difficile* strains from clinical and nonclinical sources. *Journal of Clinical Microbiology* **22**:873–876.

91. **Borriello SP, Davies HA, Kamiya S, Reed PJ, Seddon S.** 1990. Virulence factors of *Clostridium difficile*. *Clin. Infect. Dis.* **12**:S185–S191.
92. **Seddon SV, HEMINGWAY I, Borriello SP.** 1990. Hydrolytic enzyme production by *Clostridium difficile* and its relationship to toxin production and virulence in the hamster model. *Journal of Medical Microbiology* **31**:169–174.
93. **KARASAWA T, Ikoma S, Yamakawa K, Nakamura S.** 1995. A defined growth medium for *Clostridium difficile*. *Microbiology (Reading, Engl.)* **141**:371–375.
94. **Pitts AC, Tuck LR, Faulds-Pain A, Lewis RJ, Marles-Wright J.** 2012. Structural insight into the *Clostridium difficile* ethanolamine utilisation microcompartment. *PLoS ONE* **7**:e48360.
95. **Köpke M, Straub M, Dürre P.** 2013. *Clostridium difficile* is an autotrophic bacterial pathogen. *PLoS ONE* **8**:e62157.
96. **Sebahia M, Wren BW, Mullany P, Fairweather NF, Minton N, Stabler R, Thomson NR, Roberts AP, Cerdeño-Tárraga AM, Wang H, Holden MT, Wright A, Churcher C, Quail MA, Baker S, Bason N, Brooks K, Chillingworth T, Cronin A, Davis P, Dowd L, Fraser A, Feltwell T, Hance Z, Holroyd S, Jagels K, Moule S, Mungall K, Price C, Rabinowitsch E, Sharp S, Simmonds M, Stevens K, Unwin L, Whithead S, Dupuy B, Dougan G, Barrell B, Parkhill J.** 2006. The multidrug-resistant human pathogen *Clostridium difficile* has a highly mobile, mosaic genome. *Nat Genet* **38**:779–786.
97. **Scaria J, Janvilisri T, Fubini S, Gleed RD, McDonough SP, Chang YF.** 2011. *Clostridium difficile* Transcriptome Analysis Using Pig Ligated Loop Model Reveals Modulation of Pathways Not Modulated In Vitro. *J Infect Dis* **203**:1613–1620.
98. **Janoir C, Denève C, Bouttier S, Barbut F, Hoys S, Caleechum L, Chapetón-Montes D, Pereira FC, Henriques AO, Collignon A, Monot M, Dupuy B.** 2013. Adaptive strategies and pathogenesis of *Clostridium difficile* from in vivo transcriptomics. *Infection and Immunity* **81**:3757–3769.
99. **Blottiere HM, de Vos WM, Ehrlich SD, Doré J.** 2013. Human intestinal metagenomics: state of the art and future. *Current Opinion in Microbiology* **16**:232–239.
100. **Staib L, Fuchs TM.** 2014. From food to cell: nutrient exploitation strategies of enteropathogens. *Microbiology*.
101. **HAFIZ S, OAKLEY CL.** 1976. *Clostridium difficile*: isolation and characteristics (Plate VIII). *Journal of Medical Microbiology* **9**:129–136.

102. **Wilson KH, Sheagren JN, Freter R.** 1985. Population dynamics of ingested *Clostridium difficile* in the gastrointestinal tract of the Syrian hamster. *J INFECT DIS* **151**:355–361.
103. **Wilson KH, Sheagren JN, Freter R, Weatherbee L, Lyerly D.** 1986. Gnotobiotic models for study of the microbial ecology of *Clostridium difficile* and *Escherichia coli*. *J INFECT DIS* **153**:547–551.
104. **Freter R, Stauffer E, Cleven D, Holdeman LV, Moore WE.** 1983. Continuous-flow cultures as in vitro models of the ecology of large intestinal flora. *Infection and Immunity* **39**:666–675.
105. **Freter R, Brickner H, Botney M, Cleven D, Aranki A.** 1983. Mechanisms that control bacterial populations in continuous-flow culture models of mouse large intestinal flora. *Infection and Immunity* **39**:676–685.
106. **Freter R, Brickner H, Fekete J, Vickerman MM, Carey KE.** 1983. Survival and implantation of *Escherichia coli* in the intestinal tract. *Infection and Immunity* **39**:686–703.
107. **Ozawa A, Freter R.** 1964. Ecological Mechanism Controlling Growth Of *Escherichia Coli* In Continuous Flow Cultures And In The Mouse Intestine. *J Infect Dis* **114**:235–242.
108. **Duerden BI.** 1994. Virulence factors in anaerobes. *Clin. Infect. Dis.* **18 Suppl 4**:S253–9.
109. **Corfield AP, Wagner SA, Clamp JR, Kriaris MS, Hoskins LC.** 1992. Mucin degradation in the human colon: production of sialidase, sialate O-acetyltransferase, N-acetylneuraminidase, arylesterase, and glycosulfatase activities by strains of fecal bacteria. *Infection and Immunity* **60**:3971–3978.
110. **Seddon SV, Borriello SP.** 1989. A chemically defined and minimal medium for *Clostridium difficile*. *Letters in applied microbiology* **9**:237–239.
111. **Seddon SV, Borriello SP.** 1992. Proteolytic activity of *Clostridium difficile*. *Journal of Medical Microbiology* **36**:307–311.
112. **Stickland LH.** 1934. Studies in the metabolism of the strict anaerobes (genus *Clostridium*): The chemical reactions by which *Cl. sporogenes* obtains its energy. *Biochemical Journal* **28**:1746.
113. **Garsin DA.** 2010. Ethanolamine utilization in bacterial pathogens: roles and regulation. *Nat Rev Micro* **8**:290–295.
114. **Tsoy O, Ravcheev D, Mushegian A.** 2009. Comparative genomics of ethanolamine utilization. *Journal of Bacteriology* **191**:7157–7164.

115. **Garsin DA.** 2012. Ethanolamine: a signal to commence a host-associated lifestyle? *MBio* **3**:e00172–12.
116. **Janvilisri T, Scaria J, Chang Y-F.** 2010. Transcriptional profiling of *Clostridium difficile* and Caco-2 cells during infection. *J Infect Dis* **202**:282–290.
117. **Emerson JE, Stabler RA, Wren BW, Fairweather NF.** 2008. Microarray analysis of the transcriptional responses of *Clostridium difficile* to environmental and antibiotic stress. *Journal of Medical Microbiology* **57**:757–764.

CHAPTER 2

Development of Single Chamber Human Gut Microbiota Mini-bioreactor Arrays (MBRA)

The material presented in this chapter was an equal collaboration with Jennifer M. Auchtung (Britton Lab, Department of Microbiology and Molecular Genetics MSU) and Robert D. Stedtfeld (Hashsham Lab, Department of Civil and Environmental Engineering, MSU). Robert Stedtfeld drafted the bioreactor design for fabrication, and performed the HPLC analysis for SCFA quantification. Jennifer Auchtung conducted the bioreactor community analysis and microbial ecology.

Abstract

We developed single chamber continuous-flow mini-bioreactor arrays (MBRA) for *in vitro* human fecal microbiome studies. The small size (15 ml volume) and setup allowed many individual reactors to be operated in parallel, providing flexibility in terms of testing multiple conditions and replicates simultaneously. Initially, we tested four variations of media to determine how well these media would be able to reproduce the microbial diversity and functional stability of a human fecal community. Triplicate reactors were inoculated with each medium and their stability was monitored over time (28 days). We identified one medium that best supported growth of a diverse fecal microbial community with a stable short chain fatty acid (SCFA) profile most similar to the starting fecal inoculum. Detailed analyses of communities in this medium demonstrated that the microbial community in each reactor was dynamic throughout the culture period. The largest changes in the communities were observed during the first week in culture, after which the communities stabilized to a constant low rate of change. Over time, the communities present in each replicate reactor diverged both from the starting community and from the other replicate reactors, but still shared some similarity with the starting fecal inoculum. This study demonstrates the utility of multiplexed, single chamber MBRA to support growth of complex, dynamic, functionally-stable fecal microbial communities.

Introduction

The trillions of microorganisms forming the commensal microbiota of the human gastrointestinal tract contribute to many different aspects of host physiology, including metabolism and energy stasis, maturation of the immune system, metabolism of xenobiotics, and protection from pathogen invasion (reviewed in (1-3)). Although many insights about the role of the microbiota in host health and disease have been gained by studying the microbiota in association with its human host (e.g., (4-6)), the availability of less complex models of the microbiota (i.e., conventional and humanized animal (7-10) and *in vitro* models (11-16)) have also played an important role in elucidating the roles of the microbiota. The primary advantage of using these models are the ability to perform controlled experiments at a higher throughput than can be achieved with human studies, whereas the primary disadvantage is the lack of interactions with the human host.

Several different *in vitro* models of the human intestinal tract have been developed, ranging from simple batch culture models (e.g., (17, 18)) to more complex continuous flow culture models (e.g., (11-16)). Continuous-flow culture models are beneficial for studying the complex interactions between members of the host microbiota *in vitro* because they allow for studies to be completed during an extended period of time under conditions where pH, nutrient availability and washout of waste products and dead cells can be better controlled (reviewed in (19-21)).

Three multi-stage continuous-culture models that have been well studied and validated for their use as *in vitro* models of the human microbiota are the

Simulator of Human Intestinal Microbial Ecosystem (SHIME, (14, 22, 23)), the TIM-2 *in vitro* model of the human intestine (12, 24), and the three-stage compound continuous culture system (13, 16). Although they share several features, each model has its own unique properties. The SHIME and three-stage compound continuous culture system simulate multiple colon compartments (ascending, transverse, and descending colon) with fresh nutrients coming into the system at the ascending colon. In contrast, the TIM-2 model has four chambers that simulate the proximal colon and are connected in a loop with contents circulated between the four chambers and fresh medium brought into one of the chambers through a peristaltic valve. All three models are inoculated with human feces, maintained at a constant temperature of 37°C, kept anaerobic by continuous flushing of anaerobic gas (N₂ (SHIME, TIM-2) or CO₂ (three-stage)), and incorporate dynamic pH monitoring and adjustment.

Another common feature of all three model systems described above is their size and complexity, which makes high numbers of biological replication of experiments challenging. The goal of our study was to develop a simpler, continuous-flow *in vitro* model that would support growth of complex human fecal microbial communities but also facilitate higher throughput studies. We developed mini-bioreactor arrays (MBRAs) that allow for simultaneous operation of up to 24 independent reactors in a single anaerobic chamber. After testing four different media, we identified a single medium that best supported growth of microbial communities that were functionally and ecologically similar to the initial fecal

community. Based upon these results, we anticipate that our MBRA model will be a useful tool for moderate throughput studies of human fecal microbial communities.

Materials and Methods

Design of mini-bioreactor arrays (MBRA). MBRAs were designed using CAD software (Argon, Asheller-Vellum), and fabricated with DSM Somos Watershed XC 11122 via stereolithography (FineLine prototyping). In detail, six reactors with an internal volume of 25 mL were designed into a single strip with 200mm x 47 mm x 36 mm dimensions (Fig. 1A). Reactors were drawn with 25 x 25 x 40 mm dimensions, including 10 mm radial blends on the bottom corners (to prevent buildup of cells and other insoluble materials), and 5 mm radial blends on the top. Reactors were spaced 32.5 mm center to center to match dimensions on the selected stir plate (described below). Three 5.55 mm diameter holes (influent, effluent, inoculation/sampling) were placed into the top of each reactor, and spaced 16 mm apart center to center. Holes were tapped with threads to fit with conventional leur connectors. Inner walls of the reactors were placed 2 mm from the bottom of the strip, 5 mm from the top of the strip, 5 mm from the side of the strip, and 3.25 mm into the strip. A 1.25 x 16 x 31 mm intrusion was designed into the bottom corners of the MBRA for fixing into a custom built acrylic block that held the reactors upright and properly aligned with the stir-plate. A CAD file (.stl) that can be used directly for fabrication via stereolithography is available in the supplemental material.

Collection of fecal samples. Fecal samples were donated by twelve healthy, anonymous donors that were between the ages of 25 and 64, had not taken antibiotics for at least two months and had refrained from consuming products containing intentionally-added live microbes for at least two days prior to donation. Fresh samples were collected into sterile containers, which were then packed in wet ice in a sealed (8.1 quart, Sterilite Ultraseal) container with two anaerobic gaspaks (BD biosciences) and transported to the laboratory within 24 hours. Protocols for participation of human subjects were reviewed and approved by the Institutional Review Board of Michigan State University.

Preparation of fecal samples. Once received in the laboratory, samples were transferred to an anaerobic chamber and manually mixed with sterile equipment (spatula and/or pestle). Aliquots were transferred to sterile cryogenic vials and stored at -80°C until use. Prior to inoculation into the bioreactors, aliquots from each donor were thawed in the anaerobic chamber and resuspended in sterile, phosphate-buffered saline with 0.1% cysteine at a concentration of 20% w/v. Samples were vortexed vigorously for 5 min, then allowed to settle for 5 min prior to removal of the supernatant, which was used for inoculation into the reactors. Inoculum was introduced into each reactor through an ethanol-sterilized rubber septum via a sterile syringe and needle. The final concentration of inoculum in each reactor was 1%. Excess fecal slurry was diluted 30% with sterile glycerol to a final concentration of 15% glycerol, aliquoted into 1 ml volumes in sterile cryovials, flash frozen in liquid nitrogen, and stored at -80°C. Two aliquots of excess fecal slurry

were used for analyzing the SCFA and microbial community composition of the fecal inoculum.

Media. One liter of BRMW was composed of tryptone (1g), proteose peptone #3 (2g), yeast extract (2g), arabinogalactan (1g), maltose (1.5g), D-cellobiose (1.5g), sodium chloride (0.4g), hemin (5mg), magnesium sulfate (1mg), calcium chloride (1mg), tween 80 (2ml), taurocholate (1g), D-glucose (400mg), inulin (2g), sodium bicarbonate (2g), potassium phosphate monobasic (6.1g), potassium phosphate dibasic (7.6g), and vitamin K₃ (1mg). The composition of BRMW₁₀ was the same as BRMW with the exception of 10-fold reductions in the concentration of arabinogalactan, maltose, D-cellobiose, D-glucose, and inulin. One liter of BRMG was composed of trypticase peptone (2g), yeast extract (1g), D-glucose (0.4g), cellobiose (1g), maltose (1g), fructose (1g), beef extract (5g), magnesium sulfate heptahydrate (32 mg), sodium chloride (80mg), calcium chloride (0.8mg), iron sulfate (2.5mg), hematin (1.2mg), histidine (31mg), tween 80 (0.5ml), ATCC vitamin mix (10% v/v), boric acid (30µg), manganese chloride (600µg), cobalt (II) chloride (190µg), nickel (II) chloride (124µg), copper (II) chloride (102µg), zinc sulfate (144µg), sodium molybdate (36µg), sodium metavanadate (25µg), sodium tungstate (25µg), sodium selenite (6µg), isovaleric acid (0.1ml), propionic acid (2ml), butyric acid (2ml), taurocholate (1g), sodium bicarbonate (2g), potassium phosphate monobasic (6.1g), potassium phosphate dibasic (7.6g), and vitamin K₃ (1mg). The composition of BRMG₁₀ was the same as BRMG with the exception of 10-fold reductions in the concentration of maltose, D-cellobiose, D-glucose, and fructose. We adjusted the pH

of all four media to 6.8 and sterilized by a combination of autoclaving and filter sterilization of heat labile reagents.

MBRA operating conditions and sampling. Media were transferred from the source bottles through a combination of 1/8 in inner diameter (ID) C-flex tubing (6424-67, Cole-Parmer) and 0.89 mm ID 2-stop Tygon lab tubing supplied to the reactors via a 24-channel peristaltic pump (IPC-24, Ismatec). The waste line in each MBRA was set to maintain a working volume of 15 ml and the pumps were calibrated for a flow rate of 0.625 ml/hr (24 hr retention time). Waste was removed from the reactors through a combination of 1/8 in ID C-flex tubing and 1.14 mm ID 2-stop Tygon lab tubing drawn from the reactors via the same 24-channel peristaltic pump. Omnifit caps were used to connect media and waste bottles to tubing.

Reactors were stirred using magnetic stir bars driven by independent magnets on a 60-spot magnetic stir plate (VarioMAG HP 60, Vario-MAG USA). Assembled MBRA were sterilized by autoclaving and were operated in an anaerobic chamber (5% H₂, 5% CO₂, 90% N₂) maintained at 37°C. MBRA and source media were allowed to equilibrate to the anaerobic environment of the chamber for at least 72 hours prior to use. Media was pumped through tubing into the reactors and allowed to equilibrate for 48 hrs in the reactors prior to inoculation to ensure sterility. 1 ml samples were removed for SCFA and microbial ecological analyses every two days by sterile needle and syringe through ethanol-sterilized septa. (Removal of 1 ml of sample decreases the total volume of the culture in the reactor by 6.7%. Reactor volume returns to the pre-sampling volume of 15 ml within 1.6 hours of sampling

through the addition of fresh medium. During these 1.6 hours, waste is unlikely to be removed since the volume of the reactor is below the threshold volume for waste removal.) Samples were centrifuged for 1 min at maximum speed, supernatants were removed from cell pellets, and both pellets and supernatants were stored at -80°C until further processing. The pH of thawed supernatant samples was tested with pH strips (pHydrion papers, pH 4.5-7.5, MicroEssential Laboratories).

HPLC of SCFA. To ensure cells were removed, thawed supernatant samples were centrifuged at maximum speed for an additional 15 min. Centrifuged reactor samples were filtered through 0.22- μm -pore-size filters (SLGS033SS, Millipore) and acidified with 0.1 M H_2SO_4 . SCFAs were analyzed with a high-performance liquid chromatograph (HPLC) equipped with a 250 x 4.6 mm Discovery C8 column (59354-U, Supelco Analytical) connected to a UV/Vis absorbance detector (Series 200, Perkin Elmer) set at 210 nm. The mobile phase was 25 mM potassium phosphate adjusted to a pH of 2.8 with phosphoric acid, at a flow rate of 1 ml/min, and 100 μl was injected into the HPLC using an autosampler (Series 200, Perkin Elmer). All compounds detectable with the UV/Vis absorbance detector within 50 min were monitored. Lactate, acetate, butyrate, propionate, and isobutyrate were identified by their retention times compared to those of standards.

SCFA Analysis. The area under peaks were calculated using TotalChrom Navigator (Perkin Elmer), and the concentration of SCFA was derived via standard dilutions of lactate, acetate, butyrate, propionate, and isobutyrate run in parallel. Pearson

Product Moment Correlation Coefficients were calculated using the Pearson function in Microsoft Excel. Additional transformations of the data are reported in the figure or table legend.

DNA extraction. We extracted DNA from samples using bead beating followed by cleanup with a Qiagen DNEasy Tissue Kit. Samples were resuspended in 360 μ l buffer ATL (Qiagen), transferred to a MoBio fecal bead tube, and homogenized on full speed for 1 min. Homogenates were incubated with proteinase K (40 μ l of >600 mAU/ml, Qiagen) for 1 hour at 55°C, followed by incubation with 200 μ l of buffer AL for 10-30 minutes at 70°C. 200 μ l of ethanol was added prior to loading on the column. Column washing was as described in the Qiagen protocol and samples were eluted in 100 μ l of Buffer AE. DNA concentrations were determined with Quant-IT (Invitrogen) according to the manufacturer's protocol.

Preparation of 16S rRNA amplicons for sequencing. We used 40 ng of each DNA sample as template in PCR with the following final concentrations of reagents: 200 nM 357F primer, 200 nM 926R primer, 1X AccuPrime PCR Buffer II (Invitrogen), 0.75 U of AccuPrime Taq DNA High Fidelity (Invitrogen). 357F/926R were designed by the Human Microbiome Project, amplify the V3-V5 variable regions of the 16S *rRNA* gene, and contain unique barcodes that can be used to multiplex sequencing reactions (25). Each reaction was set up in triplicate and amplified using the following cycle: 95°C for 2 min, followed by 30 cycles of 95°C for 20 sec, 50°C for 30 sec, and 72°C for 5 min, with a final extension at 72°C for 5 min. Successful PCR

amplification products from triplicate reactions were pooled and cleaned with Agencourt AMPure XP beads essentially according to protocol with minor modifications (Beckman-Coulter). Briefly, products were resuspended with a 0.7X volume of beads, washed twice with 70% ethanol, and eluted with 25 μ l of low EDTA TE Buffer (10 mM Tris, 0.1 mM EDTA). Concentrations of purified DNA samples were determined using Quant-IT (Invitrogen) according to the manufacturer's protocol and were pooled in equimolar amounts. Nucleotide sequencing was performed on a 454 GS Junior (Roche Diagnostics) at Michigan State University according to the manufacturer's protocols. Four sequencing runs were performed. Run 1 included BRMW & BRMW₁₀ Reactors 1, 2 & 3 on days 2, 4, 8, 14, and 28 and BRMG Reactors 1, 2, & 3 on days 2, 4, 8, 14, 22, and 28 in culture; Run 2 included BRMW & BRMW₁₀ Reactors 1, 2, & 3 on day 20 in culture; Run 3 included BRMW₁₀ Reactors 1, 2, & 3 on days 2, 4, 6, 8, 10, 12, 14, 16, 18, and 20 in culture as well as two independently prepared replicates of the fecal slurry; Run 4 was an in-depth analysis of the two replicates of the fecal slurry.

Analysis of amplicon data. All sequence data were analyzed using mothur (26) Version 1.27.0 (August 2012). The sequences from the four sequencing runs described above were initially processed independently and were quality trimmed and filtered to remove those sequences that had any ambiguous bases, mismatches to the reverse primer or barcode, homopolymeric stretches longer than 8 nt, were shorter than 200 nt, and/or had an average quality score over a 50 nt window less than 30 (27). Sequences from all four runs were then compiled into a single fasta file

and aligned to the SILVA reference alignment using the NAST-based aligner in mothur, trimmed to ensure that sequences overlapped, and pre-clustered, allowing a difference between sequences of 2 bp or less (27). Potentially chimeric sequences were removed using the mothur-implementation of UChime (28); remaining sequences were classified using RDP training set version 9 (March 2012) and mothur's implementation of the kmer-based Bayesian classifier. Sequences that classified as Mitochondria, Chloroplasts, Eukarya or unknown were removed prior to further analysis. Sequences were binned into Operational Taxonomic Units (OTUs) with $\leq 3\%$ sequence dissimilarity using the average neighbor algorithm of mothur. Taxonomy was assigned to each OTU based upon the majority sequence consensus within that OTU (29).

Comparison of cultures grown in BRMW, BRMW₁₀ and BRMG to the fecal slurry. In order to determine the differences in microbial community structure and composition within and between cultures grown in BRMW, BRMW₁₀, BRMG and the fecal slurry, we extracted these samples (from Runs 1 (all samples included), 2 (all samples included), and 3 (fecal slurry only)) from the larger pool of samples prior to further analysis. For OTU-based analyses, we then removed those sequences that were represented by only a single sequence across the samples studied (singletons). Before determining alpha-diversity measures (Inverse Simpson, Chao Richness, Simpson Evenness) for the communities using the calculators present in mothur, we randomly subsampled our data to the maximum number of sequences present in the smallest group (nseqs=554) ten times and presented the mean \pm standard deviations of these calculations. We also used one iteration of our randomly

subsampled data to calculate the theta dissimilarity measure described by Yue and Clayton (θ_{YC} (30)) using the calculators present in mothur.

For taxonomic-based analyses, we classified sequences using the RDP training set and the mothur-implementation of the RDP-classifier as described above. Sequences that were classified to the same taxonomic-level (Genus, Family, Order, Class, or Phylum) were binned together into phylotypes. Prior to calculation of the θ_{YC} dissimilarity index, those phylotypes that were represented by a single sequence across the samples were removed and the data was randomly subsampled to the largest number of sequences present in the smallest sample (nseqs=557).

For analysis of phylogenetic diversity, we randomly subsampled our data to the maximum number of sequences present in the smallest group (nseqs=557), calculated an uncorrected pairwise distance matrix between the aligned sequences, and then built a relaxed neighbor joining phylogenetic tree of the sequence data using the mothur-implementation of clearcut (31). We calculated the phylogenetic distance between samples using the mothur-implementation of weighted unifrac (32). We used the mothur-implementation of principal coordinates analysis (PCOA), ANOSIM, and AMOVA for analysis of θ_{YC} Dissimilarity Indices. PCOA data was plotted in R whereas other distance measures were plotted in Microsoft Excel.

The percent abundance of each phylotype at the class-level was based upon analysis of total sequences present in the indicated samples (not subsampled). The percent abundance in the fecal slurry samples was based upon the in-depth sequencing (nseqs = 38,169 and 44,792) of duplicate fecal slurry samples (Sequencing Run 4).

Analysis of variation in cultures grown in BRMW₁₀ and comparison to the starting fecal inoculum. In order to calculate the differences that occurred between the three reactors grown in BRMW₁₀ and between BRMW₁₀ and the fecal inoculum, we extracted sequence data from all three reactors on Day 2, 4, 6, 8, 10, 12, 14, 16, 18 and 20 and the two replicates of the fecal slurry samples (Sequencing Run 3). For OTU-based analyses, we removed sequences represented by only a single sequence across the data points and randomly subsampled all groups to the largest number present in the smallest sample (nseqs=1814 for comparisons without fecal slurry samples; nseqs=1582 for comparisons with fecal slurry samples). For taxonomic-based analyses, we classified sequences using the RDP-classifier and binned into phylotypes, removed singletons, and subsampled as described above. We calculated the θ_{YC} dissimilarity index, and ANOSIM and AMOVA of the θ_{YC} distance matrix as described above. We calculated the Pearson Product Moment Correlation Coefficient using the Pearson function in Microsoft Excel. Data was plotted in Microsoft Excel.

Results

Mini-bioreactor design. After evaluating different materials for use in the MBRA, we determined that DSM Somos Watershed XC 11122 was the most appropriate material due to its transparency, resistance to water and humidity, durability after autoclaving, previous use in microbiological studies (33), and its ability for use with enclosed 3D fabrication. Stereolithography was used to create blocks of six bioreactor chambers within each mini-bioreactor array (Fig. 2.1A). We chose

stereolithography for synthesis in order to have a completely enclosed reactor design, thereby minimizing points at which contaminants could be introduced into the reactors. The interior volume of each reactor was designed to allow a 15 ml medium volume and a 10 ml headspace volume. This reactor volume was chosen to allow for a less drastic change in volume of medium upon sampling (<10% for a 1 ml sample) while still maintaining sufficient headspace within the reactor to reduce the risk of contamination of the source medium. Further, the small medium volume (compared to liter scale reactors) reduced medium consumption and waste production, thereby limiting expense of operation.

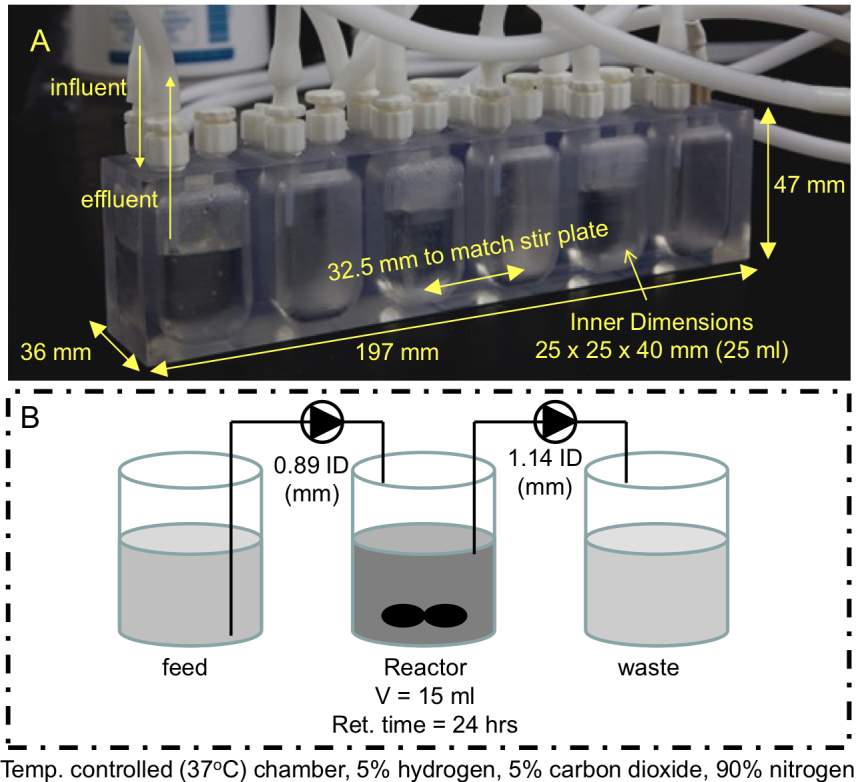


Figure 2.1. Schematic of MBRA design and set-up. (A) Picture of a single mini-bioreactor (MBRA) strip with dimensions indicated. (B) Schematic of bioreactor setup. Each mini-bioreactor was operated with a total volume of 15 ml. We used peristaltic pump tubing with 0.89 mm inner diameter (ID) and the lowest peristaltic pump setting to produce a flow rate from the feed of 0.625 ml/hr (24 hr retention time). We used 1.14 ID peristaltic tubing on the waste lines to prevent clogging. Each reactor was constantly stirred using a magnetic stir bar driven by a stir plate. Reactors were maintained in an anaerobic chamber (5% H₂, 5% CO₂, 90% N₂) at 37°C.

MBRA operation. We operated the MBRA as continuously-stirred tank bioreactors with a retention time of 24 hours (Fig. 2.1B). Similar operating conditions have been used in other *in vitro* colonic models of the distal colon that supported growth of diverse microbial communities (14, 34). These operating conditions allowed us to monitor growth of our fecal communities in culture for 28 days. In order to facilitate

growth of strict anaerobes, we maintained the MBRA in a 37°C anaerobic chamber with 5% CO₂, 5% H₂ and 90% N₂ atmosphere. We evaluated four different types of media, which were variations of media developed in the Wilcox (13) and Gordon (8) laboratories for culturing diverse fecal communities. We named the media variations BRMW (Bioreactor Medium Wilcox), BRMG (Bioreactor Medium Gordon), BRMW₁₀ and BRMG₁₀. BRMW₁₀ and BRMG₁₀ are modifications of BRMW and BRMG that contain 10% of the carbohydrates found in the original media, which we evaluated because previous work with the three-stage compound continuous culture system had shown that the majority of carbohydrates in the medium are depleted prior to reaching the third chamber of the system that mimics the distal colon (34). The media were buffered with both phosphate buffer and bicarbonate, which was sufficient to maintain a relatively constant pH without addition of acid or base (pH was between 6.5 and 7.0 across all twelve reactors, when measured every 2 days).

Short chain fatty acid profiles of cultures grown in each medium revealed that BRMW₁₀ communities were highly stable and most similar to the fecal inoculum. One key function the gut microbiota provides to its host is the fermentation of otherwise indigestible polysaccharides to short chain fatty acids (SCFAs), which can both be used by the host for energy metabolism and influence a wide array of host functions (reviewed in (3)). Changes in the concentration and proportion of individual SCFAs correlate with changes in bacterial groups (35-37), thus monitoring SCFAs can be a good measure of community functional stability.

Using HPLC, we monitored the concentrations of five SCFAs (acetate, butyrate, isobutyrate, lactate and propionate) in our reactors over time and compared these concentrations to the starting fecal inoculum. While the low concentration of isobutyrate, an isoform of butyrate, is typically neglected, it was monitored in this study because it has been described, along with butyrate, as the most rapid indicators for monitoring process instability (38, 39).

We found considerable differences in SCFA profiles and concentrations across the four different media (Figure 2.2, Figure S2.1). For an individual reactor in a given medium, we generally observed that stabilization in the SCFA profile, which we defined as a Pearson Product Moment Correlation Coefficient > 0.8 from one sample day to the next (as had been previously reported to represent stability (23, 40)), occurred by day two of growth in culture and persisted throughout the remainder of time in culture (Fig 2.3A-D). The two exceptions to this trend were from a single reactor grown in BRMG and another reactor grown in BRMG₁₀ where the correlation coefficient dropped to 0.73 and 0.77, respectively during single two-day windows. In general, the correlation coefficient was above 0.9 for most points in culture. A notable exception occurred between day 18 and 20 in culture in BRMG and BRMG₁₀ where the correlation coefficient dropped quickly then returned to stability. This time frame corresponded to a change from one batch of source medium to a new batch of source medium.

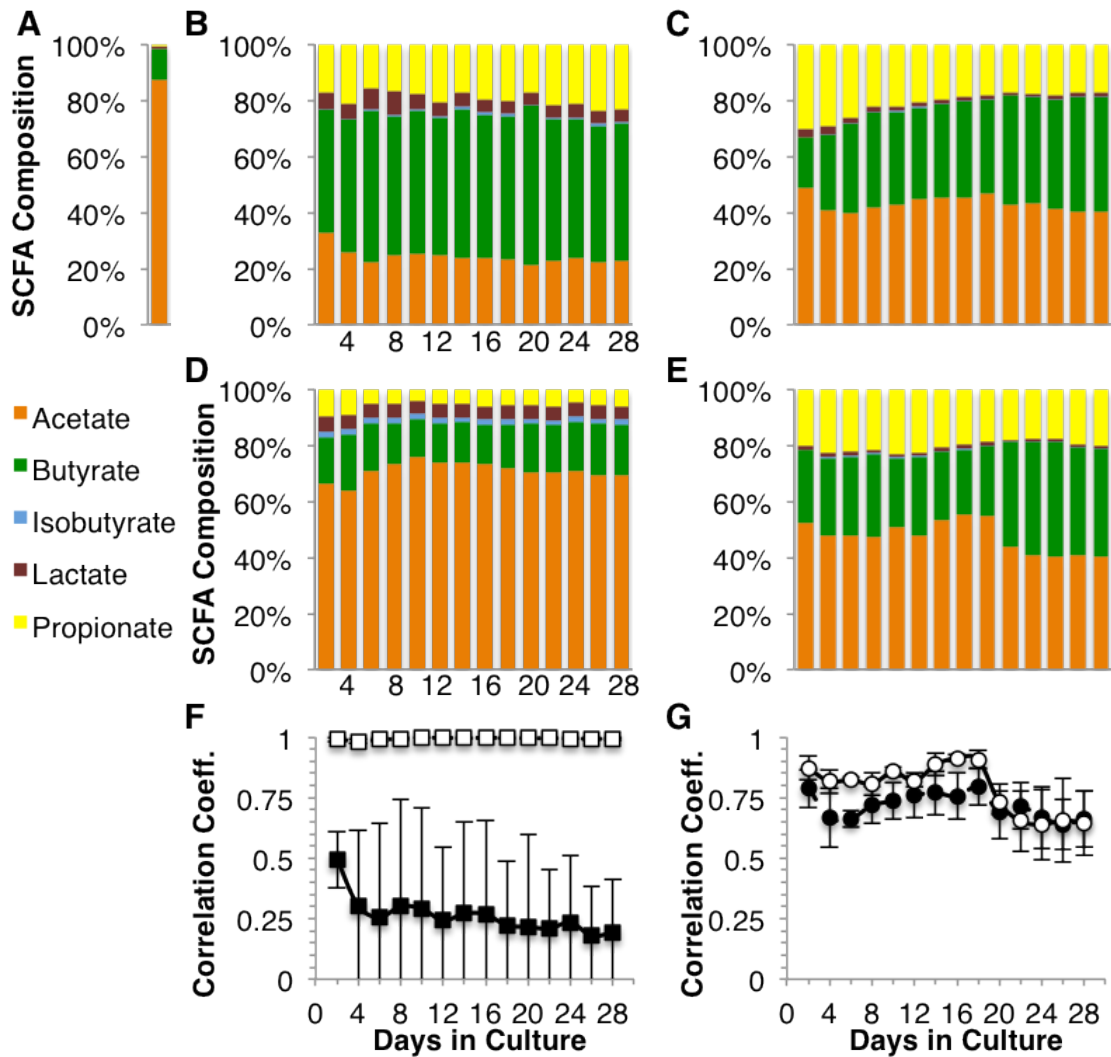


Figure 2.2. Short Chain Fatty Acid analysis of bioreactor cultures. Comparison of the Short Chain Fatty Acid Profiles of the fecal inoculum to bioreactors cultured in BRMW, BRMG, BRMW₁₀, or BRMG₁₀. (A-E) Mean Percent Abundance of SCFA in duplicate samples of original fecal inoculum (A) and from triplicate reactors cultured in BRMW(B), BRMG(C), BRMW₁₀(D), or BRMG₁₀ (E) sampled on every two days. (F-G) We calculated Pearson Product Moment Correlation Coefficients of the SCFA composition (percent abundance of acetate, butyrate, isobutyrate, lactate, and propionate) for each day in culture compared to the initial fecal inoculum. Data presented are the mean of triplicate reactors (error bars=SD of mean). Symbols represent cultures grown in BRMW (■), BRMW₁₀ (□), BRMG (●) or BRMG₁₀ (○).

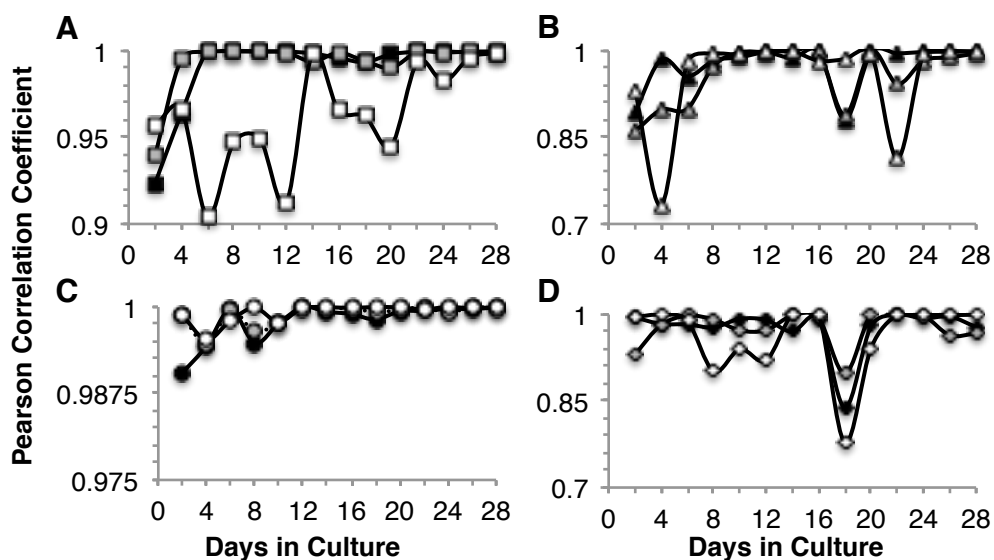


Figure 2.3. Pearson Product Moment Correlation Coefficient of the SCFA composition in bioreactor cultures. For each individual reactor grown in BRMW(A), BRMG(B), BRMW₁₀ (C), or BRMG₁₀(D), we calculated the Pearson Product Moment Correlation Coefficient of the SCFA composition from day X to day X+2 in culture (X=2-28 at two day intervals) and plotted this as a function of day X. Black symbols represent the data from reactor 1, gray symbols represent the data from reactor 2, and white symbols represent the data for reactor 3 in each panel.

The similarity in SCFA profiles that we observed from one replicate reactor to another varied by the type of medium evaluated. Bioreactor communities established in BRMW₁₀ were highly similar to one another, with a mean correlation coefficient from one replicate to another on the same day in culture of >0.99 (Figure S2.2B). In contrast, one of the replicate reactors grown in BRMW diverged drastically from the other two replicates by day 4 in culture (Figure S2.2A). In this case, the SCFA profiles of two reactors were highly similar (mean correlation coefficient across all days sampled >0.99), whereas the third reactor had a SCFA profile dissimilar to either of the reactors (mean correlation coefficient across all days sampled of 0.46 and 0.41). The replicate cultures grown in BRMG and BRMG₁₀

were intermediate between these two extremes, with mean correlation coefficients amongst reactors ranging from 0.82 to 0.98 (Figure S2.2C and S2.2D)

We also compared the similarity of the SCFA profiles of our different bioreactor cultures to the starting fecal slurry. The SCFA profile of our fecal slurry (87% acetate, 11% butyrate, 1% propionate, and 1% lactate, Table 2.1) was similar to previously reported fecal SCFA profiles (35, 41). Cultures grown in BRMW₁₀ had a SCFA profile most similar to the fecal inoculum (Fig. 2.2F), although acetate concentrations were 15% lower than in the fecal inoculum with increased concentrations of the remaining four SCFAs (Table 2.1). Cultures grown in BRMW had a SCFA profile least similar to the fecal inoculum (Fig. 2.2F). Acetate concentrations dropped to 24% of the total SCFA pool with large increases in butyrate (50%) and propionate (20%, Table 2.1). Cultures grown in BRMG and BRMG₁₀ had SCFA profiles more similar to the fecal inoculum than those grown in BRMW, but less similar than cultures grown in BRMW₁₀ (Fig. 2.2F & 2.2G). As expected, concentrations of acetate, butyrate, and propionate were higher in cultures grown in BRMG or BRMG₁₀ (Fig. S2.1), which contain added SCFAs (acetate, 29.6 mM; butyrate, 21.6 mM; propionate, 26.5 mM). However, even after correcting for the calculated levels of SCFAs in the starting media, cultures grown in BRMG and BRMG₁₀ still had reduced acetate concentrations (47% and 55%, respectively, Table 2.1) and higher concentrations of butyrate (41% and 33%, respectively, Table 2.1) than the fecal inoculum.

Table 2.1. SCFA profiles for fecal inoculum and MBRA cultures.

	Acetate	Butyrate	Propionate	Lactate	Isobutyrate
Fecal	87% ±	10% ± 1.5%	1.0% ± 0.4%	1.0 ± 0.0%	ND
Inoculum ¹	1.1%				
BRMW ²	24.1 ± 2.6%	50.7 ± 2.9%	19.9 ± 2.5%	5.3 ± 1.2%	ND
BRMW ₁₀ ²	70.5 ± 2.9%	16.5 ± 1.9%	6.1 ± 1.3%	4.7 ± 0.2%	1.9 ± 0.09%
BRMG ^{2,3}	43.2 ± 2.6%	33.9 ± 6.1%	21 ± 4.5%	1.7 ± 0.6%	0.09 ± 0.1%
BRMG ₁₀ ^{2,3}	47.3 ± 5.5%	30.8 ± 6.6%	20.4 ± 1.9%	1.2 ± 0.2%	0.2 ± 0.2%

¹ Values reported are the mean of duplicate slurry samples for fecal inoculum ± SD

² Values reported are the mean of samples collected every two days for 28 days across triplicate bioreactors ± SD

³ Background concentrations of acetate, butyrate and propionate (29.6 mM, 21.6 mM, and 26.5 mM, respectively) in BRMG and BRMG₁₀ were subtracted prior to determining the mean percent abundance of each SCFA species.

Comparison of MBRA microbial composition and structure demonstrates that communities cultured in BRMW₁₀ are most similar to the fecal inoculum. In order to study how culturing in the bioreactors influenced the structure of the microbial communities, we analyzed 16S rRNA gene diversity of samples collected from triplicate reactors grown in BRMW, BRMG, and BRMW₁₀ at several points during growth as well as from duplicate samples of the initial fecal slurry. We did not include cultures grown in BRMG₁₀ in these analyses because preliminary 16S rRNA gene sequence analyses of BRMG₁₀ communities revealed that the cultures were dissimilar from the fecal inoculum (data not shown).

Overall, culturing in any of the three media resulted in significant decreases in microbial diversity and species richness and an increase in species evenness compared to the fecal inoculum (Fig 2.4A-C). The highest levels of diversity and richness were seen in the communities cultured in BRMW₁₀, whereas the lowest levels of diversity and richness were seen in the communities cultured in BRMG. As might be expected based upon the changes in diversity, richness and evenness, culturing also resulted in changes in overall community structure (Fig. 2.4D-F). We examined the changes in community structure at multiple taxonomic levels (Order, Genus, and operational taxonomic units (OTUs) with sequence dissimilarity $\leq 3\%$ in Fig. 2.4D, 2.4E, and 2.4F, respectively) using the dissimilarity measure described by Yue and Clayton (θ_{YC} (30)), which compares community structures based upon shared community membership and abundance. We found that the communities cultured in BRMG were least similar to the starting fecal inoculum at all taxonomic levels (Fig. 2.4D-F, scaled from 0 to 1, with 1 being least similar). When examined at the Order level, communities cultured in BRMW appeared slightly more similar to the starting fecal inoculum than communities cultured in BRMW₁₀ throughout their time in culture, although these differences were not statistically significant (student's two-tailed t-test, $p > 0.07$ for all time points). As expected, comparing the BRMW and BRMW₁₀ communities at finer taxonomic resolution (Fig. 2.4E and 2.4F) revealed more dissimilarity to the starting fecal inoculum after culture in either medium. Culturing in either medium produced similar levels of change in the community structure relative to the fecal inoculum, with exception of the bioreactor communities in BRMW reactors on day 4, which were much more similar to the

starting fecal inoculum. Similar differences in community structure among the three media were also observed when we compared their 16S *rRNA* gene diversity using shared phylogenetic distance with weighted Unifrac ((32), data not shown).

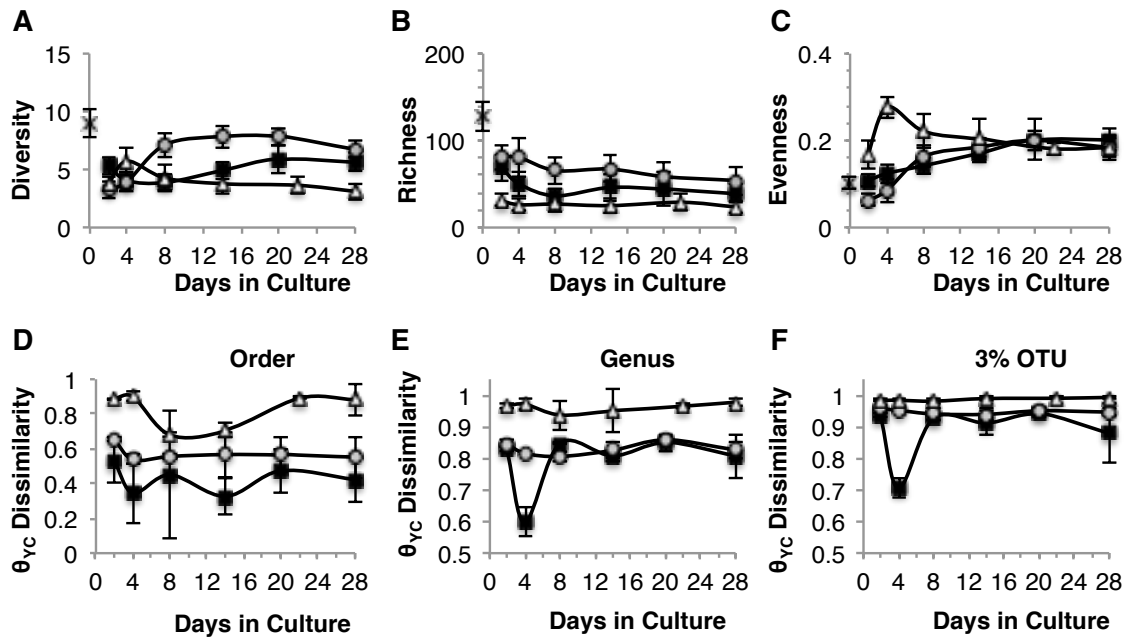


Figure 2.4. Microbial ecology of bioreactors compared to the fecal inoculum.

We compared the composition and structures of microbial communities cultured in BRMW, BRMW₁₀, or BRMG medium to the fecal inoculum by analysis of 16S *rRNA* gene diversity. We partitioned sequences with $\leq 3\%$ sequence dissimilarity into operational taxonomic units (OTUs, A-C, G) as well as examining shared community composition at the Order (E) and Genus (F) levels. Triplicate BRMW or BRMW₁₀ bioreactor communities were analyzed on days 2, 4, 8, 14, 20, and 28 in culture; triplicate BRMG bioreactor communities were analyzed on days 2, 4, 8, 14, 22, and 28. In (A-C), we determined the mean (A) microbial diversity (Inverse Simpson (1/D)), (B) species richness (Chao Richness Estimate), and (C) species evenness (Simpson Evenness) of triplicate bioreactor communities after the indicated times in culture in BRMW (■), BRMW₁₀ (●), and BRMG (△) to the fecal inoculum (×). In (D-F), we compared the differences in the overall community structure (Yue and Clayton θ Dissimilarity Index (θ_{YC}) at the Order (E), Genus (F), and 3% OTU (G) levels between each day in culture in BRMW (■), BRMW₁₀ (●), or BRMG (△) to the fecal inoculum. We plotted the mean of the dissimilarity index for each triplicate set of reactors as a function of the day in culture. Error bars represent the standard deviation of the mean.

Examining how the community composition varied amongst media, we found that each medium supported a microbial community that was distinct in structure from the other media tested. We found that both analysis of similarities (ANOSIM (42), Fig. S2.3) as well as analysis of molecular variance (AMOVA (43)), indicated that the composition and structure of each community was distinct ($P < 0.001$). These observations held true whether we examined shared community structure as measured by common OTUs (Fig. S2.3) or phylogenetic distance (data not shown).

Comparison of class-level differences among reactor communities revealed the extent of reorganization of the microbial community during culture.

Examining the class-level distribution of organisms in the different media after 4 weeks in culture (Day 28), we found that in all three media there was a significant decrease in the relative abundance of *Clostridia* (Fig. 2.5). This decrease in the abundance of *Clostridia* was observed by the second day in culture (Fig S2.4). In cultures grown with BRMW or BRMW₁₀, this decrease in *Clostridia* correlated primarily with increased representation of *Bacteroides* (Fig. 2.5). In two of the three reactors cultured in BRMG, the loss of *Clostridia* correlated with a much higher population of γ -*Proteobacteria* (~50% of all organisms present), whereas in the third reactor there was a bloom of *Bacilli*. Two other classes of Bacteria that significantly expanded in culture were the *Synergistia* and *Fusobacteria*, with the largest expansions observed in reactors cultured with BRMW₁₀ and BRMG.

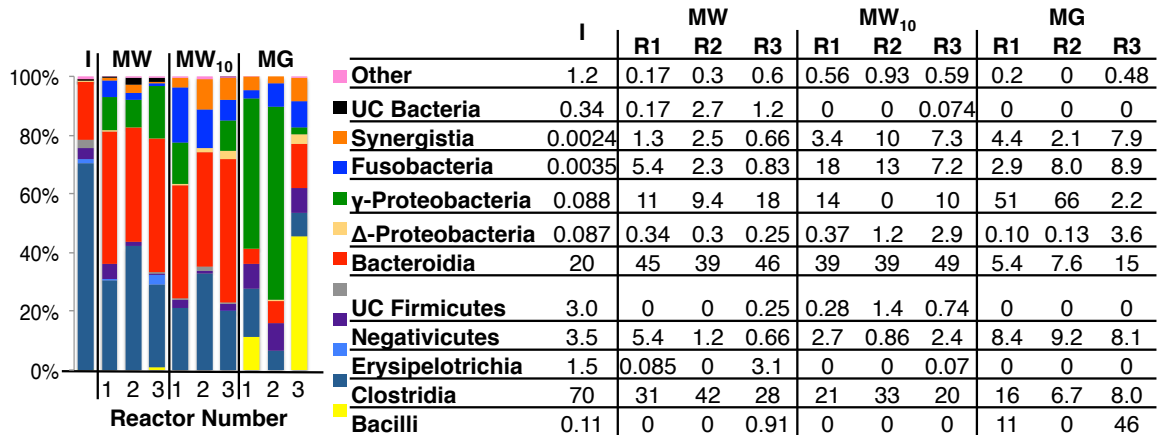


Figure 2.5. Comparison of the class-level distribution of microbes in bioreactors and the fecal inoculum. Comparison of the class-level distribution of microbes on day 28 in culture in BR(MW), BR(MW₁₀), or BR(MG) to the fecal (I) inoculum. The percent abundance of each class of Bacteria in the individual bioreactor samples is shown as is the mean percent abundance of each class in duplicate fecal inoculum samples. Reactor numbers correspond to those given in Figures 3 and 4. UC Bacteria and UC Firmicutes indicate phylotypes that could not be classified with greater than 80% confidence beyond the Domain (Bacteria) and Phylum (Firmicutes) levels by the ribosomal database project classifier release 9. Phylotypes classified as “Other” were present in <1% abundance in any of the samples and include Actinobacteria, Unclassified Bacteroidetes, Lentisphaeria, Methanobacteria, α-Proteobacteria, β-Proteobacteria, Unclassified Proteobacteria, and Verrucomicrobiae.

Examining the microbial community structure in BRMW₁₀ communities at more frequent time intervals revealed how communities diverge from day-to-day and reactor-to-reactor. After examining the SCFA profiles and community composition, it was clear that the cultures grown in BRMG were least similar to the starting fecal inoculum and were not further studied. Because cultures grown in BRMW₁₀ had a SCFA profile that was more similar to the fecal inoculum (Fig. 2.2), showed lower inter-reactor variation in SCFA profiles across replicates (Fig. 2.3, Fig. S2.2), and maintained levels of microbial diversity, species richness, evenness, and

community composition with as much similarity to the fecal inoculum as cultures grown in BRMW (Fig. 2.5), we focused on the microbial communities that were established in these reactors in more detail. We examined changes in microbial community composition in the triplicate reactors grown in this medium every two days for the first twenty days in culture in order to determine the extent of intra- and inter-reactor variation that occurred over time in culture.

Two overall trends were apparent from these analyses: 1) the communities present in each individual reactor changed over time in culture with larger changes in community structure at earlier times in culture (Fig. 2.6), and 2) the structures of the microbial communities in replicate reactors diverged from each other over time (Fig. 2.7). We determined the average θ_{YC} dissimilarity of each day in culture from all other days in culture in each replicate reactor (a similar measure of community stability based upon average Unifrac distances was described by Werner (44)). Upon plotting these dissimilarities as a function of the day in culture, we found that the communities present early during cultivation (Days 2-6) were less similar to the overall communities present later in culture (Days 8-20, Fig. 2.6A). The statistical significance of the differences was supported by both ANOSIM and AMOVA (Fig. 2.6B).

We also examined the variation in community structure between replicate reactors over time in culture. We found that the variation between replicate reactors was smallest during the first week in culture and increased between the replicate reactors in subsequent weeks (Fig. 2.7A). This pattern is most obvious when comparing reactors 1 and 3, where both ANOSIM and AMOVA revealed

statistically significant differences in community structure during the last two weeks in culture that were absent during the first week of culture (Fig. 2.7B). In contrast, the community present in reactor 2 had statistically significant differences in structure compared to reactors 1 and 3 throughout its time in culture (Fig. 2.7A and 2.7B), although the differences in community structure between these reactors early in culture indicated by the ANOSIM values (R=0.78 between reactors 1 & 2 and reactors 2 & 3), were not statistically significant.

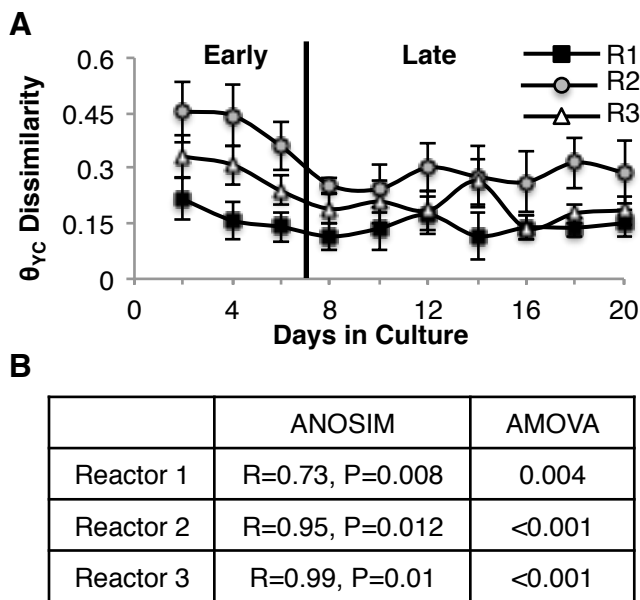


Figure 2.6. Analysis of changes in community structure across time in replicate reactors. We examined the changes that occurred in the structure of microbial communities based upon changes in shared OTUs ($\leq 3\%$ sequence dissimilarity) every two days from Day 2 to Day 20 during culturing in triplicate reactors grown in BRMW₁₀. In (A), we compared the mean distance from each day in culture from all other days in culture in Reactor 1 (■), Reactor 2 (●), or Reactor 3 (△) using the θ_{YC} (A) Dissimilarity Indices. Error bars reflect the standard errors of the mean. In (B), we calculated ANOSIM and AMOVA between early (Days 2-6) and late (Days 8-20) days in culture for each individual reactor based upon θ_{YC} Dissimilarity Indices.

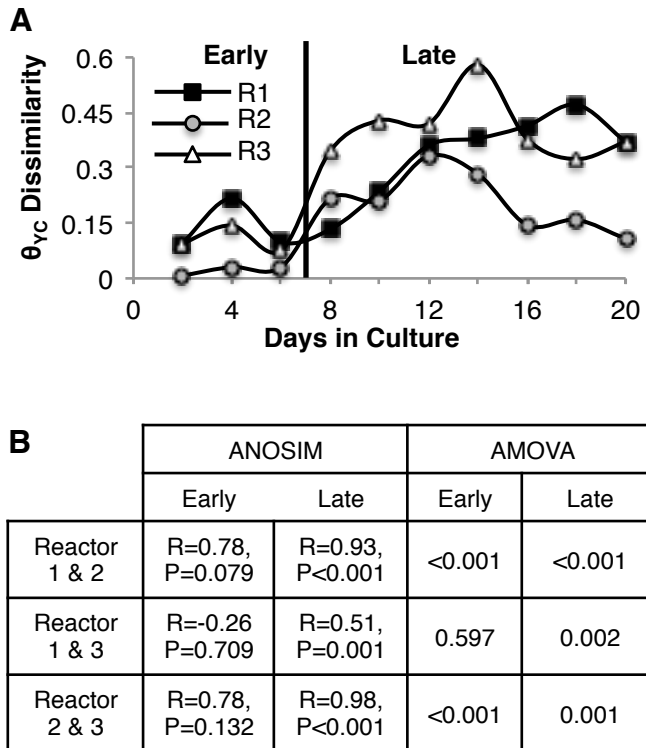


Figure 2.7. Pairwise analyses of changes in community structure across time between reactors. We compared the changes that occurred in the structure of microbial communities between triplicate reactors grown in BRMW₁₀ based upon changes in shared OTUs ($\leq 3\%$ sequence dissimilarity) every two days from Day 2 to Day 20. In (A), we plotted the θ_{VC} (C) Dissimilarity Indices between Reactors 1 and 2 (■), Reactors 1 and 3 (●), or Reactors 2 and 3 (△) on each day as a function of that day in culture. In (B), we calculated ANOSIM and AMOVA between reactors during early (Days 2-6) and late (Days 8-20) days in culture based upon θ_{VC} (C) or Jaccard (D) Dissimilarity Indices.

Discussion

We developed relatively simple, single-stage bioreactors that allow for higher throughput *in vitro* studies of fecal microbial communities. We tested four different media (BRMW, BRMW₁₀, BRMG, and BRMG₁₀) and identified a medium, BRMW₁₀, that best supported cultivation of microbially-diverse, functionally-stable human fecal communities. BRMW₁₀ communities produced the short chain fatty acids acetate, butyrate, isobutyrate, lactate, and propionate in highly stable proportions throughout their time in culture and at levels that were most similar to the starting human fecal inoculum. Further, 16S *rRNA* gene sequence analysis revealed that cultures grown in BRMW₁₀ were most similar to the fecal inoculum, having the highest levels of microbial diversity and richness of the media tested, as well as overall community composition and structure that was as or more similar to the fecal inoculum than the other media tested.

From our comparisons of microbial community structure between the initial fecal inoculum and the communities cultured in the BRMW, BRMW₁₀ and BRMG (Fig. 2.4), it was clear that the communities we cultivated in all three media were significantly different from the initial fecal inoculum, with decreases in microbial diversity and richness and increases in evenness, and that these changes occurred by day two in culture. Many factors might have contributed to our inability to cultivate organisms from the original fecal sample. One of these factors is likely the absence of specific nutrients in our media that are required for growth of these fecal organisms. Because our assessment of the composition of the initial fecal inoculum is based upon 16S *rRNA* gene analysis, we also do not know what fraction of the

community we sequenced represents non-viable cells that could not be cultivated under any condition. Although our protocol for sample collection and processing was intended to minimize damage to sensitive anaerobic bacteria, it is possible that immediate cultivation from freshly voided fecal samples could produce better results. In addition, since our initial fecal inoculum was pooled from twelve distinct fecal donors, each with a different microbial community (data not shown), it is possible that competitive forces that shaped each individual microbiota would make it unlikely that all of these microbes would coexist in a single community under *in vitro* or *in vivo* conditions. Comparing the impact of cultivation on inocula from an individual donor to pooled communities could provide some insight into this question. Finally, because our MBRA were designed as continuously-stirred tank bioreactors that are operated anaerobically, they provide fewer niches than would be available within the host. The increased evenness of our communities in culture could indicate that there has been a reduction in available niches that promote growth in different proportions. It is possible that coexistence of this community requires further niches to be present, such as those that could be provided by including beads coated with mucin or glycopeptides typically found in the distal colon.

Based upon in-depth analysis of the communities cultivated in BRMW₁₀, it was clear that adaptation to growth in culture caused the biggest change in the structure of the microbial community, with the largest changes observed between the initial fecal inoculum and Day 2 in culture (Fig. 2.4). However, it was also evident that there was continuous change in the community composition and

structure throughout cultivation, with the largest changes observed during the first week in culture (Fig. 2.6). Further, these changes appeared to follow an independent path in each replicate reactor, resulting in communities in each reactor at the end of cultivation that were more dissimilar than at the beginning of cultivation (Fig. 2.6, 2.7). In spite of these changes in community composition, SCFA production remained highly stable throughout the time in culture, indicating that in these communities, functional stability can be obtained in the presence of ongoing changes in community structure at the species-level.

Other significant changes that were apparent in the BMRW₁₀ reactor communities relative to the fecal inoculum were the increases in the abundance of γ -*Proteobacteria*, *Fusobacteria* and *Synergistetes* (Fig. 2.5). The γ -*Proteobacteria* detected were primarily classified with $\geq 80\%$ confidence as members of the *Enterobacteriaceae* family. The *Enterobacteriaceae* are facultative anaerobes that have a large number of readily cultivable representatives (e.g., *Escherichia*, *Salmonella*, *Shigella*). It is unclear what niche they may be occupying in these cultures that allow for their expansion. *In vivo*, high levels of *Enterobacteriaceae* correlate with inflammation, colitis, and colorectal cancer (e.g., (45)). Similarly, we cannot predict what niche *Fusobacteria* may be filling within the reactor communities, but their abundance has also been correlated with colorectal cancer *in vivo*, although it is unclear whether these organisms may play a causative role or be a secondary invader (46, 47). All of the *Synergistetes* isolates that were identified classified as members of the genus *Cloacibacillus*. *C. evryensis*, a cultured representative of the genus *Cloacibacillus* was isolated from an anaerobic sludge

digestor of a wastewater treatment plant and characterized by its ability to ferment amino acids to acetate, butyrate, H₂ and CO₂ (48). Subsequently, *Synergistetes*, including organisms classified as *Cloacibacillus*, have been found as naturally occurring members of the human microflora, but have also been implicated as opportunistic pathogens, being cultured from infections of the peritoneal fluid, a sacral pressure ulcer, and a blood culture ((49), and references therein).

The immediate stability that we observed in the SCFA profiles (between the first two time points tested, Day 2 and Day 4) in the MBRAs differs from other studies, in which functional stability was not reached until two to three weeks after inoculation (23, 40). We suspect that this difference may be due to the fact that there are initially large changes seen as the inoculum acclimates to growth in culture (differences between the inoculum and day 2 in culture) and that once established, the simplistic continuous-flow setup of the reactors causes less perturbation to the functional activity of the communities.

Comparison of community ecology in BRMW₁₀ reactors to previously published models reveals similar trends among the *in vitro* models. It is somewhat difficult to compare the changes observed between the communities cultured in BRMW₁₀ and the fecal inoculum with those previously reported for other gut models. In the three-stage compound continuous culture system developed by Macfarlane et al. (1998), community composition is assessed by plating on selective media, which does not resolve differences in community structure at the genus and species level. Both Van den Abeele (2010) and Rajilic-Stojanovic (2010) used a

phylogenetic microarray (HITChip) to compare the composition of their reactors (SHIME and TIM-2, respectively) to their fecal inoculum. HITChip has a much finer phylogenetic resolution than selective plating, but still produces signals at a variety of phylogenetic distances (60% of signals at 98% identity phylotype level, 29% of signals at genus-level identity, and 9% of signals at order-level identity (50)).

Van den Abeele reported the similarity in composition between their twin SHIME reactors at the Phylum and Group levels (23). They found differences at both the Phylum and Group levels after 19 and 26 days in culture, with a ~1.5-fold increase in *Bacteroidetes* and an ~3-fold decrease in *Firmicutes*. Similarly, we observed a ~2-fold increase in *Bacteroidetes* and a ~2-3-fold decrease in *Firmicutes* on Day 28 in culture for BRMW₁₀ reactors compared to the fecal inoculum (Fig. 2.5). Rajilic-Stojanovic (2010) reported the overall similarity of their fecal inoculum to culturing in the TIM-2 model for up to 72 hours and found that the mean similarity was 50% based upon Pearson Product Moment Correlation Coefficients of their HITChip profiles of cultured populations and the fecal inoculum. When we calculated the Pearson Product Moment Correlation Coefficient for our data at different taxonomic levels, we found that it increased at increasing taxonomic levels (mean $r^2 = 29.7\%$ at the Genus-level; mean $r^2 = 31.0\%$ at the Family-level; mean $r^2 = 66\%$ at the Order-level). Rajilic-Stojanovic also observed significant increases in *Bacteroidetes* in culture, whereas the differences amongst *Firmicutes* were more obvious at the Class-level, with increases in *Bacilli* and decreases in *Clostridia*. We did not observe significant increases in *Bacilli* in reactors cultured in BRMW₁₀. These differences may be due to differences in media or inoculum preparation or

due to the operation of our reactors in an anaerobic chamber as opposed to maintaining anaerobicity through streaming of O₂-free gas. With our reactor setup, we found that streaming of O₂-free gas was not sufficient to maintain a strict anaerobic environment due to the multiple points at which O₂ could diffuse into the system (data not shown).

Conclusions. Although the MBRA lack the more complex interactions that are possible through *in vivo* models (e.g., lack of immune interaction, absorption/excretion of water and SCFA between the host and microbiota), they represent an excellent opportunity to study microbial interactions in a more structured, high-throughput environment. When MBRA were operated with BRMW₁₀ medium, we found that they developed dynamic human fecal microbial communities that produced SCFA profiles very similar to the starting fecal inoculum. Thus, the BRMW₁₀ medium and MBRA represent an exciting avenue for future studies of human fecal microbiota community dynamics.

Acknowledgements

The authors would like to acknowledge Byron Smith, Alec Bonifer, and Lilian Jensen for technical assistance, as well as Terrence Marsh and Thomas Schmidt for constructive comments on the manuscript. This research was funded as part of the Michigan State University Enteric Research Investigation Network award from that National Institutes of Health to Robert Britton (Project Number 5U19AI090872-02).

APPENDIX

Appendix

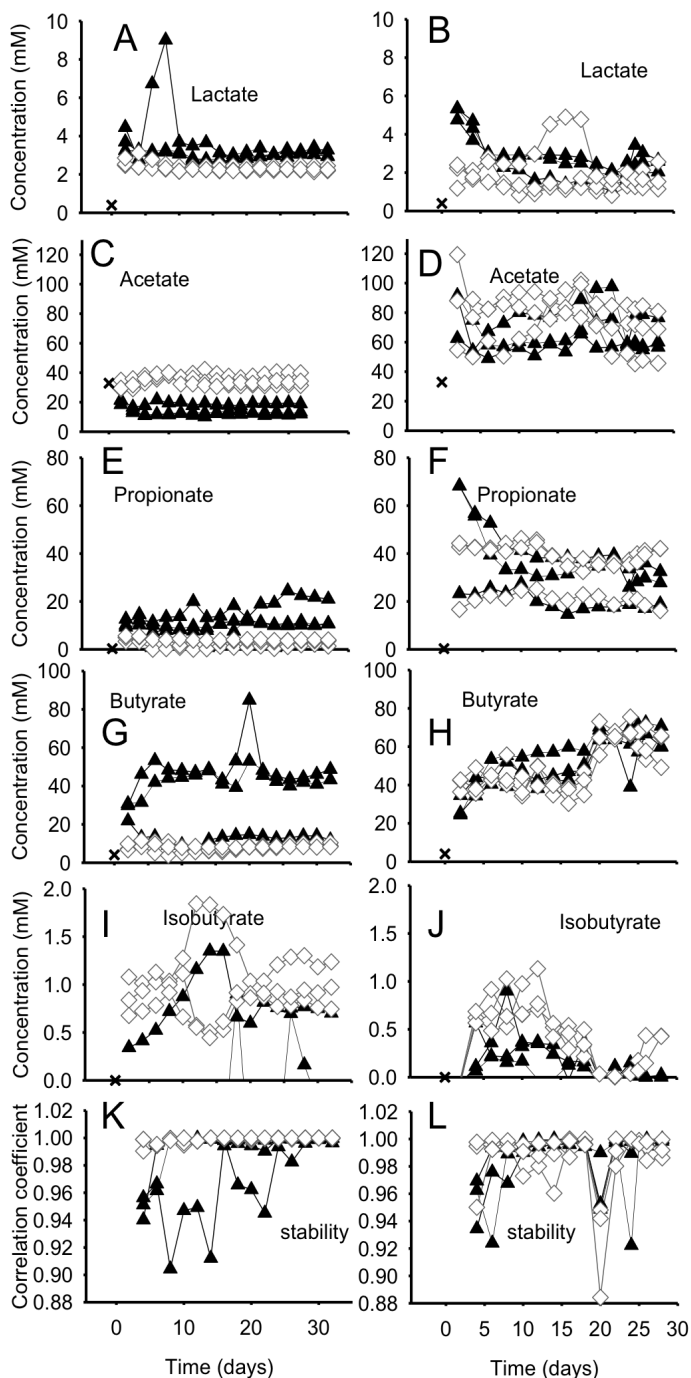


Figure S2.1. SCFA concentrations in bioreactor cultures. SCFA concentrations measured in reactors cultured with BRMW (\blacktriangle)/ BRMW₁₀ (\diamond ; A, C, E, G) or BRMG (\blacktriangle)/BRMG₁₀ (\diamond ; B, D, F, H) media. Similarity indices based on Pearson product-moment correlation coefficients generated between day X and day X-2 (K, L) for samples taken at 2, 4, 6, 8, 10, 12, 14, 16, 18, 20, 22, 24, 26, and 28 days.

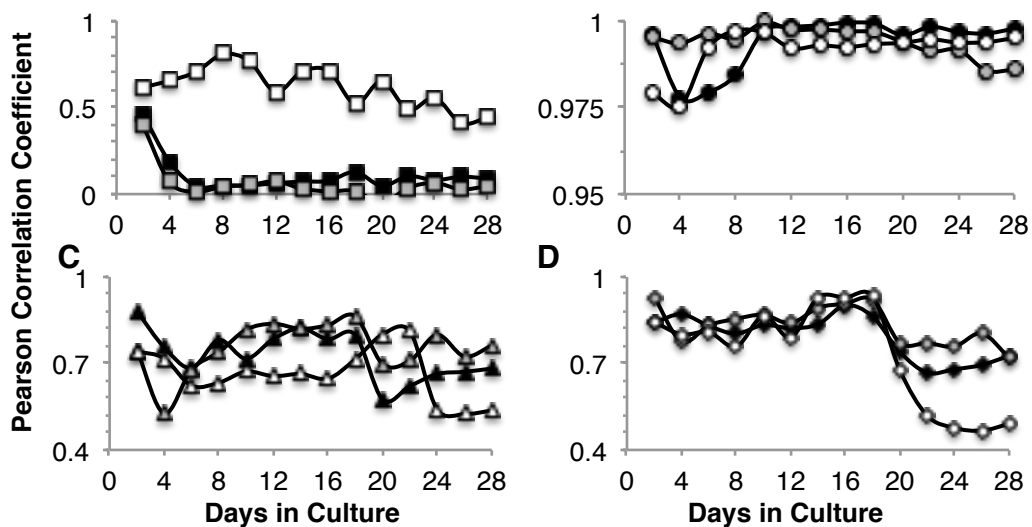
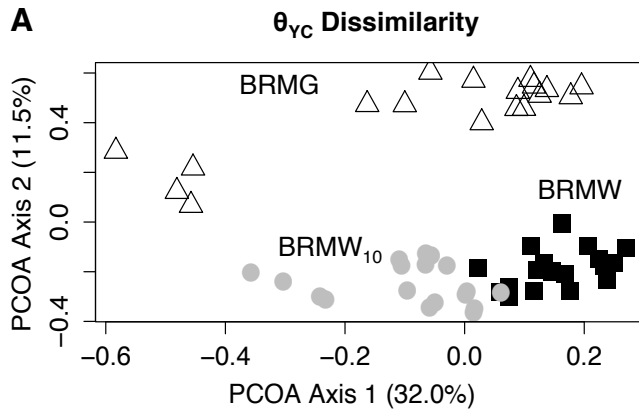


Figure S2.2. Pearson Product Moment Correlation Coefficient of the SCFA profiles. We calculated the Pearson Product Moment Correlation Coefficient of the SCFA profiles (percent abundance of acetate, butyrate, isobutyrate, lactate, and propionate) on each day across the three reactors grown in in BRMW(A), BRMW₁₀(B), BRMG(C), or BRMG₁₀(D) and plotted this as a function of day in culture. Black symbols represent the comparison between reactors 1 and 2, gray symbols represent the comparison between reactors 2 and 3, and white symbols represent the comparison between reactors 1 and 3. Reactor numbering is the same as in Figure 2.3.



B

	BRMW	BRMW ₁₀
BRMW ₁₀	R = 0.34 P < 0.001	
BRMG	R = 0.76 P < 0.001	R = 0.79 P < 0.001

Figure S2.3. Shared community structure of bioreactor cultures. Analysis of shared community structure of cultures grown in BRMW, BRMW₁₀, and BRMG evaluated using OTUs with $\leq 0.03\%$ sequence dissimilarity in the 16S *rRNA* gene. (A) Principle Coordinates Analysis of the θ_{YC} Dissimilarity measures among triplicate bioreactor communities cultured in BRMW (■), BRMW₁₀ (●), or BRMG (△) and sampled on Day 2, 4, 8, 14, 20/22, and 28 (Day 20 for BRMW and BRMW₁₀; Day 22 for BRMG reactors). (B) ANOSIM θ_{YC} Dissimilarity (D) of communities plotted in A.

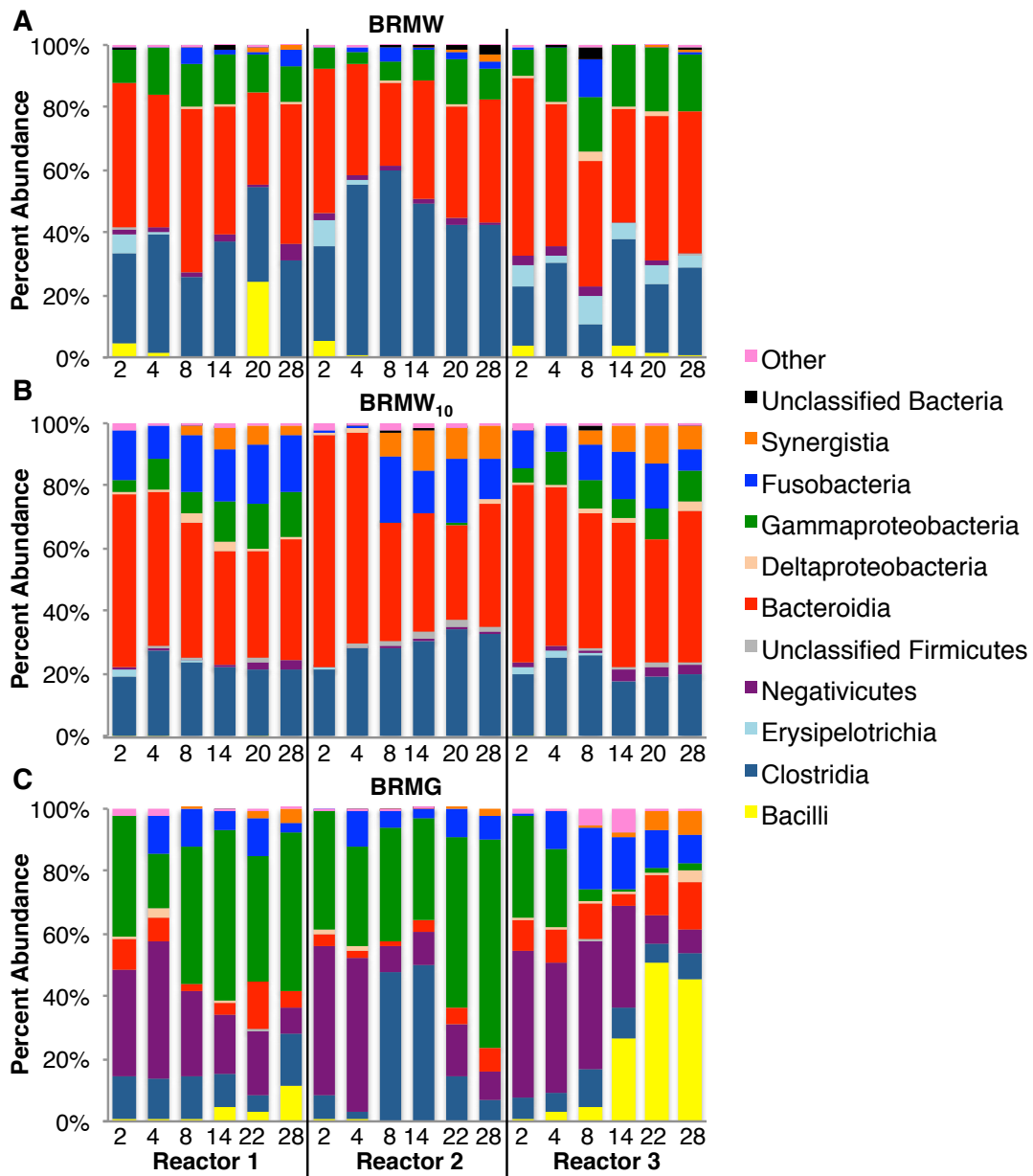


Figure S2.4. Class-level community analysis of replicate reactors in different media. We compared the class-level distribution of community members on Day 2, 4, 8, 14, 20 or 22 (BRMW/BRMW₁₀ and BRMG, respectively), and 28 in culture across triplicate reactors. The percent abundance of each class of Bacteria in the individual bioreactor samples is shown. Reactor numbers correspond to those given in Figures 2.3, 2.4, and 2.6. UC Bacteria and UC Firmicutes indicate phlotypes that could not be classified with greater than 80% confidence beyond the Domain (Bacteria) and Phylum (Firmicutes) levels by the ribosomal database project

Figure S2.4 (cont'd)
classifier release 9. Phylotypes classified as “Other” were present in <1% abundance in any of the samples and include Actinobacteria, Unclassified Bacteroidetes, Lentisphaeria, Methanobacteria, α -Proteobacteria, β -Proteobacteria, Unclassified Proteobacteria, and Verrucomicrobiae.

REFERENCES

REFERENCES

1. **Blumberg R, Powrie F.** 2012. Microbiota, Disease, and Back to Health: A Metastable Journey. *Science Translational Medicine* **4**:137rv7–137rv7.
2. **Hooper LV, Littman DR, Macpherson AJ.** 2012. Interactions Between the Microbiota and the Immune System. *Science* **336**:1268–1273.
3. **Nicholson JK, Holmes E, Kinross J, Burcelin R, Gibson G, Jia W, Pettersson S.** 2012. Host-Gut Microbiota Metabolic Interactions. *Science* **336**:1262–1267.
4. **Wu GD, Chen J, Hoffmann C, Bittinger K, Chen YY, Keilbaugh SA, Bewtra M, Knights D, Walters WA, Knight R, Sinha R, Gilroy E, Gupta K, Baldassano R, Nessel L, Li H, Bushman FD, Lewis JD.** 2011. Linking Long-Term Dietary Patterns with Gut Microbial Enterotypes. *Science* **334**:105–108.
5. **Sokol H, Pigneur B, Watterlot L, Lakhdari O, Bermúdez-Humarán LG, Gratadoux J-J, Blugeon S, Bridonneau C, Furet J-P, Corthier G, Grangette C, Vasquez N, Pochart P, Trugnan G, Thomas G, Blottiere HM, Doré J, Marteau P, Seksik P, Langella P.** 2008. Faecalibacterium prausnitzii is an anti-inflammatory commensal bacterium identified by gut microbiota analysis of Crohn disease patients. *Proc. Natl. Acad. Sci. U.S.A.* **105**:16731–16736.
6. **Chang JY, Antonopoulos DA, Kalra A, Tonelli A, Khalife WT, Schmidt TM, Young VB.** 2008. Decreased Diversity of the Fecal Microbiome in Recurrent Clostridium difficile–Associated Diarrhea. *J Infect Dis* **197**:435–438.
7. **Wang Z, Klipfell E, Bennett BJ, Koeth R, Levison BS, DuGar B, Feldstein AE, Britt EB, Fu X, Chung Y-M, Wu Y, Schauer P, Smith JD, Allayee H, Tang WHW, DiDonato JA, Lusis AJ, Hazen SL.** 2011. Gut flora metabolism of phosphatidylcholine promotes cardiovascular disease. *Nature* **472**:57–63.
8. **Goodman AL, Kallstrom G, Faith JJ, Reyes A, Moore A, Dantas G, Gordon JL.** 2011. Extensive personal human gut microbiota culture collections characterized and manipulated in gnotobiotic mice. *Proceedings of the National Academy of Sciences* **108**:6252–6257.
9. **Bäckhed F, Ding H, Wang T, Hooper LV, Koh GY, Nagy A, Semenkovich CF, Gordon JL.** 2004. The gut microbiota as an environmental factor that regulates fat storage. *Proc. Natl. Acad. Sci. U.S.A.* **101**:15718–15723.
10. **Gootenberg DB, Turnbaugh PJ.** 2011. Companion animals symposium: humanized animal models of the microbiome. *J. Anim. Sci.* **89**:1531–1537.
11. **Allison C, McFarlan C, Macfarlane GT.** 1989. Studies on mixed populations

- of human intestinal bacteria grown in single-stage and multistage continuous culture systems. *Appl Microbiol* **55**:672–678.
12. **Minekus M, Smeets-Peeters M, Bernalier A, Marol-Bonnin S, Havenaar R, Marteau P, Alric M, Fonty G, Huis in't Veld JH.** 1999. A computer-controlled system to simulate conditions of the large intestine with peristaltic mixing, water absorption and absorption of fermentation products. *Appl Microbiol Biotechnol* **53**:108–114.
 13. **Freeman J.** 2003. Effects of cefotaxime and desacetylcefotaxime upon *Clostridium difficile* proliferation and toxin production in a triple-stage chemostat model of the human gut. *Journal of Antimicrobial Chemotherapy* **52**:96–102.
 14. **Molly K, Vande Woestyne M, Verstraete W.** 1993. Development of a 5-step multi-chamber reactor as a simulation of the human intestinal microbial ecosystem. *Appl Microbiol Biotechnol* **39**:254–258.
 15. **Honda H, Gibson GR, Farmer S, Keller D, McCartney AL.** 2011. Use of a continuous culture fermentation system to investigate the effect of GanedenBC30 (*Bacillus coagulans* GBI-30, 6086) supplementation on pathogen survival in the human gut microbiota. *Anaerobe* **17**:36–42.
 16. **Macfarlane G, Macfarlane S, Gibson G.** 1998. Validation of a Three-Stage Compound Continuous Culture System for Investigating the Effect of Retention Time on the Ecology and Metabolism of Bacteria in the Human Colon. *Microbial Ecology* **35**:180–187.
 17. **WANG X, Gibson GR.** 1993. Effects of the in vitro fermentation of oligofructose and inulin by bacteria growing in the human large intestine. *J. Appl. Bacteriol.* **75**:373–380.
 18. **Kim B-S, Kim JN, Cerniglia CE.** 2011. In Vitro Culture Conditions for Maintaining a Complex Population of Human Gastrointestinal Tract Microbiota. *J. Biomed. Biotechnol.* **2011**:1–10.
 19. **Gibson GR, Fuller R.** 2000. Aspects of in vitro and in vivo research approaches directed toward identifying probiotics and prebiotics for human use. *The Journal of nutrition* **130**:391S–395S.
 20. **Macfarlane GT, Macfarlane S.** 2007. Models for intestinal fermentation: association between food components, delivery systems, bioavailability and functional interactions in the gut. *Current Opinion in Biotechnology* **18**:156–162.
 21. **Sousa T, Paterson R, Moore V, Carlsson A, Abrahamsson B, Basit AW.** 2008. The gastrointestinal microbiota as a site for the biotransformation of

- drugs. *International Journal of Pharmaceutics* **363**:1–25.
22. **Molly K, Woestyne MV, Smet ID, Verstraete W.** 1994. Validation of the simulator of the human intestinal microbial ecosystem (SHIME) reactor using microorganism-associated activities. *Microb Ecol Health Dis* **7**:191–200.
 23. **Van den Abbeele P, Grootaert C, Marzorati M, Possemiers S, Verstraete W, Gerard P, Rabot S, Bruneau A, Aidy El S, Derrien M, Zoetendal E, Kleerebezem M, Smidt H, Van de Wiele T.** 2010. Microbial Community Development in a Dynamic Gut Model Is Reproducible, Colon Region Specific, and Selective for Bacteroidetes and Clostridium Cluster IX. *Applied and Environmental Microbiology* **76**:5237–5246.
 24. **Rajilic-Stojanovic M, Maathuis A, Heilig HGJ, Venema K, de Vos WM, Smidt H.** 2010. Evaluating the microbial diversity of an in vitro model of the human large intestine by phylogenetic microarray analysis. *Microbiology* **156**:3270–3281.
 25. **Consortium THMP.** 2012. Structure, function and diversity of the healthy human microbiome. *Nature* **486**:207–214.
 26. **Schloss PD.** 2009. A High-Throughput DNA Sequence Aligner for Microbial Ecology Studies. *PLoS ONE* **4**:e8230.
 27. **Schloss PD, Gevers D, Westcott SL.** 2011. Reducing the Effects of PCR Amplification and Sequencing Artifacts on 16S rRNA-Based Studies. *PLoS ONE* **6**:e27310.
 28. **Edgar RC, Haas BJ, Clemente JC, Quince C, Knight R.** 2011. UCHIME improves sensitivity and speed of chimera detection. *Bioinformatics* **27**:2194–2200.
 29. **Schloss PD, Westcott SL.** 2011. Assessing and improving methods used in operational taxonomic unit-based approaches for 16S rRNA gene sequence analysis. *Applied and Environmental Microbiology* **77**:3219–3226.
 30. **Yue J, Clayton M.** 2005. A Similarity Measure Based on Species Proportions. *Communications in Statistics: Theory and Methods* **34**:2123–2131.
 31. **Evans J, Sheneman L, Foster J.** 2006. Relaxed Neighbor Joining: A Fast Distance-Based Phylogenetic Tree Construction Method. *Journal of Molecular Evolution* **62**:785–792.
 32. **Lozupone CA, Hamady M, Kelley ST, Knight R.** 2007. Quantitative and qualitative beta diversity measures lead to different insights into factors that structure microbial communities. *Applied and Environmental Microbiology* **73**:1576–1585.

33. **Stoner DL, Watson SM, Stedtfeld RD, Meakin P, Griffel LK, Tyler TL, Pegram LM, Barnes JM, Deason VA.** 2005. Application of Stereolithographic Custom Models for Studying the Impact of Biofilms and Mineral Precipitation on Fluid Flow. *Applied and Environmental Microbiology* **71**:8721–8728.
34. 2009. Validation of a Three-Stage Compound Continuous Culture System for Investigating the Effect of Retention Time on the Ecology and Metabolism of Bacteria in the Human Colon 1–8.
35. **Schwartz A, Taras D, Schäfer K, Beijer S, Bos NA, Donus C, Hardt PD.** 2009. Microbiota and SCFA in Lean and Overweight Healthy Subjects. *Obesity* **18**:190–195.
36. **Flint HJ, Bayer EA, Rincon MT, Lamed R, White BA.** 2008. Polysaccharide utilization by gut bacteria: potential for new insights from genomic analysis. *Nat Rev Micro* **6**:121–131.
37. **Duncan SH, Belenguer A, Holtrop G, Johnstone AM, Flint HJ, Lobley GE.** 2007. Reduced Dietary Intake of Carbohydrates by Obese Subjects Results in Decreased Concentrations of Butyrate and Butyrate-Producing Bacteria in Feces. *Applied and Environmental Microbiology* **73**:1073–1078.
38. **Ahring BK, Sandberg M, Angelidaki I.** 1995. Volatile fatty acids as indicators of process imbalance in anaerobic digestors. *Appl Microbiol Biotechnol* **43**:559–565.
39. **Ito Y, Moriwaki H, Muto Y, Kato N, Watanabe K, Ueno K.** 1997. Effect of lactulose on short-chain fatty acids and lactate production and on the growth of faecal flora, with special reference to *Clostridium difficile*. *Journal of Medical Microbiology* **46**:80–84.
40. **Possemiers S, Verthé K, Uyttendaele S, Verstraete W.** PCR-DGGE-based quantification of stability of the microbial community in a simulator of the human intestinal microbial ecosystem. *FEMS Microbiology Ecology* **49**:495–507.
41. **Kotani A, Miyaguchi Y, Kohama M, Ohtsuka T, Shiratori T, Kusu F.** 2009. Determination of short-chain fatty acids in rat and human feces by high-performance liquid chromatography with electrochemical detection. *Analytical sciences : the international journal of the Japan Society for Analytical Chemistry* **25**:1007–1011.
42. **CLARKE KR.** 1993. Non-parametric multivariate analyses of changes in community structure **18**:117–143.
43. **Excoffier L, Smouse PE, Quattro JM.** 1992. Analysis of molecular variance inferred from metric distances among DNA haplotypes: application to human

mitochondrial DNA restriction data. *Genetics* **131**:479–491.

44. **Werner JJ, Knights D, Garcia ML, Scalfone NB, Smith S, Yarasheski K, Cummings TA, Beers AR, Knight R, Angenent LT.** 2011. Bacterial community structures are unique and resilient in full-scale bioenergy systems. *Proceedings of the National Academy of Sciences* **108**:4158–4163.
45. **Arthur JC, Perez-Chanona E, Mühlbauer M, Tomkovich S, Uronis JM, Fan T-J, Campbell BJ, Abujamel T, Dogan B, Rogers AB, Rhodes JM, Stintzi A, Simpson KW, Hansen JJ, Keku TO, Fodor AA, Jobin C.** 2012. Intestinal inflammation targets cancer-inducing activity of the microbiota. *Science* **338**:120–123.
46. **Kostic AD, Gevers D, Pedamallu CS, Michaud M, Duke F, Earl AM, Ojesina AI, Jung J, Bass AJ, Tabernero J, Baselga J, Liu C, Shivdasani RA, Ogino S, Birren BW, Huttenhower C, Garrett WS, Meyerson M.** 2012. Genomic analysis identifies association of *Fusobacterium* with colorectal carcinoma. *Genome Research* **22**:292–298.
47. **Castellarin M, Warren RL, Freeman JD, Dreolini L, Krzywinski M, Strauss J, Barnes R, Watson P, Allen-Vercoe E, Moore RA, Holt RA.** 2012. *Fusobacterium nucleatum* infection is prevalent in human colorectal carcinoma. *Genome Research* **22**:299–306.
48. **Ganesan A, Chaussonnerie S, Tarrade A, Dauga C, Bouchez T, Pelletier E, Le Paslier D, Sghir A.** 2008. *Cloacibacillus evryensis* gen. nov., sp. nov., a novel asaccharolytic, mesophilic, amino-acid-degrading bacterium within the phylum “Synergistetes,” isolated from an anaerobic sludge digester. *Int. J. Syst. Evol. Microbiol.* **58**:2003–2012.
49. **Marchandin H, Damay A, RoudiEre L, Teyssier C, Zorogniotti I, Dechaud H, Jean-Pierre H, Jumas-Bilak E.** 2010. Phylogeny, diversity and host specialization in the phylum Synergistetes with emphasis on strains and clones of human origin. *Research in Microbiology* **161**:91–100.
50. **Rajilić-Stojanović M, Heilig HGJ, Molenaar D, Kajander K, Surakka A, Smidt H, de Vos WM.** 2009. Development and application of the human intestinal tract chip, a phylogenetic microarray: analysis of universally conserved phlotypes in the abundant microbiota of young and elderly adults. *Environ Microbiol* **11**:1736–1751.

CHAPTER 3

Epidemic *Clostridium difficile* strains demonstrate increased competitive fitness over non-epidemic isolates

These results have been published in the article: Robinson*, C.D, J. M. Auchtung*, J. Collins, and R. A. Britton. Epidemic *Clostridium difficile* strains demonstrate increased competitive fitness over non-epidemic isolates. *Infection and Immunity*. Published ahead of print April 14, 2014.

*Co-first authors

Copyright © American Society for Microbiology, *Infection and Immunity*, 82:7, 2014, 2815-2825, DOI: 10.1128/IAI.01524-14

Development of the *in vitro* *C. difficile* infection model was an equal collaboration with Jennifer M. Auchtung. Jennifer Auchtung conducted the community analysis and microbial ecology of the bioreactors. James Collins developed the humanized mouse infection model and facilitated the mouse competition experiments.

Abstract

Clostridium difficile infection (CDI) is the most common cause of severe cases of antibiotic associated diarrhea (AAD) and is a significant health burden. Recent increases in the rate of CDI have paralleled the emergence of a specific phylogenetic clade of *C. difficile* strains (ribotype 027, North American Pulsed-Field Electrophoresis (NAP) 1, Restriction Endonuclease Analysis (REA) Group BI). Initial reports indicated that ribotype 027 strains were associated with increased morbidity and mortality and may be hypervirulent. Although subsequent work has cast some doubt as to whether ribotype 027 strains are hypervirulent, these strains are considered epidemic isolates that have caused severe outbreaks across the globe. We hypothesized one factor that could lead to the increased prevalence of ribotype 027 strains would be if these strains had increased competitive fitness compared to strains of other ribotypes. We developed a moderate throughput *in vitro* model of *C. difficile* infection and used it to test competition between four ribotype 027 clinical isolates and clinical isolates of four other ribotypes (001, 002, 014, and 053). We found that ribotype 027 strains out-competed strains of other ribotypes. A similar competitive advantage was observed when two ribotype pairs were competed in a mouse model of *C. difficile* infection. Based upon these results we conclude that one possible mechanism that ribotype 027 strains have caused outbreaks worldwide is due to their increased ability to compete in the presence of a complex microbiota.

Introduction

Diarrhea and colitis are some of the most common side effects of antibiotic treatment (1). The generally accepted paradigm of antibiotic-associated diarrhea (AAD) is that antibiotics cause a perturbation of the intestinal microbiota, presenting conditions that allow for the growth of toxigenic bacteria and viruses. It was not until the late 1970's that toxigenic *C. difficile* was identified as a common causative agent of AAD and colitis (2). It is now estimated that 30% of antibiotic-associated diarrhea cases are attributable to *C. difficile* (3) and that healthy GI microbial communities play an essential role in providing colonization resistance to *C. difficile* infection (1, 4, 5).

The incidence of *C. difficile* infection (CDI) has been steadily rising over the past decade, with CDI recently becoming the most common nosocomial infection in the United States (2, 6). This rise in the rate of CDI has co-occurred with an increased prevalence of infection caused by a specific phylogenetic clade of strains characterized as ribotype 027 (3, 7). Initial clinical and epidemiological studies reported ribotype 027 strains as being associated with increased rates of morbidity and mortality, leading to the hypothesis that these strains are hypervirulent (7-13). However, subsequent analyses comparing the outcomes of endemic CDI caused by ribotype 027 strains to CDI caused by strains of other *C. difficile* ribotypes have yielded conflicting results. Several studies have found that infection with ribotype 027 strains did not result in more severe clinical outcomes across a number of institutions (14-17); whereas other studies have seen higher mortality caused by ribotype 027 strains compared to strains from some of the other *C. difficile*

ribotypes (18, 19). What is clear, however, is that ribotype 027 strains have been associated with several large outbreaks, have undergone rapid, global spread since their emergence, and have become a prevalent ribotype in many hospitals and regions (20, 21), and references therein). Therefore, rather than ribotype 027 strains being hypervirulent (capable of causing more severe *C. difficile* disease), we hypothesized that ribotype 027 strains may instead have increased ecological fitness over strains of other *C. difficile* ribotypes.

In order to test this hypothesis, we examined competition between several ribotype 027 and non-027 strains in human fecal bioreactors. Fecal bioreactors have previously been used to study *C. difficile* invasion of complex microbial communities *in vitro*, as well as the effects of potential antibiotic and probiotic treatments (e.g., (4, 22-24)). When developing our fecal bioreactors, we modified parameters of design and operation used in other established models to allow for simpler, higher-throughput fecal mini-bioreactor arrays (MBRA). Using these fecal MBRA, we examined competition between four different pairs of ribotype 027 and non-027 clinical isolates. We found that in all competitions studied, ribotype 027 strains demonstrated a clear competitive advantage over non-027 strains, often increasing in abundance more than two to three orders of magnitude by the end of the experiment. We then performed similar competitions between ribotype 027 and non-027 strains in a mouse model of *C. difficile* infection and saw similar increased competitive advantage of the ribotype 027 strains. These results support our hypothesis that ribotype 027 strains have become more prevalent due to increased ecological fitness compared to strains of other *C. difficile* ribotypes.

Materials And Methods

Mini-bioreactor array (MBRA) design and operation. MBRAs were designed using CAD software (Argon, Asheller-Vellum), and fabricated with DSM Somos Watershed XC 11122 via stereolithography (FineLine prototyping, Fig. 3.1). Each MBRA consisted of six reactors with an internal volume of 25 ml and a working volume of 15 ml. MBRA were operated under an atmosphere of 5% CO₂/5% H₂/90% N₂ at 37°C in a heated anaerobic chamber. Media was continuously replenished and waste removed at a flow rate of 1.875 ml/hr. Prior to use, MBRA and media were sterilized by autoclaving and allowed to equilibrate to the anaerobic environment for ≥72 hrs. Reactor contents were continuously stirred. Additional details regarding MBRA design and operation are available in the Supplementary Methods.

Strains, media, and growth conditions. All *C. difficile* strains used in this study are clinical isolates obtained from the Michigan Department of Community Health (MDCH, Table 3.1). They were collected from Michigan hospitals between December 2007 and May 2008. MDCH determined strain toxinotype and NAP status. Ribotyping was determined by Seth Walk (University of Michigan). All growth studies were carried out in a 37° C anaerobic chamber (Coy, Grass Lake, MI) under 5% CO₂/5% H₂/90% N₂ atmosphere using pre-equilibrated media.

Table 3.1. Characterization of Strains Used in this Study.

Strain	Toxinotype	PFGE Type (NAP status)	Ribotype
CD1014	0	MI-NAP4	014
CD2015	III	MI-NAP1	027
CD2048	0	MI-NAP3	053
CD3014	0	MI-NAP2	001
CD3017	III	MI-NAP1	027
CD4004	0	MI-NAP6	002
CD4010	III	MI-UN13	027
CD4015	III	MI-NAP1	027

BHIS and TCCFA were made as previously described (25), except that cysteine was excluded from both media. One liter of bioreactor medium (BRM) contained: 1 g tryptone, 2 g proteose peptone #3, 2 g yeast extract, 0.1 g arabinogalactan, 0.15 g maltose, 0.15 g D-cellobiose, 0.4 g sodium chloride, 5 mg hemin, 0.1 g magnesium sulfate, 0.1 g calcium chloride, 0.4 g potassium phosphate monobasic, 0.4 g potassium phosphate dibasic, and 2 ml tween 80; which were adjusted to pH 6.8 and autoclaved at 121°C for 30 min. Following autoclaving, a filter-sterilized mix of 1 g taurocholic acid, sodium salt, 40 mg D-glucose, 0.2 g inulin, 2 g sodium bicarbonate, and 1 mg vitamin K3 was added. When needed to solidify media, Bacto agar was added to a final concentration of 1.5 % w/v.

Collection and preparation of fecal samples for fecal MBRA experiments. Fecal

samples were donated by twelve healthy, anonymous donors that were between the ages of 25 and 64, had not taken antibiotics for at least two months and had not consumed probiotic products for at least two days prior to donation. Fresh samples were collected into sterile containers, which were then packed in wet ice in a sealed (8.1 quart, Sterilite Ultraseal) container with two anaerobic gaspaks (BD biosciences) and transported to the laboratory within 24 hours. Samples were then transferred to an anaerobic chamber and manually mixed with sterile equipment. Aliquots were transferred to sterile cryogenic vials and stored at -80°C until use. Prior to inoculation, aliquots were resuspended in sterile, anaerobic phosphate-buffered saline at a concentration of 25% w/v. Samples (pooled at equal volumes) were vortexed vigorously for 5 min, large particulates were removed by centrifugation at 201 X g for 5 min, and supernatants were used for inoculation of the reactors.

***C. difficile* invasion and competition growth studies in fecal community MBRA.**

Reactors were inoculated with 4 ml of 25% fecal slurry inoculum and allowed to grow in batch culture for 16-18 hr. After 16-18 hrs, fresh media flow and waste removal was initiated. 36 hrs later, we began dosing clindamycin (500 µg/ml final concentration) or an equivalent volume of water (solvent for clindamycin; both stored aerobically at 4° C until use) twice daily for 4 days. 1 ml samples were removed from the excess fecal slurry sample, and from reactors prior to the initiation of dosing, and daily thereafter throughout the experiment. Samples were

centrifuged at 21000 X g for 1 min, supernatants discarded, and cell pellets were stored at -80°C until subjected to further analyses.

For invasion studies with CD2015, CD2015 was grown in BRM broth batch culture overnight and reactors were inoculated with either a 1:100 dilution of the overnight culture (Fig. 3.2) or from dilutions of the exponentially growing subculture in BRM broth (Fig. 3.3; CD2015 concentrations specified in figure) on day 7 of operation. Prior to inoculation, reactors were tested for *C. difficile* contamination by selective plating of an aliquot of each reactors' contents on TCCFA supplemented with rifampicin (rif, 50 µg/ml) and erythromycin (erm, 20 µg/ml) and by qPCR with *C. difficile* specific primers (methods described below). Additional 200 µl samples were removed from each reactor either 15 min (Fig. 3.3) or 3 hrs (Fig. 3.2) post-inoculation and CD2015 levels were determined by selective plating on TCCFA rif erm. On subsequent days of MBRA operation, *C. difficile* levels were determined via selective plating of an appropriately diluted 100 µl aliquot from the 1 ml daily sample as well as by *C. difficile* specific qPCR at the times indicated.

For competition studies, bioreactors were set-up following the *C. difficile in vitro* invasion model described above with the following modifications. Strains were inoculated into 5 ml BRM overnights, which were subcultured into 10-30 ml BRM media and allowed to grow at 37° C for 4 hr before inoculation into the reactors to ensure active growth at the time of inoculation. Subcultures were mixed at various ratios (1:1, 1:2, or 1:5 027:non-027 as indicated) and inoculated into the reactors. For replicates indicated in Table S1 (three replicates of two competition pairs, CD3017/CD3014 and CD4010/CD4004), *C. difficile* was inoculated into reactors on

day 8 of operation instead of day 7. 0.5 ml samples were removed from the reactors immediately prior to *C. difficile* inoculation and 2 hr after inoculation and processed as described above. 0.25 ml of the aliquots collected prior to *C. difficile* inoculation were used in qPCR reactions (described below) to detect possible *C. difficile* contamination. MBRA were run for an additional 10-12 days and sampled daily as described above.

Quantitative PCR of *tcdA* gene to quantify *C. difficile* invasion. Frozen culture cell pellets were resuspended in 0.5 ml sterile water and transferred to 2 ml screw-top tubes containing ~200 μ l 0.1 mm silica beads (Biospec Products). The samples were homogenized by bead-beating (BioSpec Products) on the homogenize setting for 1.5 min, centrifuged for 1 min at 21000 X g, and the supernatant was transferred to a new tube. When not in use, processed supernatants were stored at -20°C. *C. difficile* levels were determined by qPCR with primers specific to the *C. difficile* Toxin A gene (*tcdA*, Table S3.2).

We calibrated the *tcdA* signal observed in our reactors to a known concentration of *C. difficile* cells grown under fecal bioreactor conditions in the MBRA and enumerated by plate counting. We processed the samples as described above and spiked them into pooled supernatant samples prepared from bioreactors prior to *C. difficile* inoculation. We generated 10-fold dilutions of *C. difficile* in this background community DNA and used them to generate a standard curve for determining the absolute amounts of *C. difficile* in our bioreactor samples. We also used 10-fold dilutions of community DNA alone to generate a standard curve for

assessing the total bacterial signal from our reactors using universal 16S primers (Table S3.2).

Real-time PCR reactions were performed in triplicate and contained the following components: 4 μ l supernatant (undiluted (*tcdA*) or 1:500 dilution in sterile water (universal 16S *rRNA*)), 12.5 μ L Power SYBR Green PCR Master Mix (ABI, Carlsbad, CA), 0.25 μ L each primer (5 μ M) (Table S3.2), and 8 μ L Milli-Q water. Real-time PCR was performed using an Eppendorf Mastercycler PCR machine under the following conditions: 95°C 10 min, 40 cycles of 95°C for 15 sec followed by 60°C for 1 min. A 20 min melting curve was also performed from 60°C to 95°C. We calculated the *tcdA* copies/ml from our experimental samples using the C_T values and concentrations from our standard curve described above. If a sample's C_T value fell below the lowest concentration from our standard curve, it was designated below the limit of detection, which was 1000 *tcdA* copies/ml. We also determined the total bacterial load per sample based upon C_T value with broad-host range 16S *rRNA* primers (Table S3.2). We used these C_T values, which varied by less than 3 cycles across all samples ($C_T=18.75-21.97$, Fig. S3.1), to normalize the *tcdA* copy numbers that are reported in Fig. 3.2.

Preparation of 16S rRNA amplicon sequencing. We extracted DNA from samples using bead beating followed by modified cleanup with a Qiagen DNEasy Tissue Kit as described (26). DNA concentrations were determined by spectrophotometry at 260 and 280 nm (Nanodrop). We used 40 ng of each DNA as template in PCR with the following final concentrations of reagents: 200 nM 357F primer, 200 nM 926R

primer, 1X AccuPrime PCR Buffer II (Invitrogen), 0.75 U of AccuPrime Taq DNA High Fidelity (Invitrogen). 357F/962R were designed by the Human Microbiome Project, amplify the V3-V5 variable regions of the 16S *rRNA* gene, and contain unique barcodes that can be used to multiplex sequencing reactions (27). Each reaction was set up in triplicate and amplified using the following cycle: 95°C for 2 min, followed by 30 cycles of 95°C for 20 sec, 50°C for 30 sec, and 72°C for 5 min, with a final extension at 72°C for 5 min. Successful PCR amplification products from triplicate reactions were pooled and cleaned with Agencourt AMPure XP (Beckman-Coulter). Products were resuspended with a 0.7X volume of beads, washed twice with 70% ethanol, and eluted with 25 µl of low EDTA TE Buffer (10 mM Tris, 0.1 mM EDTA). Concentrations of purified DNA were determined using Quant-IT (Invitrogen) according to the manufacturer's protocol and were pooled in equimolar amounts. Nucleotide sequencing was performed on a 454 GS Junior (Roche Diagnostics) at MSU according to the manufacturer's protocols.

Processing and analysis of Sequencing Data. All sequence data was processed using mothur (28) Version 1.29.1 (January 2013). Sequences were initially quality filtered using the mothur-implementation of PyroNoise to remove low quality sequences as well as trimmed and filtered to remove those sequences that had any ambiguous bases, mismatches to the reverse primer or barcode, homopolymeric stretches longer than 8 nt, and were shorter than 200 nt (29). Sequences from independent sequencing runs were then compiled into a single fasta file and aligned to the SILVA reference alignment using the NAST-based aligner in mothur, trimmed

to ensure that sequences overlapped, and pre-clustered, allowing a difference between sequences of 2 bp or less (29). Potentially chimeric sequences were removed using the mothur-implementation of UChime (30); remaining sequences were classified using RDP training set version 9 (March 2012) and mothur's implementation of the kmer-based Bayesian classifier. Sequences were binned into Operational Taxonomic Units (OTUs) with $\leq 3\%$ sequence dissimilarity using the average neighbor algorithm of mothur. Taxonomy was assigned to each OTU based upon the majority sequence consensus within that OTU (31). Number of OTUs, evenness (Simpson Evenness) and diversity (Inverse Simpson) were calculated using mothur. Differences in OTU abundances between treated and untreated bioreactors was determined using the mothur-implementation of metastats (32). Bray-Curtis dissimilarities were calculated from the OTU distributions of each sample, which were \log_{10} transformed and normalized by dividing the abundance of each OTU in a sample by the maximum abundance observed for that OTU followed by normalizing the total abundance of OTUs across each sample to the same number using the vegan package in R (33). The metaMDS function of vegan was used to determine the optimal ordination distances for the Bray-Curtis dissimilarities, which were also plotted in R. The significance of community differences was determined by Analysis of Similarities (ANOSIM), which was calculated in R.

Quantitative PCR Analysis of Competition Cultures and Calculations of

Competitive Index. Strain-specific genes *thyA* (027) and *thyX* (non-027) were used to differentiate strains in competitions. We first identified the strain specificity of

these thymidylate synthase genes while doing *in silico* genomic comparisons of *C. difficile* genomes. We then screened a collection of 88 strains belonging to several NAP groups, including all of the strains used in this study, for the presence of *thyA* or *thyX* (Fig. S3.2), and verified that *thyA* was unique to NAP1 (ribotype 027) strains by screening. This correlation of *thyA* with ribotype 027 strains has been noted earlier. (34).

Frozen culture cell pellets (from 0.5 or 1 ml cells) were washed in the same volume of sterile water, resuspended in the same volume of sterile water, and transferred to 2 ml screw-top tubes containing ~200 μ L 0.1 mm silica beads. The samples were then placed in a BeadBeater cell disruptor (BioSpec Products, Bartlesville, OK) on the homogenize setting for 1 min, centrifuged at 21000 X g for 1 min, and diluted 1:10 in sterile water. Real-time PCR reactions were set-up by combining the following components: 12.5 μ L Power Sybr Green PCR Master Mix (ABI, Carlsbad, CA), 0.25 μ L each primer (100 μ M), 11 μ L Mili-Q water, 1 μ L diluted culture supernatant. Primers used are described in Table S3.2. PCR was performed using the conditions described above. All PCR reactions were performed in technical triplicate and the C_T values are an average of the triplicate data points. The amplification efficiency (E) of each primer set was determined by plotting the C_T values of a standard curve generated by serial 4-log dilutions of *C. difficile* template; the sample with the highest signal was diluted into sample with no *C. difficile* inoculated (community background DNA). Primer efficiencies were calculated using the method described by Pfaffl *et al.*; $E = 10^{(-1/\text{slope})}$ (35). Competitive Indices (CI) were calculated by dividing the end point ribotype 027:non-027 ratio by the ratio at

T_0 (Ratio= $2^{C_T(\text{non-027})-C_T(027)}$). Primer efficiencies were not factored into the CI calculations; however, they differ by <5% ($E_{\text{thyA}}=2.04$; $E_{\text{thyX}}=1.95$) when calculated from reactions using sample containing *C. difficile* diluted into fecal community background DNA.

***C. difficile* competition experiments in humanized microbiota mice (^{hm}mice).**

Germ free C57/B6 mice were gavaged with fecal slurry pooled from the twelve human fecal donors described above. Following initial establishment a stable humanized microbiota was passed from ^{hm}mice to their progeny. Descendants of these original ^{hm}mice were maintained under specific pathogen free conditions and used for all experiments. To induce susceptibility to *C. difficile* infection (36), an antibiotic mixture of kanamycin (0.4 mg/ml), gentamicin (0.035 mg/ml), colistin (850 U/ml), metronidazole (0.215 mg/ml), and vancomycin (0.045 mg/ml) was administered in drinking water ad libitum for 3 days and then replaced with fresh drinking water. After 24 hours of plain drinking water, mice were treated intraperitoneally with clindamycin (10 mg/kg) and 24 hours post injection challenged with either 10^4 pure or mixed 027/non-027 *C. difficile* spores. Spores were cultivated by spread plating overnight BHIS cultures of *C. difficile* on BHIS medium and incubating anaerobically at 37°C for 5 days. Cells were scraped from the plates and resuspended in sterile water, heat-treated at 60°C for 30 min to kill vegetative cells, and the number of viable spores were enumerated by plating appropriate serial dilutions on BHIS supplemented with 0.1% taurocholic acid. Spore preparations were diluted in sterile water to yield the desired concentrations

($\sim 10^4$ or $\sim 10^5$ spores/ml), then mixed, when appropriate, prior to gavaging a total of $\sim 10^4$ spores/mouse. For competition experiments, mice were gavaged with the following ratios of ribotype 027:non-027 spores: 1:14 for CD3017 + CD1014 and 1:50 for CD4015 + CD2048. Mice were observed daily for disease symptoms and morbidity. Fecal samples were collected daily and frozen until analyzed.

C. difficile levels were quantified in fecal samples by plating. Fecal samples were weighed, diluted in 500 μ l sterile water, and heat-treated at 65°C for 30 min to reduce background growth of mouse fecal microbiota. Total heat-resistant CFU/g of feces were determined by spotting appropriate serial dilutions on BHIS plates supplemented with 0.1% taurocholic acid. Ribotype 027-specific heat-resistant CFU/g of feces were determined by spotting appropriate serial dilutions on BHIS plates supplemented with 0.1% taurocholic acid and either 50 μ g/ml rifampicin and 10 μ g/ml erythromycin (CD4015 + CD2048 competition samples) or 10 μ g/ml erythromycin only (CD3017 + CD 1014 competition samples). Plates were incubated anaerobically for 24-48 hrs. Colonies formed on antibiotic-supplemented medium represented levels of ribotype 027 strains (CD3017 and CD4015). Non-027 ribotype strain levels were determined by subtracting the number of colonies formed on selective plates from the number on non-selective plates (total *C. difficile*). The fecal sample weights were then used to determine CFU/g feces. CI's were calculated by dividing the ribotype 027:non-027 strain ratios at day 4 by the ratios in the gavaged spore mixtures. In cases where the number of colonies on selective plates were the same as the number on non-selective plates, the ribotype 027:non-027 ratio was set to 10. This was determined as a reasonable level for the non-027 limit of detection

based on this type of subtractive analysis taking into account plating error and would most likely result in an underestimate of the ribotype 027 CI.

Because we used subtractive plating to measure the levels of ribotype 027:non-027 spores and our detection limit set the maximum observable ratio between ribotype 027:non-ribotype 027 strains at 10:1, we found that starting with the ribotype 027 strain in the minority provided a larger dynamic range that allowed us to more readily detect an increase in the ribotype 027 strain levels compared to non-027 levels. Although the ratios of ribotype 027:non-ribotype 027 spores gavigated were lower than originally intended, placing the ribotype 027 strains in the minority ensures that the 027 strains do not have an advantage by being even at a slightly higher proportion in the mixed spore preparations, since there is always a low level of error in diluting and plating

Results

Fecal mini-bioreactors (MBRA) provide an *in vitro* model to study *C. difficile* invasion in complex microbial communities. Our objective was to design human fecal bioreactors that recapitulated antibiotic- induced *C. difficile* invasion of a resistant community that also allowed for testing of multiple experimental parameters in replicate reactors simultaneously. Therefore, we pursued a relatively simple bioreactor design, an array of six single vessel chambers (mini-bioreactor array, MBRA) with modest operating volume (15 ml) that would allow us to operate up to 24 continuous-flow fecal bioreactors simultaneously in the same anaerobic chamber (Fig. 3.1). The reactors were fabricated with DSM Somos Watershed XC

11122 resin, which allowed for direct observation of the reactor contents and the ability to autoclave and reuse the reactors.

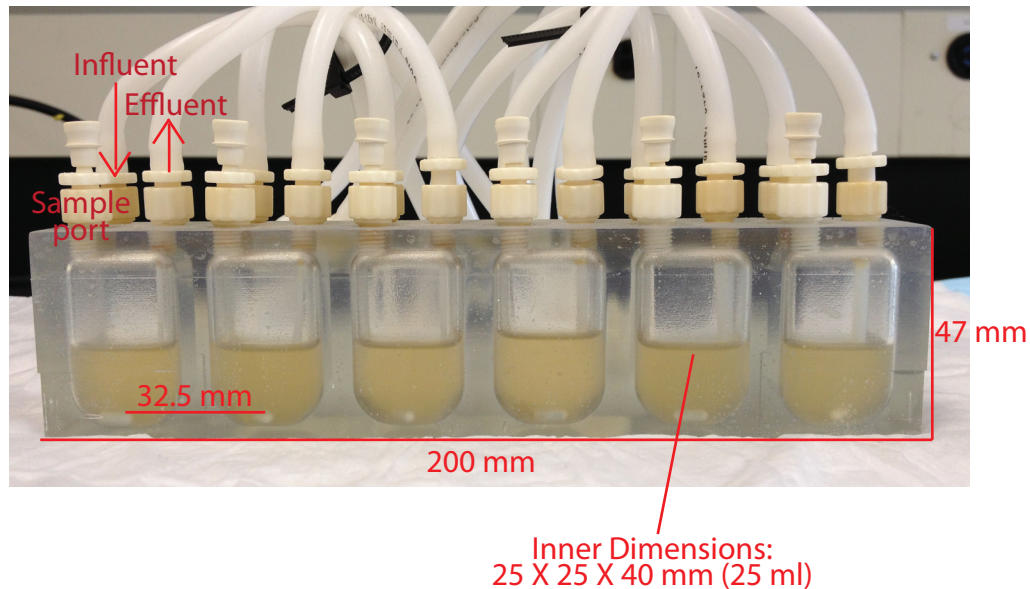


Figure 3.1. An example of a minibioreactor array (MBRA) used for cultivation of fecal microbial communities. The placement of the influent, effluent and sample port for one of the six bioreactor chambers is indicated as are some of the key dimensions.

Continuous-flow MBRAs were inoculated with fecal samples pooled from twelve healthy, *C. difficile*-negative donors and bacterial communities were allowed to adapt to growth in culture before challenging the communities with clindamycin, an antibiotic known to support *C. difficile* invasion (37). Initial studies compared the ability of three clindamycin-treated and three mock-treated communities to resist invasion by *C. difficile*. We found that in mock-treated communities challenged with 10^6 vegetative cells of *C. difficile*, *C. difficile* levels were reduced to below the level of

detection in replicate reactors within one to four days following inoculation (Fig. 3.2, open symbols). In contrast, when MBRAs were treated twice daily with clindamycin for four days prior to *C. difficile* inoculation, *C. difficile* levels were maintained at the same high levels at which they were inoculated for eight days following inoculation (Fig. 3.2, closed symbols).

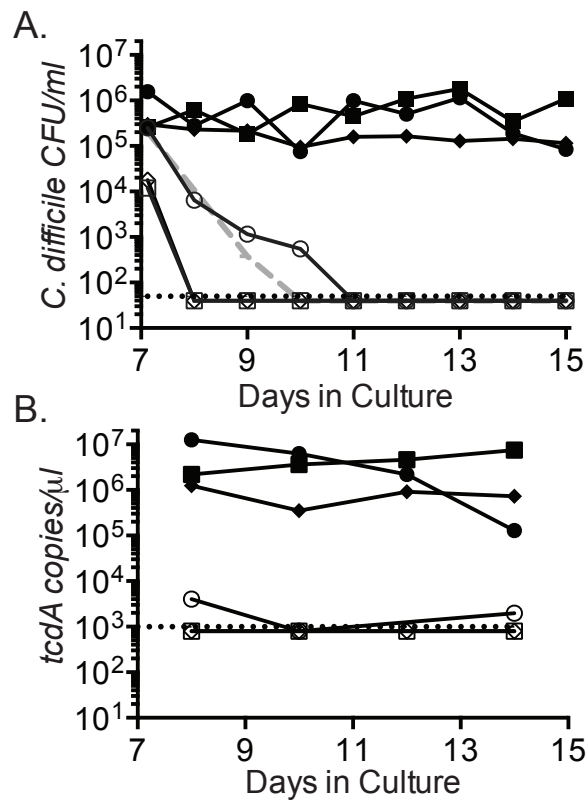


Figure 3.2. Fecal bioreactor communities prevent invasion by *C. difficile* unless disrupted by treatment with clindamycin. We monitored *C. difficile* proliferation in three independent fecal bioreactors that were either clindamycin-treated (reactors 1-3; closed squares, circles and diamonds, respectively) or mock-treated (reactors 4-6; open squares, circles and diamonds, respectively) through selective plating (A) or quantitative PCR (B). The gray dashed line in panel A represents the theoretical washout rate of non-proliferating *C. difficile* cells. The black dashed line represents the limit of detection for selective plating (A) or qPCR (B) in our experiments.

Because we used such a high inoculum in this initial experiment, we were interested in establishing the minimal number of *C. difficile* cells required for invasion. We found that inoculation with 10^4 or 150 cells was sufficient to allow clindamycin-induced invasion by *C. difficile*, and that the final cfu/ml reached 10^5 - 10^6 (Fig. 3.3A). These levels are only ~10-100-fold lower than the 10^7 cfu/ml that pure *C. difficile* reaches in reactors operating under these continuous-culture conditions (Fig. 3.3B).

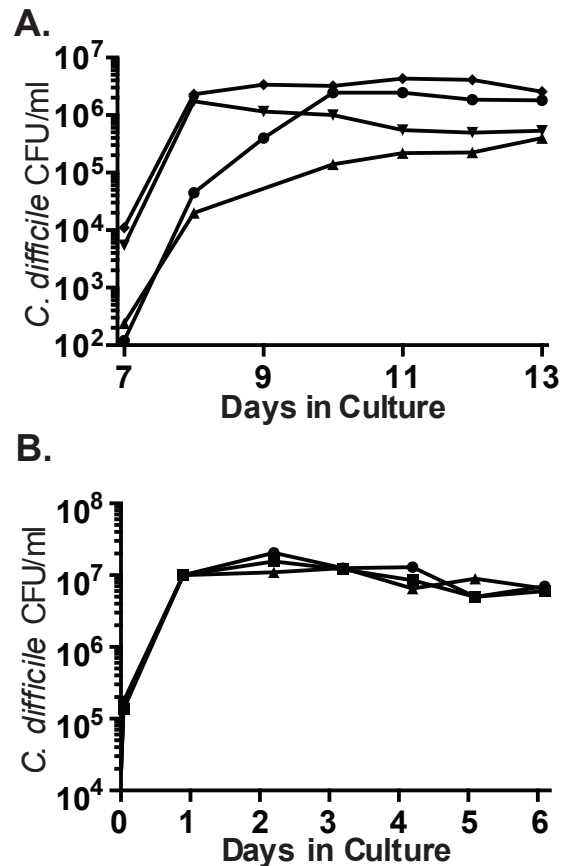


Figure 3.3. *C. difficile* proliferation was assayed in fecal bioreactors with different levels of inoculum and in pure culture under the continuous-culture conditions used for bioreactors. In (A), we monitored *C. difficile* proliferation in four independent fecal bioreactors that were clindamycin-treated and inoculated at the indicated densities. In (B), we measured *C. difficile* proliferation in pure culture in three replicate continuous-culture bioreactors operated under flow conditions used for fecal bioreactors.

In addition to the invasion that we observed for the single ribotype 027 strain (CD2015) shown in Fig. 3.2, we found similar invasion dynamics for other ribotype 027 strains (CD3017, CD4010, and CD4015) as well as strains from other ribotypes (CD1014, CD3014, and CD4004, data not shown). Based upon these results, we concluded that the communities established in our fecal MBRA demonstrated the key attribute of an *in vitro* *C. difficile* invasion model that we intended to achieve - the ability to resist invasion by *C. difficile* until disrupted by antibiotic treatment.

MBRAs support complex fecal microbial communities. In order to investigate whether the resistance to invasion that we observed in our unperturbed MBRA communities was due to the presence of complex microbial communities or simple communities composed of a few strains that were inhibitory to *C. difficile* growth, we sequenced the V3-V5 hypervariable region of the 16S *rRNA* gene from samples collected from the triplicate clindamycin and mock-treated reactors through pyrosequencing. Samples were collected prior to antibiotic treatment (day 2) and every two days after the initiation of treatment (days 4, 6, 8, 10 and 12; *C. difficile* was added to all reactors on day 7) and sequencing data from these samples were compared to duplicate samples from the initial fecal inoculum.

At the sequence depth examined (1053 sequences/sample), we detected a mean of 69 operational taxonomic units (OTUs; 97% sequence similarity) in the untreated (day 2, all reactors) and mock-treated (days 4, 6, 8, 10 and 12) bioreactor

communities (Fig. 3.4A). The number of OTUs observed in untreated or mock-treated reactors was ~2.4-fold lower than that observed in the original fecal inoculum (mean=168 OTUs, Fig. 3.4A).

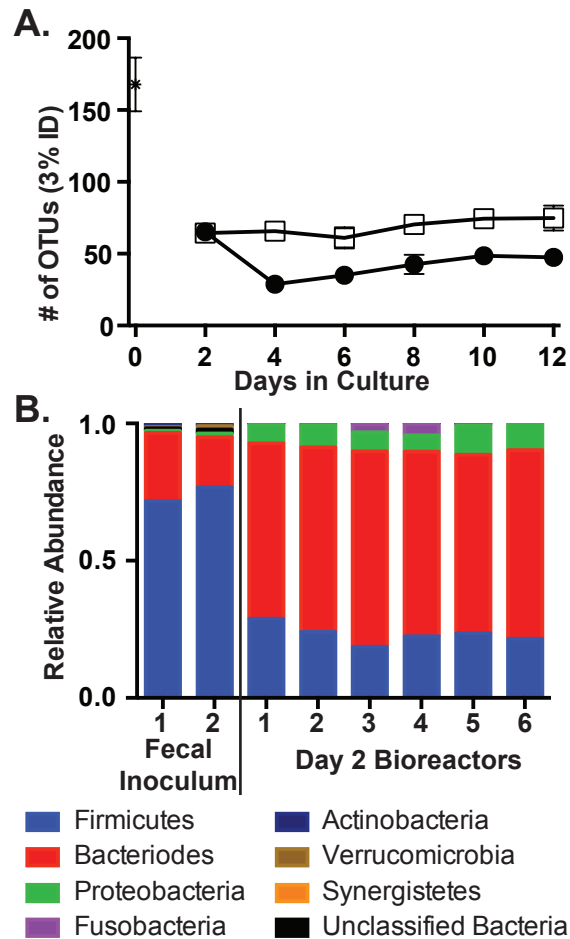


Figure 3.4. Comparison of the community structure between fecal samples, mock-treated and clindamycin-treated reactors. We analyzed the 16S rRNA gene abundances from the three mock-treated and clindamycin-treated communities described in Fig. 3.2 on days 2, 4, 6, 8, 10 and 12 in MBRAs as well as duplicate samples from the initial fecal inoculum. In (A), we plotted the mean number of OTUs in the fecal inoculum (asterisks), and clindamycin (closed circles) and mock-treated (open squares) communities \pm the standard deviations. In (B), we classified each sequence to the phylum level with at least 80% confidence (sequences <80% were designated “Unclassified Bacteria”). We then plotted the relative abundance of each phylum in the duplicate samples of initial fecal inoculum and the six replicate bioreactor samples from day 2 prior to the initiation of treatment. Reactors are numbered as in Fig 3.2.

When we compared the composition of the original fecal inoculum community to the bioreactor communities, we found a significant shift in composition upon culturing in the bioreactors, even by day 2 (Fig. 3.4B). The fecal inoculum was dominated by members of the *Firmicutes* phylum, which comprised $74\% \pm 3\%$ of the sequences. In contrast, members of the *Bacteroides* phylum were dominant members of the bioreactor communities on day 2 in culture (Fig. 3.4B), comprising $67\% \pm 3\%$ of the sequences in all six replicate reactors studied.

Bioreactor community composition changes in response to clindamycin

treatment. Because clindamycin-treated bioreactor communities become susceptible to *C. difficile* invasion (Fig. 3.2), we anticipated that we would observe changes in the microbial composition of these communities compared to the mock-treated communities, and that these changes would be consistent with previously published models of *C. difficile* invasion. One significant change we observed in our clindamycin-treated communities was a significant reduction in the number of OTUs compared to mock-treated reactors (Fig. 3.4A, $p < 0.01$ for days 4-12 with student's t-test). The ability of antibiotic treatment to significantly reduce species complexity has been previously reported (26, 38). Although the species richness declined, quantitative PCR with broad-range 16S rRNA gene primers indicated the total amount of bacteria in the reactors was equivalent to untreated reactors after clindamycin treatment (Fig. S3.1), indicating that *C. difficile* invasion was not dependent upon a decreased bacterial load in the bioreactors.

This change in microbial composition was also evident when comparing the composition of the communities using the Bray-Curtis dissimilarity measure, which compares the relative abundances of shared OTUs between communities. When we plotted these data using nonmetric multi-dimensional scaling (NMDS, Fig. 3.5), we found that all six bioreactor communities were highly similar prior to treatment on day 2 and that bioreactor communities diverged in response to clindamycin-treatment as well as time in culture. Analysis of similarities (ANOSIM, (39)) found strong statistical support ($p < 0.05$) for the distinct partitioning of the communities into pre-treatment, mock-treatment and clindamycin-treatment groups, with clindamycin-treatment causing a more significant shift in community structure than time in culture. Using metastats (32), we identified several specific OTUs that were significantly different between treated and untreated communities. We observed decreases in specific members of Ruminococcaceae, Lachnospiraceae, and Clostridiaceae families that were consistent with changes observed in previous animal and human studies (40, 41), providing further support for the relevance of this model for studying aspects of *C. difficile* invasion *in vitro*.

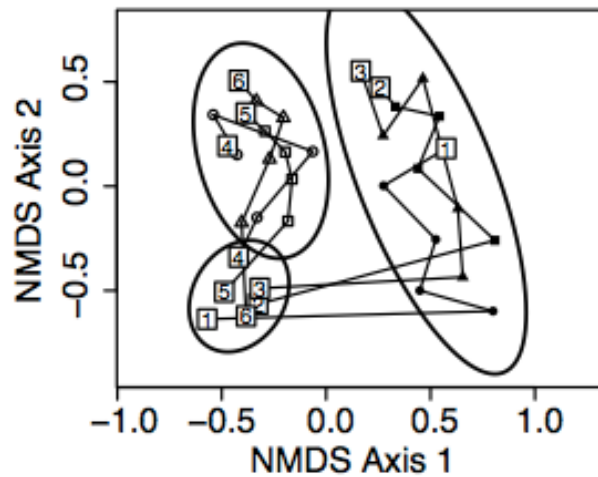


Figure 3.5. Community structure changes in response to clindamycin-treatment. We plotted the Bray-Curtis dissimilarity (3% OTUs) between samples using nonmetric multidimensional scaling (NMDS). Samples were plotted from three clindamycin-treated replicates (1-3; closed symbols) and three mock-treated replicates (4-6; open symbols) every two days from day 2 (pre-treatment) through day 12. Data was normalized prior to analysis as described in the methods. The numbers in boxes indicate the points for the indicated reactors on day 2 and day 12 and correspond to the reactor numbers indicated in Fig. 3.4. Intervening time points are represented by symbols and are connected in sequential order by lines. The ellipses indicate the 95% confidence intervals for the indicated groups (pre-treatment; mock-treatment; clindamycin-treatment.) Distinct distributions between clindamycin and early/mock-treated samples were also supported by ANOSIM, with p-values less than 0.001. The plot stress was 0.171.

Ribotype 027 strains exhibit a competitive advantage over non-027 strains in the presence of a complex microbiota. Having developed the MBRA *C. difficile*

invasion model, we investigated if ribotype 027 strains were able to better compete than non-027 ribotype strains for their available niche after antibiotic treatment in the presence of the complex MBRA communities. We chose to study recent clinical isolates of ribotype 027 and non-027 *C. difficile* strains collected by the Michigan

Department of Community Health in order to avoid confounding effects of strain adaptation to laboratory conditions. Eighty-eight isolates were characterized by North American Pulsed-Field Electrophoresis (NAP) fingerprint, toxinotype, and ribotype; we selected eight strains for further study (Table 3.1). Four different ribotype 027 strains were competed against four different non-027 ribotype strains in order to avoid selecting strains with unrepresentatively high or low competitive fitness for either ribotype group. For the non-027 ribotypes, we selected strains that were different ribotypes and had different NAP designations to broaden the phylogenetic breadth of strains tested.

Exponentially growing pure cultures of ribotype 027 and non-027 *C. difficile* strains were mixed together and inoculated into clindamycin-treated MBRAs. At days 3, 7, and 11 post-inoculation samples were taken and quantitative PCR was conducted to determine the relative ratios of the competing strains. Plotted in Fig. 3.6 are the competitive indices (CI) of ribotype 027 strains at day 7 for all of the replicates in each competition pair, calculated as the ratio of 027:non-027 at day 7 divided by the ratio at day 0. The mean competitive indices (range) for these competitions are 7.8 (0.5 to 22.4) for CD2015, 832.4 (21.9 to 3993.2) for CD3017, 131.4 (1.4 to 593.4) for CD4015, and 327.9 (30.3 to 764.9) for CD4010. Fig. S3.3 shows the 027:non-027 ratios plotted across time for each individual reactor of all competition pairs. The competition dynamics vary between replicates both within and across competition pairs. However, there is a strong trend of increasing ratios over time for the ribotype 027 strains, even when started at different initial input ratios, further supporting their competitive advantage. The competitive indices

calculated from these ratios across all time points (days 3, 7, and 11; some days vary, see figure legend) are reported in Table S3.1. Across all 22 competition replicates, only two CIs were <1.0 at day 7; these account for two of the six replicates of the CD2015 (ribotype 027) + CD3014 (ribotype 001) competition pair. This competition pair was particularly interesting in that this ribotype 027 strain (CD2015) displayed an initial drop in strain ratio in the majority of the competition replicates, sometimes emerging as low as 2% of the total *C. difficile* population at day 3 (Fig. S3.3). Nevertheless, CD2015 was able to recover and eventually outcompete the non-027 ribotype strain by the end of the competitions. At the day 11 time point of these replicates, the ratios continued to increase resulting in CI's close to or >1 (Table S3.1).

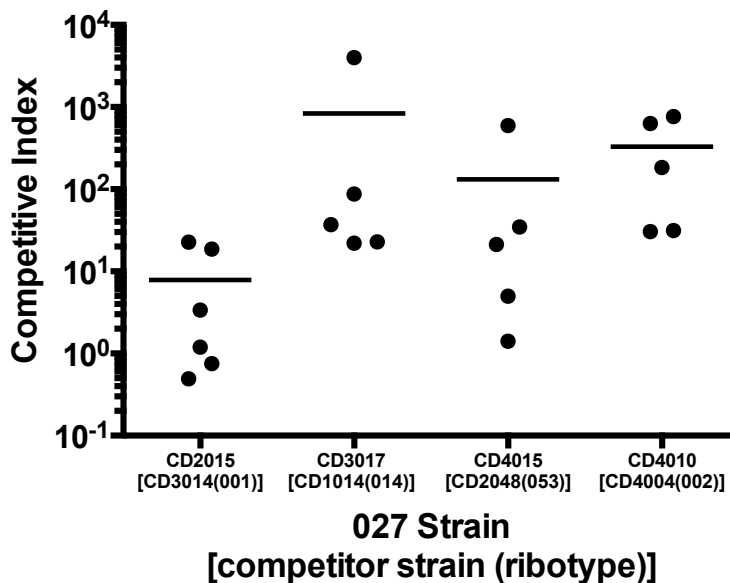


Figure 3.6. Competitive indices of ribotype 027 strains relative to non-027 strains in the presence of MBRA fecal communities. Clindamycin-treated bioreactors were inoculated with the indicated mixtures of strains at various ratios and the abundance of each strain was monitored over time by qPCR to measure ribotype 027:non-027 ratios. Plotted here is the competitive index of the ribotype 027 strains for each replicate competition, calculated as the ratio of 027:non-027 at day 7 or 8 (see Table S1) divided by the ratio at day 0. Each black circle represents an individual replicate competition. Where the non-027 strain was below the limit of detection, the ratio was determined by substituting in the highest C_T value in the linear range (detection limit) for the non-027 value. Black bars represent the mean of replicates for each competition.

One possible mechanism for ribotype 027 strains to out-compete the non-027 strains would be if the latter were inherently unable to invade the complex MBRA communities. We tested this hypothesis by inoculating fecal bioreactors with individual non-027 strains and saw that these strains were equally able to invade the microbiota as ribotype 027 strains (data not shown). In addition, the minimal

inhibitory concentrations to clindamycin of all of the strains used in this study ranged from 50 µg/ml to >100 mg/ml (data not shown), concentrations several fold higher than the calculated residual clindamycin in the reactors at the time of *C. difficile* inoculation based on theoretical washout (<9 µg/ml). Therefore, the competition outcome was not reflective of differences in clindamycin sensitivity.

Because we performed our competition experiments in fecal bioreactors that had been treated by clindamycin and did not include untreated control reactors, we wanted to verify that the communities present in our clindamycin-treated competition reactors were similar to those previously established and characterized in our *in vitro* invasion model. Therefore, we sequenced the V3-V5 hypervariable region of 16S rRNA gene from our competition bioreactor samples at day 7, just prior to *C. difficile* inoculation, by pyrosequencing and compared these sequences to the previous data we had collected from our *in vitro* invasion model (Fig. 3.4 and 3.5). We found that the richness, diversity, and evenness of the competition communities were similar to those of the other clindamycin-treated communities on day 6 (Fig. S3.4). When we compared the microbial community structures of the competition bioreactor samples using the Bray-Curtis dissimilarity measure and plotted them with the previous clindamycin-treated and mock-treated samples with NMDS, we found that they grouped together with the clindamycin-treated communities (Fig. S3.5). These community comparisons show that the strains were competed in the presence of complex, diverse fecal communities and not community anomalies made up of unexpectedly low richness or diversity.

Ribotype 027 strains display a competitive advantage *in vivo*. In order to address if ribotype 027 strains are capable of outcompeting non-027 ribotype strains in the intestinal tract, we competed two ribotype 027 and non-027 strains in a humanized microbiota mouse model of *C. difficile* infection. Mice were treated with an antibiotic cocktail (36) for three days, followed by a single dose of clindamycin. 24 hours later mice were gavaged with *C. difficile* spores. Under these conditions, strains CD3017 and CD4015 (ribotype 027) and strains CD1014 and CD2048 (ribotypes 014 and 053, respectively) were able to transiently colonize the intestinal tracts of mice when infected individually without causing severe disease (Fig. S3.6).

To compare the relative fitness between ribotype 027 and non-027 strains, antibiotic-treated animals were treated with a mixture of 10^4 spores from strains CD3017 (027) and CD1014 (014) (ratio of 1:14) or CD4015 (027) and CD2048 (053) (ratio of 1:50). The abundance of each strain was monitored daily by selective plating of mouse feces. The 027 strain competitive indices in replicate mice for both competition groups are plotted in Fig. 3.7. Competitive indices are calculated by dividing the 027:non-027 ratios at day 4 by the ratios present in the gavaged spore mixtures.

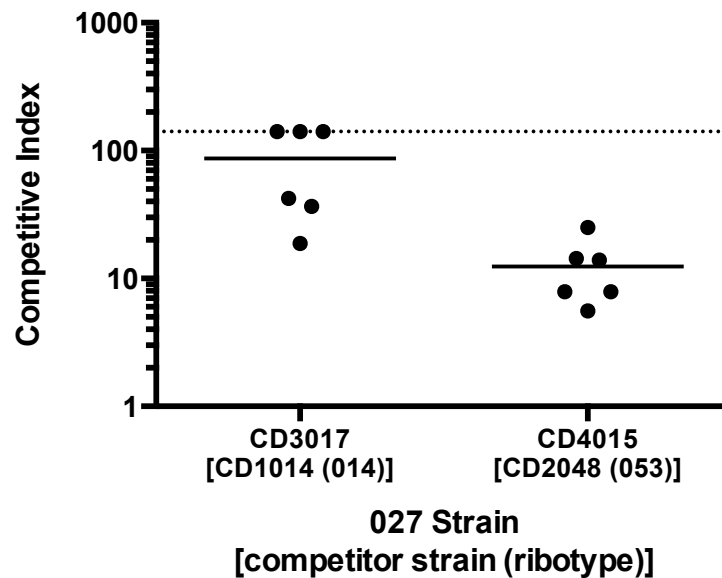


Figure 3.7. Competitive indices of ribotype 027 strains relative to non-027 strains in a mouse model of *C. difficile* infection. After antibiotic treatment, mice were gavaged with mixtures of 027 and non-027 ribotype strain spores. *C. difficile* abundance for the indicated strains was determined by selective plating of the fecal samples. Plotted here is the competitive index of the 027 strains for each replicate mouse competition as the ratio of 027:non-027 at day 4 divided by the ratio at day 0 (ratio in spore mixes). Black bars represent the mean of replicates for each competition. The dotted line on the Y-axis represents the upper CI limit for the CD3017/CD1014 competition based on the plating limit of detection.

In both competitions, we noted that the ribotype 027 strains had a competitive advantage when directly competing in the mouse intestinal tract (Fig. 3.7). CD3017 displayed a dramatic expansion over days 2-4 when competed against CD1014; at day 4, the mean CI for 3017 was 86.7 (range=18.8 to 140.9). CD4015 also displayed a competitive index that showed it had a competitive advantage over CD2048, and although the CI was not as robust as observed with CD3017, it had a competitive advantage with a CI of 12.4 (range= 7.9 to 25.0). These data

demonstrate that ribotype 027 strains have a competitive advantage over non-027 strains *in vivo*.

Discussion

Ribotype 027 strains have been frequently shown to be overrepresented in hospital outbreaks and have been linked to increased morbidity and mortality. Although this association with a hypervirulent state is controversial, the fact that ribotype 027 strains have swept across the globe implies they have acquired an increased ability to cause disease. We hypothesized that differences in strain physiology could give ribotype 027 strains a competitive advantage over strains of other ribotypes, thereby leading to the increased prevalence of ribotype 027 strains. We used the MBRA *C. difficile* invasion model to demonstrate that ribotype 027 strains were able to outcompete strains of other ribotypes in the presence of complex fecal bacterial communities. We then demonstrated similar competitive advantages of ribotype 027 strains to strains of other ribotypes in a mouse model of *C. difficile* infection.

Our work demonstrates that ribotype 027 strains can directly outcompete strains of other ribotypes. Because we used four independent ribotype 027 strains competed against four independent strains of varying ribotypes, we do not expect that the observed increase in competitive fitness of the ribotype 027 strains was due to strain selection. In the majority of competition pairs we studied, the ribotype 027 strains became the dominant *C. difficile* strain in the community, sometimes leading to the complete loss of the non-027 strain. This dominance was observed in all

bioreactor communities studied, as well as in the mouse competition between the ribotype 027 strain CD3017 and the ribotype 014 strain CD1014. However, in the second mouse competition between ribotype 027 strain CD4015 and ribotype 053 strain CD2048, the ratio of CD4015 to CD2048 increased over time, from a 1:50 ratio at the beginning of the experiment to a mean 1:4 ratio (range=1:10-1:2) at the end of the experiment, but CD4015 did not become the dominant *C. difficile* strain in the community. Although we interpret these results to indicate that CD4015 was outcompeting CD2048 for available niche space and would likely have led to its loss from the community if the experiment had been continued further, we cannot exclude the hypothesis that both strains would have reached a steady level of co-existence. Interestingly, when comparing CI's of competition pairs in the MBRA or mice, similar trends were observed, with the CD3017 CI higher than the CD4015 CI in each model, supporting that the MBRA model can recapitulate *C. difficile* dynamics that occur *in vivo*, and further demonstrating the validity of the MBRA model as a precursor for *in vivo* experiments (Fig. S3.7).

However, it is currently unclear what physiological differences present in ribotype 027 strains allow these strains to outcompete strains of other ribotypes. Although it is possible that ribotype 027 strains are capable of directly antagonizing strains of other ribotypes, we favor the model that ribotype 027 strains are better able to proliferate within the intestinal environment and thereby indirectly lead to elimination of strains of other ribotypes.

One aspect of physiology that could potentially impact competition outcome is inter-strain variability in rates of sporulation. If one strain had a higher

proportion of the cells in its population enter into sporulation during the course of competition, that strain would have less cells in logarithmic growth, effectively reducing its competitive fitness. Although there have been some reports that ribotype 027 strains sporulate more efficiently than other strains (e.g., (42, 43), larger studies comparing multiple isolates of different ribotypes have found that there is no significant correlation between sporulation efficiency and ribotype (44, 45). Because sporulation dynamics of individual strains co-cultured within the MBRA are difficult to measure; we do not currently have data to determine whether the non-027 strains used in our study sporulate to higher levels than the 027 strains. However, when we assayed sporulation in pure culture under both batch and continuous-culture conditions, we did not observe higher rates of sporulation of these non-027 strains (data not shown). The dynamics of *C. difficile* sporulation in the context of growing in the presence of a complex fecal community is an area of current and future investigation. While it is important to consider the impact of sporulation dynamics on competition outcome, we do not believe this is the factor responsible for ribotype 027 strains outcompeting other ribotypes in our experiments.

A second aspect of physiology that could play a role in competitive fitness is differences in germination. Differential germination does not play a role in the competitive advantage of ribotype 027 strains in the MBRA, since competitions were initiated with vegetative cells. In contrast, competition in the mouse model was initiated by gavaging a mixture of spores. Recent work published by Francis *et al.* demonstrates that murine bile acids (muricholic acids) inhibit *C. difficile* spore

germination and that there is strain variability in this inhibition (46). In addition, published data shows there is significant variability in rates of germination and the compounds that serve as germinants among large sets of *C. difficile* strains of varying ribotypes, at least *in vitro* (47). However, when we compared the day one levels of *C. difficile* in the mice gavaged with individual strains of different ribotypes to the levels of spores present in the initial inoculum, we found similar increases in the abundance of *C. difficile* cells across the different strains by day one (Fig. S3.6). Based upon these results, we conclude that differences in germination rates are unlikely to play a role in the ribotype 027 competitive advantage.

Evidence suggests that factors of colonization resistance are important in preventing *C. difficile* infection, and therefore must be overcome in order for *C. difficile* to proliferate in the colon (4). Some of these factors include competition for nutrients, antagonism by production of inhibitory compounds (such as bacteriocins or short chain fatty acids), and microbiota-dependent modulation of host immune functions (reviewed in (5)). Identifying which of these factors is driving the competition outcome in our model is the next area of investigation. Comparative genomic studies have identified potential candidate genes that could provide ribotype 027 strains an increased competitive advantage over strains of other ribotypes. One such genomic difference is the presence of the thymidylate synthase gene, *thyA*, in ribotype 027 strains, which has effectively replaced the native, alternative thymidylate synthase gene, *thyX*, in the form of a four-gene insertion (34). Escartin *et al.* showed that ThyA enzymes have, on average, 10-fold faster catalytic rates than ThyX enzymes *in vitro* and are able to confer faster genome

replication rates *in vivo* (48). Based upon this work, we hypothesize that the presence of *thyA* in ribotype 027 strains may confer a growth advantage, and therefore play a role in competitive fitness. We have also begun assessing whether differences in carbohydrate metabolism between ribotype 027 strains and strains of other ribotypes could provide a competitive advantage. Preliminary studies using phenotypic arrays (Biolog) and follow-up growth studies have revealed differences in metabolism of some carbohydrates by ribotype 027 strains (C.D.R. and R.A.B., unpublished results). Moreover, we are actively investigating whether ribotype 027 strains require less of a disruption of the microbiota to invade, for example after shorter antibiotic regimens or after lower dosing of antibiotics, which would provide further evidence as to why these strains are so prevalent in many clinical locations.

Fecal MBRA as a model for *C. difficile* invasion. Our goal was to cultivate complex fecal microbial communities within the MBRA that could resist invasion by *C. difficile*, recognizing that these communities would not be 1:1 translations of the starting fecal inoculum. Relative to our initial fecal inoculum, we observed a significant shift in the ratio of *Bacteroides:Firmicutes* phylum members (Fig. 3.4B). *Bacteroides*-dominated communities have been observed in several different *in vitro* bioreactor models (22, 49-51), which often use media of similar composition for cultivation. Several parameters can affect the composition of the microbial communities that are established in fecal bioreactors, including source of fecal material and how it is processed, the media composition and turnover time used for

cultivation, and the availability of surfaces for biofilm formation (reviewed in (52)). For example, we chose to pool fecal samples from twelve donors, reasoning that this may lead to an *in vitro* community that was more representative of the microbial diversity present amongst different individuals than could be achieved from a single donor. However, by choosing this pooling strategy we may have selected for communities that would not normally co-exist. We have examined the differences between MBRA communities formed from single and pooled fecal samples and found that they exhibit similar *C. difficile* invasion dynamics (manuscript in preparation). Although modifying different aspects of the operating parameters could lead to communities with higher similarities to the starting fecal inoculum, our results demonstrate that our current model yields complex fecal MBRA communities that resist invasion by *C. difficile* when unperturbed and are susceptible when disturbed by antibiotics.

Our MBRA model does not promote invasion of antibiotic-treated communities with *C. difficile* spores and thus we cannot monitor spore germination dynamics in the presence of a fecal microbiota. We are currently attempting to modify the model to enable spore germination within the MBRAs. Determining those aspects of the current model inhibitory to spore germination and outgrowth may also provide new insights into the dynamics between *C. difficile* and the microbiota.

In spite of the limitations discussed above, the *in vitro* model that we developed allows for robust, higher throughput studies of *C. difficile* invasion on shorter time scales than can be accommodated in animal models and other more

complex bioreactor models. Therefore, this model can serve as a complement to animal studies by providing a platform for conducting initial, hypothesis-generating experiments, including those experiments regarding potential therapeutic treatment of *C. difficile* infection.

Conclusions. The data from the present study suggest that ribotype 027 strains have an ecological advantage over other *C. difficile* ribotypes in the context of the intestinal microbiota. If this competitive advantage holds true in the human colonic environment, it may explain, in part, the epidemic nature of ribotype 027 strains. Mixed species *C. difficile* infections have been found to occur in 7-13% of patients infected with disease ((53, 54), and references therein). However, it has been difficult to explore the impact of mixed infection on disease progression due to limitations in the ability to accurately quantify the rate at which mixed infections occur, or the dynamics of the mixed strains over time within individual patients (53, 54). While direct competition between strains may be occurring during co-infection in patients, we suspect that ribotype 027 strains are able to outcompete strains of other ribotypes in our models of *C. difficile* infection due to their ability to better exploit the limited resources available within the intestinal communities. Finally, this work further demonstrates that aside from virulence factors such as toxin production and antibiotic resistance, the physiology of *C. difficile* should be considered an important contributor to its success as a pathogen.

Acknowledgements

The authors acknowledge Sara McNamara (MDCH) for providing *C. difficile* strains, Seth Walk (University of Michigan) for ribotyping strains, Robert Stedtfeld (MSU) for designing the mini-bioreactor arrays, Sara Poe and Kathryn Eaton for collaboration in developing the humanized microbiota mice, and Vince Young (University of Michigan) and Richard Lenski (MSU) for helpful comments regarding the manuscript. This work was supported by award 5U19AI090872-02 from the National Institutes of Allergy and Infectious Diseases to RAB.

APPENDIX

Appendix

Supplementary Methods: MBRA Design and Operation.

As described in the Methods, MBRAs were fabricated from DSM Somos Watershed XC 11122 via stereolithography (FineLine prototyping). Six reactors with an internal volume of 25 mL were designed into a single strip with 200mm x 47 mm x 36 mm dimensions (Fig. 3.1). Reactors were drawn with 25 x 25 x 40 mm dimensions, including 10 mm radial blends on the bottom corners (to prevent buildup of cells and other insoluble materials), and 5 mm radial blends on the top. Reactors were spaced 32.5 mm center to center to match dimensions on the stir plate. Three 5.55 mm diameter holes (influent, effluent, sampling) were placed into the top of each reactor, and spaced 16 mm apart center to center. Holes were threaded to fit conventional leur connectors. Inner walls of the reactors were placed 2 mm from the bottom of the strip, 5 mm from the top of the strip, 5 mm from the side of the strip, and 3.25 mm into the strip. A 1.25 x 16 x 31 mm intrusion was designed into the bottom corners of the MBRA for fixing into a custom built acrylic block that held the reactors upright and properly aligned with the stir-plate. A CAD file (.stl) that can be used directly for fabrication via stereolithography is available upon request.

Media was transferred from the source bottles through a combination of 1/8 in inner diameter (ID) C-flex tubing (Cole-Parmer) tubing and 0.89 mm ID 2-stop Tygon lab tubing supplied to the reactors via a 24-channel peristaltic pump (205S/CA, Watson-Marlow). Waste was removed from the reactors through a

combination of 1/8 in ID C-flex tubing tubing and 1.14 mm ID 2-stop Tygon lab tubing drawn from the reactors via the same 24-channel peristaltic pump. Reactors were stirred using magnetic stir bars driven by independent magnets on a 60-spot magnetic stir plate (VarioMAG HP 60, Vario-MAG USA).

Table S3.1. Competitive indices of ribotype 027 strains at selected time points after *C. difficile* inoculation as determined by quantitative PCR.

027 CIs in Fecal Community Background Competitions			
	Days post <i>C. difficile</i> inoculation		
	3	7	11
CD2015 (027) + CD3014 (001)	0.06 ⁺	0.75 ⁺	8.09 ⁺
	0.52 ⁺	1.19 ⁺	3.74 ^{+*}
	0.22 ⁺	0.49 ⁺	0.88 ⁺
	3.30 ⁺	22.39 ^{+*}	ND
	3.19	18.59	ND
	0.11	3.36	36.17
CD3017 (027) + CD1014 (014)	119.15	36.93	3.83
	11.88	21.91	33.05
	17.15	22.84	18.13
	232.86	3993.21	ND
	8.15	86.92 [*]	23.43 [‡]
CD4015 (027) + CD2048 (053)	8.11 ⁺	4.97 ⁺	24.59 ⁺
	11.16 ⁺	34.62 ⁺	52.47 ⁺
	8.44 ⁺	1.41 ⁺	18.34 ⁺
	138.94 [*]	593.38 [*]	ND
	20.21	21.26	40.32
CD4010 (027) + CD4004 (002)	19.43	183.55	107.20 [*]
	15.24	30.34	9.14 [*]
	12.97	31.27	50.09 [*]
	27.22	627.14 [*]	ND
	43.71 [*]	764.94 [*]	1386.61 [*]

ND= not determined

* Ratio calculated based upon limit of detection for non-027 ribotype

⁺ CI's calculated 1 day later than the day indicated than the column heading.

[‡]CI's calculated 1 day earlier than the day indicated than the column heading.

Shaded rows indicate replicates where *C. difficile* was added to the MBRAs post-cessation of clindamycin dosing 24 hrs later than the other replicates.

Table S3.2. Primers used for qPCR.

Target Gene	Primer sequences (Forward & Reverse)	Citation
<i>C. difficile tcdA</i>	F: AGC TTT CGC TTT AGG CAG TG R: ATG GCT GGG TTA AGG TGT TG	This study
Bacterial 16S <i>rRNA</i>	F: ACT CCT ACG GGA GGC AGC AG R: ATT ACC GCG GCT GCT GG	(55)
<i>C. difficile thyA</i>	F: GAT GGC CAG CCT GCT CAT ACA ATA R: TGT TTC ATC AGC CCA GCT ATC CCA	This study
<i>C. difficile thyX</i>	F: CCA GTT GGG ACA GAC GAA AT R: TGA ACA AGC CCT TGA AAT ACC	This study

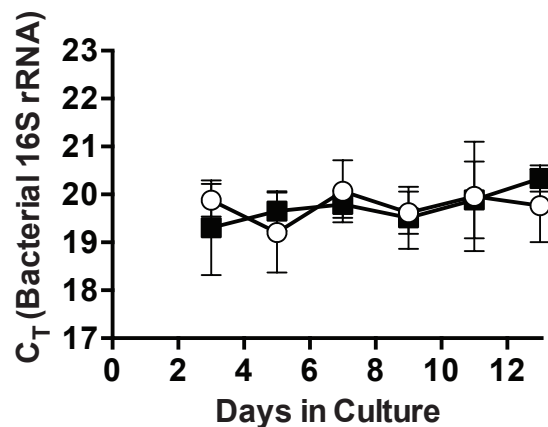


Figure S3.1. Bacterial abundance does not change significantly in clindamycin-treated reactors. We measured the relative abundance of 16S rRNA gene copies in bioreactor samples from triplicate clindamycin-treated (open circles) and mock-treated reactors (closed-squares) using quantitative PCR with previously described broad-range 16S rRNA gene qPCR primers (55). We have reported the average cycle threshold (C_T , \pm standard deviation) where the qPCR reactions began amplifying linearly. We did not determine absolute quantification of 16S rRNA gene copies in the samples because the sample populations are composed of mixtures of bacteria with different 16S rRNA gene copy numbers. Clindamycin or mock-treatment began on day 2.5 in culture and continued twice daily through day 6.

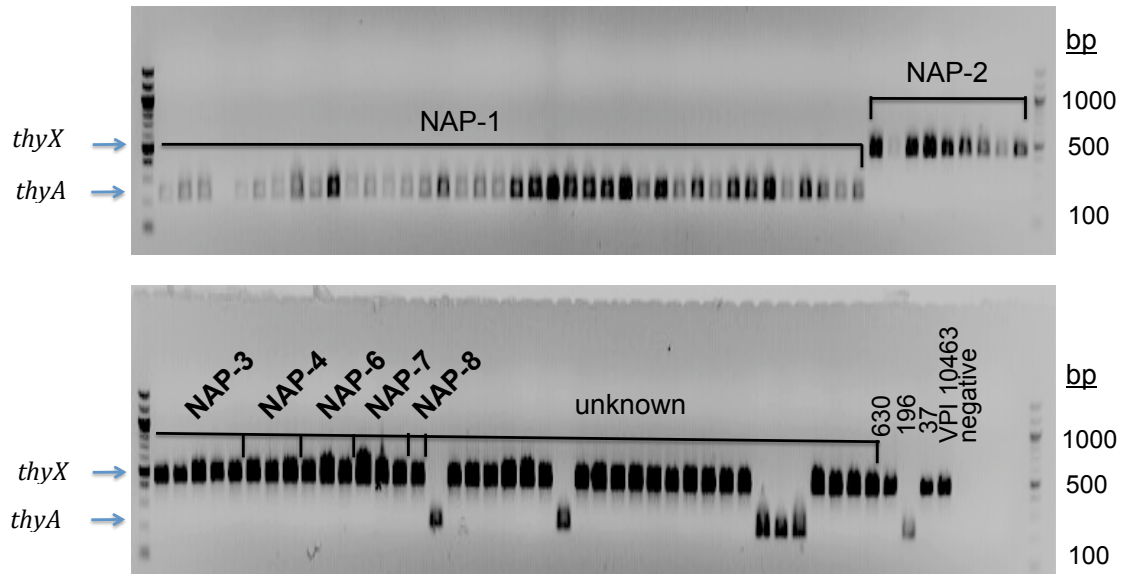


Figure S3.2. PCR screen of DNA samples from 88 strains of *C. difficile* for detection of insert containing *thyA* or the uninterrupted *thyX*.

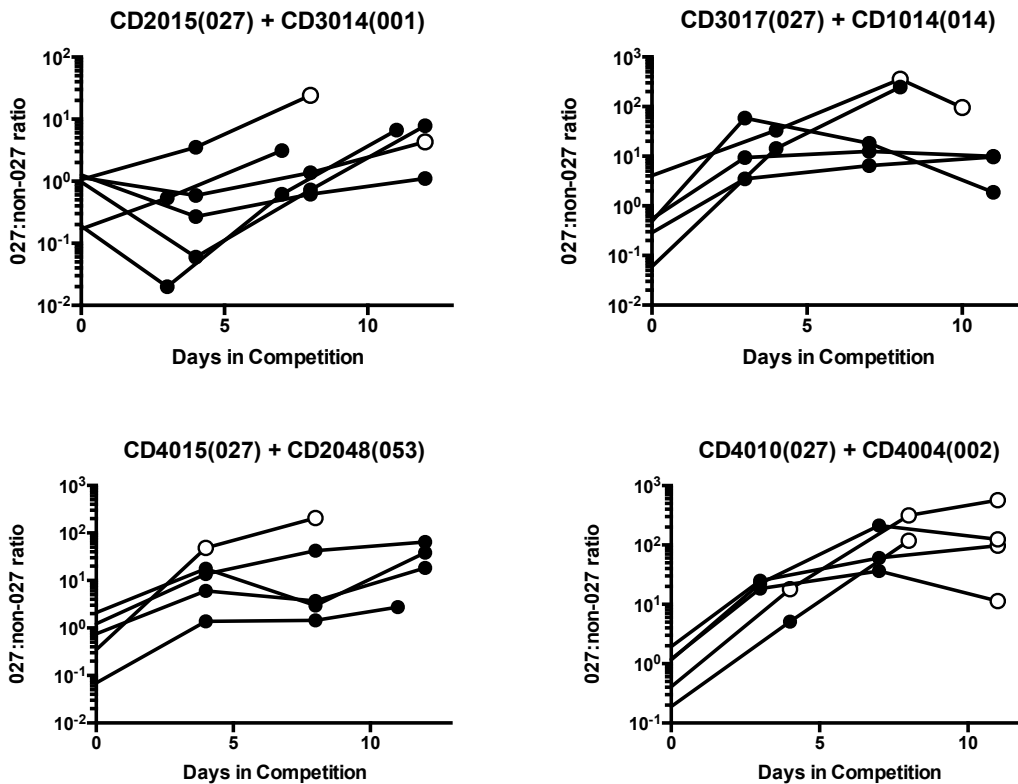


Figure S3.3. Ratios of ribotype 027:non-027 *C. difficile* strains over time in MBRA competitions. Each plot represents a different competition pair of one ribotype 027 and one non-027 ribotype strain; ribotypes indicated in parentheses above. Each line in the plots represents a replicate reactor, combined from three independent experiments. Where the non-027 ribotype strain was below the limit of detection, the ratio was determined by substituting in the highest C_T value in the linear range (detection limit) for the non-027 value (open circles).

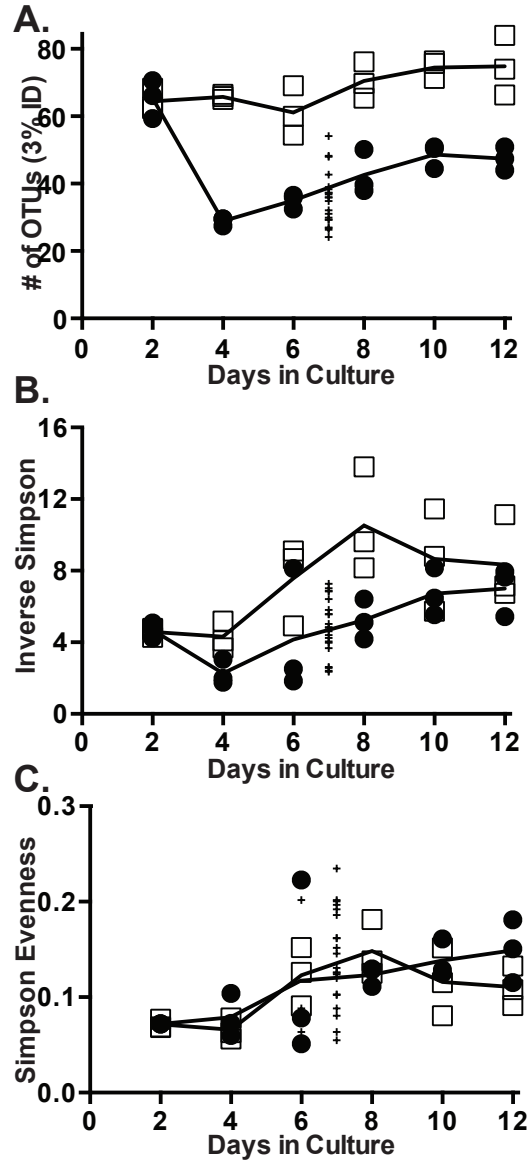


Figure S3.4. Comparison of the community structure on day 7 from clindamycin-treated reactors used for *C. difficile* competition experiments to triplicate mock-treated and clindamycin-treated reactors infected with CD2015. As described in Fig. 3.4, we analyzed the 16S *rRNA* gene abundances (binned into OTUs with 3% sequence identity) from three mock-treated and clindamycin-treated communities on days 2, 4, 6, 8, 10 and 12 in culture and compared these to samples from all competitions described (except one replicate each of 2015/3014 and 4010/4004 competitions; these are not plotted due to technical failures of the sample analysis) on day 7 just prior to the addition of *C. difficile*. We plotted the number of OTUs (A), inverse Simpson microbial diversity indicator (B), and Simpson evenness indicator (C) in the clindamycin (closed circles), mock-treated (open squares), and competition (plus symbols) communities.

The solid lines represent the mean values for the triplicate clindamycin-treated and mock-treated samples at each time point, which are reproduced from Fig. 3.4.

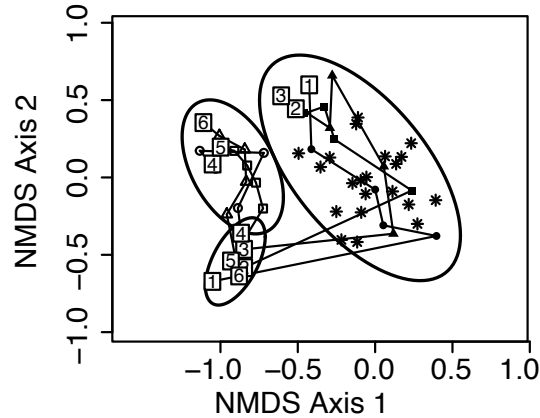


Figure S3.5. Similar community structure changes were observed in response to clindamycin-treatment in competition bioreactor communities. As described in Fig. 3.5, we plotted the Bray-Curtis dissimilarity (3% OTUs) between samples using nonmetric multidimensional scaling (NMDS). Samples were plotted from three clindamycin-treated replicates (1-3; closed symbols) and three mock-treated replicates (4-6; open symbols) every two days from day 2 (pre-treatment) through day 12. The numbers in boxes indicate the points for the indicated reactors on day 2 and day 12 and correspond to the reactor numbers indicated in Fig. 3.2. Intervening time points are represented by symbols and are connected in sequential order by lines. Asterisks represent the day 7 samples from the competition bioreactor communities described in Fig. S3.4. The ellipses indicate the 95% confidence intervals for the indicated groups (pre-treatment; mock-treatment; clindamycin-treatment.) The plot stress was 0.201.

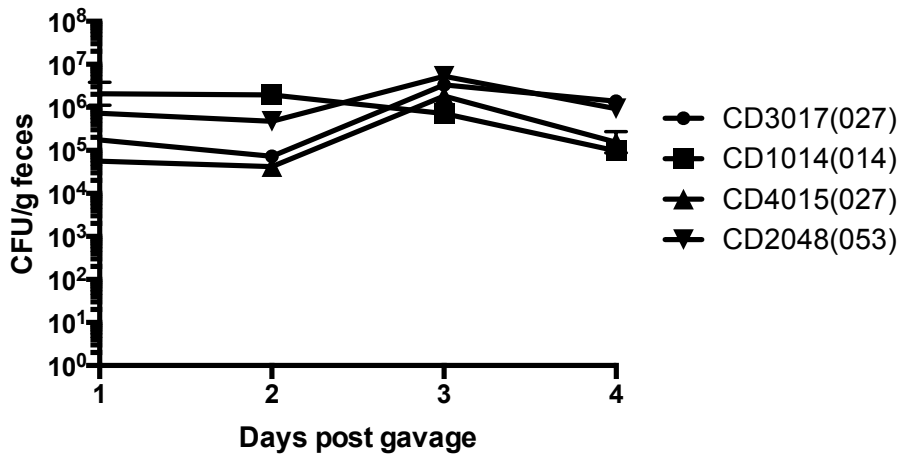


Figure S3.6. Levels of *C. difficile* strains across time in mouse model of infection as determined by plating from fecal pellets. After antibiotic treatment, mice were gavaged with spores from each individual ribotype. Fecal samples were collected daily for four days. For each time point, fecal samples were weighed, suspended in sterile water, heat killed for 30 min at 65°C, and plated on BHIS containing 0.1% taurocholic acid. Plotted here are the mean CFU/g feces from replicate mice for each strain group (with standard deviations where applicable; some data points were lost due to technical failure; two groups lost a triplicate mouse after day 1).

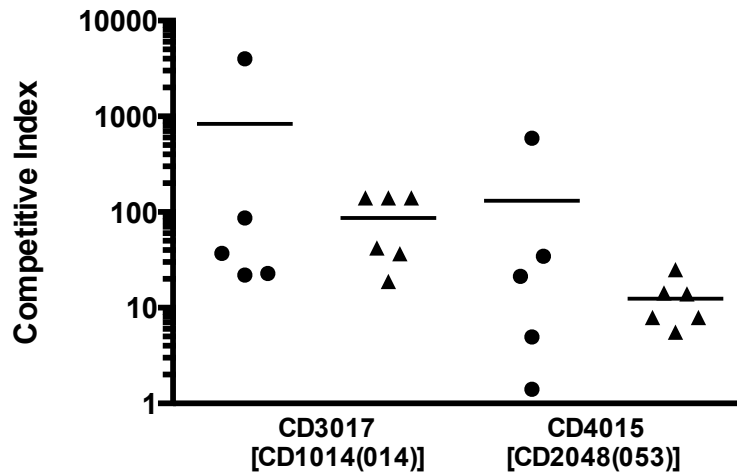


Figure S3.7. Competitive indices (CI) of two competition pairs of ribotype 027 and non-027 *C. difficile* strains in the MBRA (circles) and Mouse (triangles) models. When comparing the relative differences between the CI's of the competition pairs in each model, the mean CI of the CD3017/CD1014 competition pair is higher than the CD4015/CD2048 competition pair in both models.

REFERENCES

REFERENCES

1. **Yassin SF, Young-Fadok TM, Zein NN, Pardi DS.** 2001. Clostridium difficile-associated diarrhea and colitis. *Mayo Clin. Proc.* **76**:725–730.
2. **Bartlett JG.** 1992. Antibiotic-associated diarrhea. *Clin. Infect. Dis.* **15**:573–581.
3. **Wiström J, Norrby SR, Myhre EB, Eriksson S, Granström G, Lagergren L, Englund G, Nord CE, Svenungsson B.** 2001. Frequency of antibiotic-associated diarrhoea in 2462 antibiotic-treated hospitalized patients: a prospective study. *J. Antimicrob. Chemother.* **47**:43–50.
4. **Wilson KH, Freter R.** 1986. Interaction of Clostridium difficile and Escherichia coli with microfloras in continuous-flow cultures and gnotobiotic mice. *Infection and Immunity* **54**:354–358.
5. **Britton RA, Young VB.** 2012. Interaction between the intestinal microbiota and host in Clostridium difficile colonization resistance. *Trends in Microbiology* **20**:313–319.
6. **Miller BA, Chen LF, Sexton DJ, Anderson DJ.** 2011. Comparison of the Burdens of Hospital-Onset, Healthcare Facility–Associated Clostridium difficile Infection and of Healthcare-Associated Infection due to Methicillin-Resistant Staphylococcus aureus in Community Hospitals. *Infection Control and Hospital Epidemiology* **32**:387–390.
7. **Loo VG, Poirier L, Miller MA, Oughton M, Libman MD, Michaud S, Bourgault A-M, Nguyen T, Frenette C, Kelly M, Vibien A, Brassard P, Fenn S, Dewar K, Hudson TJ, Horn R, René P, Monczak Y, Dascal A.** 2005. A predominantly clonal multi-institutional outbreak of Clostridium difficile-associated diarrhea with high morbidity and mortality. *N. Engl. J. Med.* **353**:2442–2449.
8. **Miller M, Gravel D, Mulvey M, Taylor G, Boyd D, Simor A, Gardam M, McGeer A, Hutchinson J, Moore D, Kelly S.** 2010. Health Care–Associated Clostridium difficile Infection in Canada: Patient Age and Infecting Strain Type Are Highly Predictive of Severe Outcome and Mortality. *Clin Infect Dis* **50**:194–201.
9. **Pepin J.** 2005. Mortality attributable to nosocomial Clostridium difficile-associated disease during an epidemic caused by a hypervirulent strain in Quebec. *Canadian Medical Association Journal* **173**:1037–1042.
10. **Hubert B, Loo VG, Bourgault A-M, Poirier L, Dascal A, Fortin E, Dionne M, Lorange M.** 2007. A portrait of the geographic dissemination of the

Clostridium difficile North American pulsed-field type 1 strain and the epidemiology of *C. difficile*-associated disease in Québec. *Clin Infect Dis* **44**:238–244.

11. **Bartlett JG.** 2006. Narrative review: the new epidemic of *Clostridium difficile*-associated enteric disease. *Ann. Intern. Med.* **145**:758–764.
12. **Kuijper EJ, van Dissel JT.** 2008. Spectrum of *Clostridium difficile* infections outside health care facilities. *Canadian Medical Association Journal* **179**:747–748.
13. **McDonald LC, Killgore GE, Thompson A, Owens RC, Kazakova SV, Sambol SP, Johnson S, Gerding DN.** 2005. An epidemic, toxin gene-variant strain of *Clostridium difficile*. *N. Engl. J. Med.* **353**:2433–2441.
14. **Morgan OW, Rodrigues B, Elston T, Verlander NQ, Brown DFJ, Brazier J, Reacher M.** 2008. Clinical Severity of *Clostridium difficile* PCR Ribotype 027: A Case-Case Study. *PLoS One* **3**:e1812.
15. **Sirard S, Valiquette L, Fortier LC.** 2011. Lack of Association between Clinical Outcome of *Clostridium difficile* Infections, Strain Type, and Virulence-Associated Phenotypes. *Journal of Clinical Microbiology* **49**:4040–4046.
16. **Cloud J, Noddin L, Pressman A, Hu M, Kelly C.** 2009. *Clostridium difficile* strain NAP-1 is not associated with severe disease in a nonepidemic setting. *Clin. Gastro. Hep.* **7**:868–873.
17. **Walk ST, Micic D, Jain R, Lo ES, Trivedi I, Liu EW, Almassalha LM, Ewing SA, Ring C, Galecki AT.** 2012. *Clostridium difficile* ribotype does not predict severe infection. *Clin Infect Dis.* **55**:1661-1668.
18. **Walker AS, Eyre DW, Wyllie DH, Dingle KE, Griffiths D, Shine B, Oakley S, O'Connor L, Finney J, Vaughan A, Crook DW, Wilcox MH, Peto TEA.** 2013. Relationship Between Bacterial Strain Type, Host Biomarkers, and Mortality in *Clostridium difficile* Infection. *Clin Infect Dis.* **56**:1589-1600.
19. **Hensgens MPM, Goorhuis A, Dekkers OM, van Benthem BHB, Kuijper EJ.** 2013. All-Cause and Disease-Specific Mortality in Hospitalized Patients With *Clostridium difficile* Infection: A Multicenter Cohort Study. *Clin Infect Dis* **56**:1108–1116.
20. **Waslawski S, Lo ES, Ewing SA, Young VB, Aronoff DM, Sharp SE, Novak-Weekley SM, Crist AE, Dunne WM, Hoppe-Bauer J, Johnson M, Brecher SM, Newton DW, Walk ST.** 2013. *Clostridium difficile* ribotype diversity at six health care institutions in the United States. *Journal of Clinical Microbiology* **51**:1938–1941.

21. **He M, Miyajima F, Roberts P, Ellison L, Pickard DJ, Martin MJ, Connor TR, Harris SR, Fairley D, Bamford KB, D'Arc S, Brazier J, Brown D, Coia JE, Douce G, Gerding D, Kim HJ, Koh TH, Kato H, Senoh M, Louie T, Michell S, Butt E, Peacock SJ, Brown NM, Riley T, Songer G, Wilcox M, Pirmohamed M, Kuijper E, Hawkey P, Wren BW, Dougan G, Parkhill J, Lawley TD.** 2013. Emergence and global spread of epidemic healthcare-associated *Clostridium difficile*. *Nat Genet* **45**:109–113.
22. **Freeman J.** 2003. Effects of cefotaxime and desacetylcefotaxime upon *Clostridium difficile* proliferation and toxin production in a triple-stage chemostat model of the human gut. *Journal of Antimicrobial Chemotherapy* **52**:96–102.
23. **Honda H, Hoyles L, Gibson GR, Farmer S, Keller D, McCartney AL.** 2011. Impact of GanedenBC30 (*Bacillus coagulans* GBI-30, 6086) on population dynamics of the human gut microbiota in a continuous culture fermentation system. *Anaerobe*. **17**:36-42.
24. **Baines SD, Crowther GS, Todhunter SL, Freeman J, Chilton CH, Fawley WN, Wilcox MH.** 2013. Mixed infection by *Clostridium difficile* in an in vitro model of the human gut. *Journal of Antimicrobial Chemotherapy* **68**:1139–1143.
25. **Sorg JA, Dineen SS.** 2005. *Laboratory Maintenance of Clostridium difficile*. John Wiley & Sons, Inc., Hoboken, NJ, USA.
26. **Antonopoulos DA, Huse SM, Morrison HG, Schmidt TM, Sogin ML, Young VB.** 2009. Reproducible Community Dynamics of the Gastrointestinal Microbiota following Antibiotic Perturbation. *Infection and Immunity* **77**:2367–2375.
27. **Consortium THMP.** 2012. Structure, function and diversity of the healthy human microbiome. *Nature* **486**:207–214.
28. **Schloss PD.** 2009. A High-Throughput DNA Sequence Aligner for Microbial Ecology Studies. *PLoS ONE* **4**:e8230.
29. **Schloss PD, Gevers D, Westcott SL.** 2011. Reducing the Effects of PCR Amplification and Sequencing Artifacts on 16S rRNA-Based Studies. *PLoS ONE* **6**:e27310.
30. **Edgar RC, Haas BJ, Clemente JC, Quince C, Knight R.** 2011. UCHIME improves sensitivity and speed of chimera detection. *Bioinformatics* **27**:2194–2200.
31. **Schloss PD, Westcott SL.** 2011. Assessing and improving methods used in operational taxonomic unit-based approaches for 16S rRNA gene sequence

- analysis. *Applied and Environmental Microbiology* **77**:3219–3226.
32. **White JR, Nagarajan N, Pop M.** 2009. Statistical Methods for Detecting Differentially Abundant Features in Clinical Metagenomic Samples **5**:e1000352.
 33. **Oksanen J, Blanchet FG, Kindt R, Legendre P, Minchin PR, O'Hara RB, Simpson GL, Solymos P, Stevens MHH, Wagner H.** 2013. *vegan*: Community Ecology Package. R package version 2.0-9.
 34. **Knetsch CW, Hensgens MPM, Harmanus C, van der Bijl MW, Savelkoul PHM, Kuijper EJ, Corver J, van Leeuwen HC.** 2011. Genetic markers for *Clostridium difficile* lineages linked to hypervirulence. *Microbiology* **157**:3113–3123.
 35. **Pfaffl MW.** 2001. A new mathematical model for relative quantification in real-time RT-PCR. *Nucleic Acids Research* **29**:e45.
 36. **Chen X, Katchar K, Goldsmith JD, Nanthakumar N, Cheknis A, Gerding DN, Kelly CP.** 2008. A mouse model of *Clostridium difficile*-associated disease. *Gastroenterology* **135**:1984–1992.
 37. **Bartlett JG.** 1981. Antimicrobial agents implicated in *Clostridium difficile* toxin-associated diarrhea of colitis. *Johns Hopkins Med J* **149**:6–9.
 38. **Jernberg C, Löfmark S, Edlund C, Jansson JK.** 2010. Long-term impacts of antibiotic exposure on the human intestinal microbiota. *Microbiology* **156**:3216–3223.
 39. **CLARKE KR.** 1993. Non-parametric multivariate analyses of changes in community structure **18**:117–143.
 40. **Reeves AE, Theriot CM, Bergin IL, Huffnagle GB, Schloss PD, Young VB.** 2011. The interplay between microbiome dynamics and pathogen dynamics in a murine model of *Clostridium difficile* Infection. *gutmicrobes* **2**:145–158.
 41. **Antharam VC, Li EC, Ishmael A, Sharma A, Mai V, Rand KH, Wang GP.** 2013. Intestinal dysbiosis and depletion of butyrogenic bacteria in *Clostridium difficile* infection and nosocomial diarrhea. *Journal of Clinical Microbiology* **51**:2884–2892.
 42. **Merrigan M, Venugopal A, Mallozzi M, Roxas B, Viswanathan VK, Johnson S, Gerding DN, Vedantam G.** 2010. Human Hypervirulent *Clostridium difficile* Strains Exhibit Increased Sporulation as Well as Robust Toxin Production. *Journal of Bacteriology* **192**:4904–4911.
 43. **Akerlund T, Persson I, Unemo M, Noren T, Svenungsson B, Wullt M,**

- Burman LG.** 2008. Increased Sporulation Rate of Epidemic *Clostridium difficile* Type 027/NAP1. *Journal of Clinical Microbiology* **46**:1530–1533.
44. **Burns DA, Heeg D, Cartman ST, Minton NP.** 2011. Reconsidering the sporulation characteristics of hypervirulent *Clostridium difficile* BI/NAP1/027. *PLoS ONE* **6**:e24894.
45. **Carlson PE, Walk ST, Bourgis AET, Liu MW, Kopliku F, Lo E, Young VB, Aronoff DM, Hanna PC.** 2013. The relationship between phenotype, ribotype, and clinical disease in human *Clostridium difficile* isolates. *Anaerobe* **24**:109–116.
46. **Francis MB, Allen CA, Sorg JA.** 2013. Muricholic Acids Inhibit *Clostridium difficile* Spore Germination and Growth. *PLoS ONE* **8**:e73653.
47. **Heeg D, Burns DA, Cartman ST, Minton NP.** 2012. Spores of *Clostridium difficile* Clinical Isolates Display a Diverse Germination Response to Bile Salts. *PLoS ONE* **7**:e32381.
48. **Escartin F, Skouloubris S, Liebl U, Myllykallio H.** 2008. Flavin-dependent thymidylate synthase X limits chromosomal DNA replication. *Proceedings of the National Academy of Sciences* **105**:9948–9952.
49. **Van den Abbeele P, Grootaert C, Marzorati M, Possemiers S, Verstraete W, Gerard P, Rabot S, Bruneau A, Aidy El S, Derrien M, Zoetendal E, Kleerebezem M, Smidt H, Van de Wiele T.** 2010. Microbial Community Development in a Dynamic Gut Model Is Reproducible, Colon Region Specific, and Selective for Bacteroidetes and *Clostridium* Cluster IX. *Applied and Environmental Microbiology* **76**:5237–5246.
50. **Rajilic-Stojanovic M, Maathuis A, Heilig HGHJ, Venema K, de Vos WM, Smidt H.** 2010. Evaluating the microbial diversity of an in vitro model of the human large intestine by phylogenetic microarray analysis. *Microbiology* **156**:3270–3281.
51. **Macfarlane G, Macfarlane S, Gibson G.** 1998. Validation of a Three-Stage Compound Continuous Culture System for Investigating the Effect of Retention Time on the Ecology and Metabolism of Bacteria in the Human Colon. *Microbial Ecology* **35**:180–187.
52. **Payne AN, Zihler A, Chassard C, Lacroix C.** 2012. Advances and perspectives in in vitro human gut fermentation modeling. *Trends in Biotechnology* **30**:17–25.
53. **Eyre DW, Cule ML, Griffiths D, Crook DW, Peto TEA, Walker AS, Wilson DJ.** 2013. Detection of Mixed Infection from Bacterial Whole Genome Sequence Data Allows Assessment of Its Role in *Clostridium difficile* Transmission. *PLoS*

Comp Biol **9**:e1003059.

54. **Behroozian AA, Chludzinski JP, Lo ES, Ewing SA, Waslawski S, Newton DW, Young VB, Aronoff DM, Walk ST.** 2013. Detection of Mixed Populations of *Clostridium difficile* from Symptomatic Patients Using Capillary-Based Polymerase Chain Reaction Ribotyping. *Infection Control and Hospital Epidemiology* **34**:961–966.
55. **Fierer N, Jackson JA, Vilgalys R, Jackson RB.** 2005. Assessment of soil microbial community structure by use of taxon-specific quantitative PCR assays. *Appl Microbiol* **71**:4117–4120.

CHAPTER 4

Differential Metabolism of Trehalose by Epidemic Ribotypes of *Clostridium difficile*

Introduction

Clostridium difficile is one of the primary causative agents of antibiotic-associated diarrhea (1). While Bartlett *et al.* first described this association almost four decades ago in 1978, it is still poorly understood why disease generally only occurs following antibiotic treatment (2). Several factors from the perspectives of the host and microbiota likely contribute to the complex dynamics of both resistance and susceptibility to *C. difficile* infection (CDI). However, mechanisms of colonization resistance and competitive inhibition are believed to play a role (reviewed in (3)). Competition for nutrients is one of the mechanisms governing colonization resistance, and although evidence to support this in the case of establishment of CDI exists, we do not have a complete understanding of the role of nutrient availability (4-6). Therefore, there is still much to be learned in terms of how *C. difficile* metabolism and competition for nutrients contribute to colonization and establishment of disease. Moreover, recent increases in the incidence and severity of CDI correlate with the emergence of epidemic-associated lineages of *C. difficile*, primarily ribotype 027 (RT 027) (7-10). In chapter 3 we show that RT 027 strains are able to out-compete strains of other ribotypes in the presence of complex fecal

communities in an *in vitro* model of *C. difficile* invasion. Furthermore, we speculate that there are aspects of RT 027 strain physiology related to nutrient utilization that play a role in this increased competitive fitness.

In this chapter, I will present work that was performed to investigate carbon source utilization of *C. difficile* with particular emphasis on identifying carbon sources that RT 027 strains differentially metabolize. The primary nutrients and carbon sources utilized by *C. difficile* during outgrowth in the gastrointestinal tract are not well explored. Identifying compounds that support *C. difficile* growth in the context of the intestinal environment would increase our understanding in this area and provide insight into knowing which nutritional factors are important for *C. difficile* gut colonization. Additionally, elucidating if RT 027 strains have the ability to utilize a wider range of nutrients, or specific nutrients more efficiently, might help to explain the competitive advantage of RT 027 strains. Moreover, it would provide further evidence to support the hypothesis that these strains have become more prevalent due to differences in physiology rather than, or in addition to, differences related to traditional virulence factors.

Most of the experimental work in this chapter focuses on *C. difficile* metabolism of a glucose disaccharide sugar, trehalose. Trehalose is a naturally occurring sugar consisting of two glucose subunits linked by an α,α -1,1-glycosidic bond (11). Trehalose synthesis occurs in organisms in all three domains of life (12). Initially, trehalose was thought to primarily serve as an energy storage molecule, however, many more biological functions of this molecule have since been discovered (reviewed in (11, 13)). These functions include incorporation in cellular

structural components, transport, intracellular signaling, and regulation (11, 13). Furthermore, because of its particular chemical characteristics, intracellular accumulation of trehalose provides stabilization of biological molecules, providing protection against osmotic, heat, cold, and oxidative stresses (14-17).

Availability of trehalose in the gastrointestinal tract has not been well defined and it is not included in studies quantifying other intestinally relevant sugars such as glucose, sucrose, maltose, and lactose. Nonetheless, there are several pieces of evidence supporting its presence and potential role in colonization. First, brush border enterocytes of the small intestine express trehalase, the enzyme required to breakdown trehalose into its glucose subunits which can then be absorbed and metabolized (18). Historically, the primary dietary sources of trehalose were mushrooms, insects, lobsters and crabs, honey, and baker's yeast (13). More recently, consumption of trehalose is increasing due to increased use in commercial food production since being granted GRAS (Generally Recognized As Safe) status by the US FDA in 2000. Furthermore, other countries/regions have approved its use as a food additive including Korea and Taiwan in 1998, the UK in 1991, Canada in 2005, and Europe in 2001. An extensive report published by Hayashibara International Inc. addressing the safety of trehalose based on several toxicity studies prompted this approval in several countries (13). Trehalose has unique chemical properties that make it useful in the food industry, including use as a stabilizing agent and texturizer in various foods, cryoprotectant in freeze dried foods, and a sweetening agent. Indeed, estimates regarding consumption of trehalose by the average adult in the US are as high as 16 g/day (13). In addition, a

rare condition of trehalose intolerance in some individuals has been reported, which is caused by insufficient trehalase activity in the small intestine, and results in intestinal symptoms similar to those of lactose intolerance upon ingestion of trehalose-containing foods (19, 20).

A recent proteomic analysis of *C. difficile* proteins expressed in a pig ileal-ligated loop model reported a 2-fold increase in TreA expression *in vivo* compared to *in vitro*, supporting the presence of trehalose in the intestinal environment (21). Moreover, the role of trehalose in colonization of other intestinal pathogens has been shown (22). Martindale *et al.* used an infant rat gut model to investigate genes important for intestinal colonization of *Escherichia coli* (23). They identified a *treB* mutant of *Escherichia coli* that was defective in colonization; TreB is a trehalose-specific component of the phosphotransferase system required for uptake of trehalose.

Finally, as discussed above, many bacterial organisms are able to synthesize and maintain intracellular stores of trehalose. Indeed, if any members of the intestinal microbiota had intracellular stores of trehalose, this would present a source of trehalose upon microbial lysis after antibiotic treatment. Taken together, all of this evidence supports that trehalose is a relevant nutrient in the gastrointestinal environment and has the potential to play a role in *C. difficile* colonization.

Very little work has been done regarding metabolism of trehalose by *C. difficile*. Genome annotation data suggest that *C. difficile* solely uses trehalose as a carbon source, and that the genes required to synthesize trehalose are absent. It

only harbors *treA*, the gene that codes for the trehalase enzyme, and *treR*, the *treA* repressor. It is not surprising that it does not appear to be able to also synthesize trehalose for use in energy storage or stress resistance, as this functional capacity occurs primarily in Gram-negative bacteria (12). In terms of regulation of trehalose utilization genes, however, Antunes *et al.* used *in silico* analysis to identify predicted CcpA-dependent carbon catabolite-regulated genes in *C. difficile*, including *treR* (24).

Here we show that RT 027 strains, and strains of another highly prevalent epidemic-associated ribotype (RT 078), grow to higher cell densities on trehalose. In the case of RT 027 this is potentially due to an identified amino acid substitution in TreR within these strains. This is supported by the observation that RT 027 strains have increased *treA* expression. In addition, a *treA* knockout mutant in CD630 was generated and preliminary mouse studies using the wild-type and mutant strains suggest that trehalose plays a role in colonization and competitive fitness. Should this result translate into the human gastrointestinal tract, it is possible that the ability of RT 027 strains to grow better on trehalose would give them a competitive advantage. Furthermore, this physiological trait could partially explain the prevalence of RT 027 strains.

Materials and Methods

C. difficile strains used in this study and growth conditions

All strains (except CD630 and CD196) were provided to the Britton laboratory by the Michigan Department of Community Health, who determined the toxinotypes and did the PFGE typing (Table 4.1). Strains were collected from infected patients at either Southeast Michigan or Mid-Michigan Hospitals between 11/2007 and 5/2008. Strains CD630, CD630 Δ erm and CD196 were kindly provided by the laboratory of Lincoln Sonnenshein (Tufts University). Ribotyping of the strains was determined by Seth Walk (previously of the Young laboratory, University of Michigan). All studies requiring growth of *C. difficile* were carried out in a Coy anaerobic chamber (5% hydrogen, 90% nitrogen, 5% CO₂ atmosphere), incubated at 37°C.

Table 4.1. Characterization of strains used in this study.

Strain	toxinotype	PFGE type (NAP status)	Ribotype
CD2015	III	MI_NAP1	027
CD196	III	MI-NAP1	027
CD4015	III	MI-NAP1	027
CD4001	III	MI-UN13	027
CD4010	III	MI-UN13	027
CD630	ND	ND	012
CD3014	0	MI-NAP2	001
CD4011	0	MI-NAP2	001
CD2048	0	MI-NAP3	053
CD1007	0	MI-NAP3	053
CD1014	0	MI-NAP4	014
CD2012	0	MI-NAP6	002
CD1015	V	MI-NAP7	078
CD1018	V	MI-NAP7	078
CD2001	V	MI-NAP8	078

Identifying nutritional compounds that increase growth of *Clostridium*

difficile. Several different plates are available to screen compounds that can serve as carbon, nitrogen, phosphorus and sulfur sources as well as nutritional supplements such as peptides, fatty acids, and vitamins. A list of the different plates (PM1-PM10) and their compounds can be found at:

http://www.biolog.com/pdf/pm_lit/PM1-PM10.pdf. Selected medium was inoculated (1:100) with overnight culture (CD630 or CD2015) and then 100 μ l added to the wells of the entire Phenotype MicroArray plate. Growth was monitored using a Tecan Sunrise spectrophotometer, reading every 20 minutes (OD_{600}) for 24 hrs under anaerobic conditions at 37°C. Two types of media were used for these experiments- a defined medium developed for *C. difficile* ((25)), and modified sporulation medium. The defined medium was made following the published recipe (Table 4.2) with a few modifications; glucose was omitted for all Phenotype MicroArray plate experiments, and for plates PM3-8, only essential amino acids were added (see table legend). The other medium used is a variation of the *C. difficile* sporulation medium published by Wilson *et al.* (26), named MSM for “modified smorulation medium”. MSM contained: 22.5 g/L trypticase peptone (VWR), 1 g/L $(NH_4)_2SO_4$, and 1.5 g/L tris base (Invitrogen); adjusted to pH 7.5 and autoclaved at 121° C for 30 min. The sporulation medium was chosen because it is simple, composed only of peptones and salts, and was diluted four-fold in order to provide a low level of growth and allow for detectability of increased yields. Growth yields were determined as the maximum OD_{600} of the growth curve for individual

wells. Compounds that increased the maximum OD₆₀₀ by at least 1.5-fold were concluded to confer a growth advantage.

Table 4.2. Defined medium ingredients and concentrations. *these amino acids were the only ones added for medium used in Biolog Phenotype MicroArray plates PM3-8.

Amino acids:	mg/L	Vitamins:	mg/L
histidine	100	thiamin	1
		calcium-D-	
tryptophan*	100	pantothenate	1
glycine	100	nicotinamide	1
tyrosine	100	rioflavin	1
arginine	200	pyridoxine	1
phenylalanine	200	<i>p</i> -Aminobenzoic acid	0.05
methionine	200	folic acid	0.0125
threonine	200	biotin	0.0125
alanine	200	B ₁₂	0.005
lysine	300		
serine	300	minerals:	
valine*	300	KH ₂ PO ₄	300
isoleucine*	300	Na ₂ HPO ₄	1500
aspartic acid	300	NaCl	900
leucine*	400	CaCl ₂ .2H ₂ O	26
cysteine*	500	MgCl ₂ .6H ₂ O	20
proline*	600	MnCl ₂ .4H ₂ O	10
glutamic acid	900	(NH ₄) ₂ SO ₄	40
		FeSO ₄ .7H ₂ O	4
		CoCl ₂ .6H ₂ O	1
		NaHCO ₃	5000

Growth experiments further investigating *C. difficile* utilization of compounds identified in Phenotype MicroArray plates. Compounds initially identified to increase growth in Phenotype MicroArray plates (PM1 and PM2) were used to further assess *C. difficile* growth using additional strains. Although Biolog does not provide the specific concentrations of the components in their phenotype microarray plates, they suggest follow-up studies be done in a range of 5-50mM in their carbon source plates (PM1-2) (per email correspondence with Biolog technical support). The defined medium was used (Table 4.2; all amino acids) and supplemented with N-acetyl-glucosamine (25mM), N-acetyl-neuraminic acid (10mM), alanine and hydroxyl-proline (12 mM each), mannose (25mM), or trehalose (25mM). Cultures were grown in 96-well plates (Corning Costar #CLS3595) plates by adding 200 μ L medium (+/- compound) to selected wells and inoculating with 10 μ L MSM overnight culture of selected strains. Growth was monitored using a Tecan Sunrise spectrophotometer, reading every 20 minutes (OD_{600}) for 24 hrs under anaerobic conditions (Coy anaerobic chamber with 3% hydrogen, 97% nitrogen atmosphere) at 37°C.

Trehalose growth experiments. Selected strains were grown in DM (Table 4.2; all amino acids) supplemented with the specified trehalose concentrations. Medium (200 μ L) was added to selected wells of 96-well plate and wells were inoculated with 10 μ L of overnight culture of indicated strains. Growth was monitored using a Tecan Sunrise spectrophotometer, reading every 20 minutes (OD_{600}) for 24 hrs

under anaerobic conditions (Coy anaerobic chamber with 3% hydrogen, 97% nitrogen atmosphere) at 37°C.

RT-qPCR analysis of *treA* expression.

Cultures. Selected *C. difficile* strains were grown overnight in 5 ml DM (table 4.1), inoculated from fresh BHIS agar plates (made as previously described except without the addition of cysteine, (27)). Expression cultures were started by subculturing 100 µL of the overnight culture into 10 mL fresh DM supplemented with 25mM trehalose (by addition of 1M stock solution of trehalose dissolved in water and filter-sterilized). Cultures were incubated (anaerobic, 37°C) and OD₆₀₀ (optical density) monitored until an OD of ~0.1-0.2 was reached. The remaining culture (~8 mL) was mixed with an equal volume of ice cold ethanol:acetone (1:1) mix, placed on ice for 10 min, and stored at -80°C.

RNA extractions. Samples (culture, ethanol, acetone mix) were thawed on ice, and then pelleted by centrifugation for 10 min at 4°C, and the supernatant removed. Cell pellets were washed with 500 µL TE buffer (10mM Tris, 1mM EDTA, pH 7.6). From this point RNA was extracted using Qiagen RNeasy Kit (Qiagen #74104), following a modified version of the recommended protocol, starting with resuspension in 1 mL RLT buffer (to which 1:100 dilution of β-mercaptoethanol is added). Samples were then transferred to 2 ml screw-top tubes containing ~200 µl 0.1 mm silica beads (Biospec Products). The samples were homogenized by bead-beating (BioSpec Products) on the homogenize setting two times for 1 min (placed on ice for 1 min

between), centrifuged for 15 min at 21000 X g, and the supernatant was transferred to a new tube. Buffer RLT (+ 1:100 β -mercaptoethanol) was added to a total volume of 900 μ L, then vortexed. 500 μ L 100% ethanol was added, the sample vortexed, and then transferred to RNeasy spin column. The extraction protocol from here followed the handbook protocol. After the final wash with RPE buffer, RNA was eluted off the columns with 20 μ L RNase-free water. 1 μ L RNase Inhibitor (Roche #03335399001) was added to the extracted RNA; samples were stored at -80°C. Samples were treated with DNase to remove any contaminating genomic DNA using Ambion Turbo DNA-free Kit (Ambion AM1907).

Reverse Transcription. cDNA of RNA samples was synthesized using Invitrogen Superscript III reverse transcriptase (Invitrogen #18080-093) following the recommended protocol. Other reaction components used were random primers (Promega #C1181), and 10mM dNTP's (Promega #U1515). Approximately 1 ng of each RNA sample was used for cDNA synthesis. No reverse transcriptase controls were also set-up by replacing the 1 μ L reverse transcriptase with 1 μ L water in those reactions; all other components were the same.

Real-Time PCR reactions. Real-time PCR reactions were performed in triplicate and contained the following components: 1 μ L cDNA (undiluted (treA), 1:100 dilution in sterile water (16S *rRNA*), or 1:100 dilution of -RT control sample), 10 μ L Power SYBR Green PCR Master Mix (ABI, Carlsbad, CA), 0.25 μ L each primer (20 μ M) (Supplementary Table 4.3), and 8.5 μ L Milli-Q water. Triplicate water controls

were also run; 1 μ L water replaced the cDNA template. Real-time PCR was performed using an Eppendorf Mastercycler PCR machine under the following conditions: 95°C 10 min, 40 cycles of 95°C for 15 sec followed by 60°C for 1 min. A 20 min melting curve was also performed from 60°C to 95°C. Standard curves of cDNA were run to determine primer efficiencies. The template used for standard curves was the sample with the lowest C_T values, diluted 4 logs into sterile water. Primer efficiencies (E) were calculated by the method published by Pfaffl *et al.* (28); *treA* E= 1.95; 16s rRNA E= 1.93. Expression of *treA* at the stopping point of each culture was determined using the average of the triplicate C_T values from each sample and the following equation: $[E_{treA}(1.95)^{(25-sample C_T)}]/[E_{16s}(1.93)^{(10-sample C_T)}]$ (28). A baseline expression C_T signal for all samples was used which was approximately the average C_T value for all strains in medium supplemented with glucose instead of trehalose. This was done to normalize the variation seen in the baseline expression of *treA* in control cultures (those without trehalose) where aberrant expression levels in some replicate cultures were observed. Aberrantly high baseline expression effectively would otherwise decrease the fold-induction of *treA* in those samples and not be representative of the true levels of *treA* transcripts in the presence of trehalose.

Table 4.3. Primers used in this study.

Target Gene (reference)	Sequence
<i>C. difficile</i> <i>treA</i> (this work)	Fwd: tacgctgatggcctcctat Rev: cgctcctttataatctgtttc
<i>C. difficile</i> 16s rRNA {Rinttila:2004da}	Fwd: ttgagcgatttacttcggtaaaga Rev: ccatcctgtactggctcacct
<i>treA</i> IBS1.2_Intron retarget (this work)	atatcaagcttttgcaaccacgtcgatcgtgaataga agattattgtgcgccagatagggtg
<i>treA</i> EBS1_Intron retarget (this work)	cagattgtacaaatgtgggtataacagataagtcatta ttattaacttacctttcttgt
<i>treA</i> EBS2_Intron retarget (this work)	cgcaagtttctaatttcggttttctatcgatagaggaaa gtgtct
<i>treA</i> knock-out screen (this work)	Fwd: gcaacaatgatggataggtgatataaatgg Rev: ggaacagaaccatcaggtttagca
qPCR- wild-type specific	Fwd: ggtagctcctatgtacgtttct Rev: caaagtcactcattgtccatattt
qPCR- <i>treA</i> mutant specific	Fwd: tcctccttctattaggcattcttg Rev: ggagaacctatgggaacgaaac

Alignments of TreA amino acid sequences from *C. difficile* clinical isolates and other Gram-positive bacteria. Whole genome sequencing (Illumina MiSeq) was conducted on several of the *C. difficile* clinical isolates obtained from the MDCH used in this study by the MSU Research and Technology Support Facility. Genome sequence files were assembled *de novo* using the next generation sequencing assembly algorithm, Velvet (www.ebi.ac.uk/~zerbino/velvet/). BLAST (Basic Local Alignment Search Tool) databases were made for each genome and the *treR* sequences pulled out of the assembled contigs by searching for sequences matching the CD630 (Integrated Microbial Genomes (IMG); <https://img.jgi.doe.gov>) *treR* sequence. The *treR* sequences of other Gram-positive organisms were obtained from the public database of IMG. All alignments were done using ClustalW2 (<https://www.ebi.ac.uk/Tools/msa/clustalw2/>).

Construction of a *treA* knockout mutant in the *C. difficile* parent strain, CD630 Δ erm. We used a gene knockout system similar to the TargetTron system available through Sigma-Aldrich to generate a *treA* gene knockout mutant. This system uses a group-II intron, retargeted to the gene of interest, to generate functional knockouts. We used the protocol previously described (29, 30). Primers were designed to target the *treA* gene (CD3091) of CD630 using the *treA* gene sequence obtained from IMG (<https://img.jgi.doe.gov>). A primer design script was developed, which is a variation of the one available from Sigma for TargetTron primer design (<http://www.sigma-genosys.com/targettron/>), and was modified to be optimized to the *C. difficile* genome. The “intronator” script is available upon

request. Primers used are listed in Table 4.3. They are designed to target the intron to insert at bp 177 of *treA*. Two plasmid templates (pBL64, pBL65) were used to PCR amplify the retargeted intron fragment and ligate it into pBL100 (30). Plasmids and erythromycin-sensitive CD630 derivative strain (CD630 Δ erm) were generously provided to us by Dr. Lincoln Sonenshein's lab (Tufts University). The *treA*-targeted pBL100 plasmid was then transformed into *Escherichia coli* SD46 (provided by Dr. Craig Ellermeier, University of Iowa), and then mated into CD630 Δ erm. The resulting *treA* insertion mutant was verified by PCR using primers designed to flank the *treA* insertion site, resulting in a 350bp product for the wild-type gene and a 2.4kbp product for the gene knockout (Table 4.3).

Colonization and competition of CD630 Δ erm wild-type and *treA* mutant

strains in a mouse model of *C. difficile* infection. The previously published cefoperazone mouse model of *C. difficile* infection was used for these experiments (31). They were conducted in the laboratory of Dr. Vince Young (University of Michigan, Department of Microbiology and Immunology), by Dr. Mark Koenigskecht, a postdoctoral research associate. Four groups of C57BL/6 mice (6-8wks in age) were used in these experiments; One group (3 mice) served as no-antibiotic control, two groups (5 mice each) were infected with wild type CD630erm or *treA* knockout mutant strain, and the fourth group (5 mice) was infected with a mixture of the wild-type and mutant strains. Mice were treated with cefoperazone (0.5mg/ml) in their drinking water for 5 days, followed by two days of fresh water before oral gavage of 1×10^4 *C. difficile* spores/mouse. Spores were cultivated by

spread plating overnight BHIS cultures of *C. difficile* on BHIS medium and incubating anaerobically at 37°C for 3 days. Cells were scraped from the plates and resuspended in sterile water, heat-treated at 60°C for 30 min to kill vegetative cells, and the number of viable spores were enumerated by plating appropriate serial dilutions on BHIS supplemented with 0.1% taurocholic acid. Spore preparations were diluted in sterile water to yield $\sim 10^5$ spores/ml, then mixed, when appropriate, prior to gavaging a total of $\sim 10^4$ spores/mouse. Mice were weighed and observed daily for disease symptoms and morbidity. Fecal samples were collected daily and transferred into an anaerobic chamber within two hours of collection. Fecal samples were weighed, suspended in anaerobic PBS, serially diluted, and plated on TCCFA agar plates +/- 10 μ g/ml erythromycin. After 24-48 hrs of anaerobic incubation at 37°C, colonies were counted and the CFU/g feces was determined.

Quantitative PCR Analysis of Competitions and Calculations of Competitive

Index. For mice gavaged with a mixture of wild type and *treA* mutant strains, the strain ratios were determined by qPCR instead of plating. Strains ratios determined by qPCR will be more reflective of the actual ratios since primers are designed to specifically target each strain, while determination by plating relies on subtraction of the colonies on selective plates from the total on non-selective plates, and will be affected by inherent plating error, making small differences in ratios more difficult to resolve. DNA was extracted from fecal samples using bead beating followed by modified cleanup with a Qiagen DNEasy Tissue Kit as described (32). DNA

concentrations were determined by spectrophotometry at 260 and 280 nm (Nanodrop), and ranged from 18-48 ng/ μ L. The mixed spores preparation (1×10^5 spores/ml) used to gavage mice was treated with 0.1% taurocholate at room temperature for 20 minutes to induce germination and then bead-beated as above. The supernatant was transferred to a fresh tube and used as DNA template in the qPCR analysis. Primers were designed to specifically target the wild-type strain (flank the intron insertion site) or the *treA* mutant (intron-specific) (table 4.3). Real-time PCR reactions were set-up by combining the following components: 10 μ L Power Sybr Green PCR Master Mix (ABI, Carlsbad, CA), 0.2 μ L each primer (20 μ M), 8.6 μ L Mili-Q water, 1 μ L DNA sample. All PCR reactions were performed in technical triplicate and the C_T values are an average of the triplicate data points. The amplification efficiency (E) of each primer set was determined by plotting the C_T values of a standard curve generated by serial 4-log dilutions of the mixed-spore supernatant diluted into a DNA sample extracted from a mouse fecal pellet collected before *C. difficile* gavage (community background DNA). Primer efficiencies were calculated using the method described by Pfaffl *et al.*; $E = 10^{(-1/\text{slope})}$ (28); Efficiency_{wild-type} = 1.96, Efficiency_{mutant} = 2.03. Competitive Indices (CI) were calculated by dividing the end point wild-type:mutant ratio by the ratio at T_0 (ratio = $E_{\text{mut}}^{C_{T_{\text{mut}}}}/E_{\text{wt}}^{C_{T_{\text{wt}}}}$).

Results and Discussion

Identification of carbon sources that *C. difficile* is able to use for growth.

Phenotype MicroArray plates can be used to screen various compounds for their ability to increase the growth rate or growth yield of selected strains. Phenotype MicroArray plates are 96-well plates in which each well contains a different compound; these can be used to screen not only for phenotypic effects on strain growth but also other aspects of physiology such as sporulation, toxin production, or biofilm formation. The focus of this work was on identifying nutrients which *C. difficile* is able to use to increase growth, although these plates could also be used to identify compounds that inhibit growth. Strains CD630 and CD2015 were used for initial Phenotype MicroArray growth studies (Table 4.1). This was done because we wanted to identify compounds beneficial for *C. difficile* in general as well as ones that might be specific to the epidemic RT 027 strains. Two different media were used for initial experiments in order to detect compounds that may provide an advantage in one medium but may not be detected in the other. Table 4.4 summarizes the results from just the two carbon source plates (PM1 and PM2). Out of 190 compounds tested, a total of 16 were found to confer a growth advantage to both strains, 5 compounds to only CD630, and 3 compounds to only CD2015, (Table 4.4). However, these results are representative of only 1 replicate of each plate for each strain and each media type. More replicates or media types might have shown more conserved overlap in the utilization of these compounds by these two strains. Moreover, some compounds may have increased growth for either, or both, strains but may have not met the 1.5-fold cut-off value. This was an initial screen for

identification of compounds to follow-up in subsequent and better-replicated growth studies. Therefore, these Phenotype MicroArray plate experiments are not an exhaustive study into the metabolic capabilities of *C. difficile* and are likely to overlook some compounds that may be of interest.

Table 4.4. Compounds that conferred at least a 1.5-fold growth yield advantage Biolog PM1 and PM2 plates.^a

	Well	Compound	CD630		CD2015	
			MSM	DM-G	MSM	DM-G
PM1:	A3	N-acetyl-D-glucosamine*	+	+	ND	+
	A8	L-proline	+	-	ND	-
	A10	D-trehalose*	+	+	ND	+
	A11	D-mannose*	+	+	ND	+
	B2	D-sorbitol	-	-	ND	+
	B11	D-mannitol	+	+	ND	+
	C7	D-fructose	+	-	ND	+
	C9	α -D-glucose	+	+	ND	+
	D7	α -Keto-Butyric acid	+	+	ND	-
	G3	L-serine	+	+	ND	-
	G4	L-threonine	+	-	ND	-
H1	glycyl-L-proline	+	-	ND	-	
PM2:	B2	N-acetyl-neuraminic acid*	-	+	+	+
	B6	D-arabitol	-	-	-	+
	B8	arbutin	+	+	+	+
	C4	D-melezilose	+	+	+	+
	D2	salicin	+	+	+	+
	D6	D-tagatose	+	+	-	+
	E5	D-glucosamine	+	+	+	+
	E8	b-hydroxy-butyric acid	-	+	-	+
	E10	α -keto valeric acid	-	+	+	+
	G8	hydroxy-L-proline*	-	-	+	+
	G10	L-leucine	-	+	+	+
	G12	L-methionine	+	-	-	+

^aEach +/- symbol represents results of an individual experiment where growth was (+) or was not (-) increased by at least 1.5-fold that of the control. DM= defined medium; MSM= modified sporulation medium.

*These compounds were selected for individual growth analysis experiments.

Plates PM3-8 were also tested for increased growth. The results are presented in Supplementary Table 4.1; however, we did not do any follow-up growth studies on the compounds identified in these plates.

Compounds identified in Phenotype MicroArray plates increase growth yield of several *C. difficile* strains. Several compounds that conferred growth advantages were selected for follow-up experiments (starred in Table 4.4). These compounds were selected based on their potential for availability in the intestinal environment. For example, N-acetyl-glucosamine is a building block of bacterial peptidoglycan. This compound may have increased availability during periods of bacterial lysis due to antibiotic activity. N-acetyl-neuraminic acid is a building block of mucin, a substance secreted by the intestinal epithelium. Reduction in bacterial levels within the gastrointestinal tract following antibiotic treatment may increase access to this compound. Additionally, we know that *C. difficile* is capable of generating ATP through Stickland reactions, the coupled reduction and oxidation of amino acids (4). Alanine and hydroxy-proline have been demonstrated to serve as a Stickland pair for this reaction. Mannose is a six-carbon sugar that is naturally occurring and often a component of cell-surface glycoproteins as well as present in various dietary sources. Finally, as presented in the introduction, trehalose is a glucose disaccharide that has several lines of evidence for potential gut-availability.

Several *C. difficile* strains (3 RT 027 and 4 RT non-027) were tested for the ability to grow to higher cell densities on these selected nutrient sources; the results are presented in figure 4.1. The defined medium was used for these experiments

and compound concentrations were chosen based on the concentration range given by Biolog (5-50mM). N-acetylglucosamine (NAG) and N-acetylneuraminic acid (NANA) increased growth yield for all four of the RT non-027 strains. Of the three RT 027 strains, only CD3017 increased in the presence of NAG. Interestingly, CD2015 did not have increased growth in these experiments in the presence of NAG or NANA, while it did have an increase in the Phenotype MicroArray plates. This may be an indication that CD2015 is more sensitive to growth conditions for utilization of this compound, or that the concentrations used in the follow-up growth cultures were lower than in the Phenotype MicroArray plates. The amino acids alanine and hydroxy-proline significantly increased growth yield only for CD2015. Mannose increased growth yield for all strains except CD3014. All strains tested had significant increases in growth yield in the presence of trehalose. Interestingly, however, when comparing the fold-increase of growth in trehalose-supplemented medium to that in unsupplemented medium, the RT027 strains had an average of 3-fold increase compared to 1.2-fold increase of the non-RT 027 strains (except for CD630, which had a 5-fold increase). Taken together, these data illustrate the proof of concept that Phenotype MicroArray plates can successfully be used to identify compounds beneficial to *C. difficile* growth.

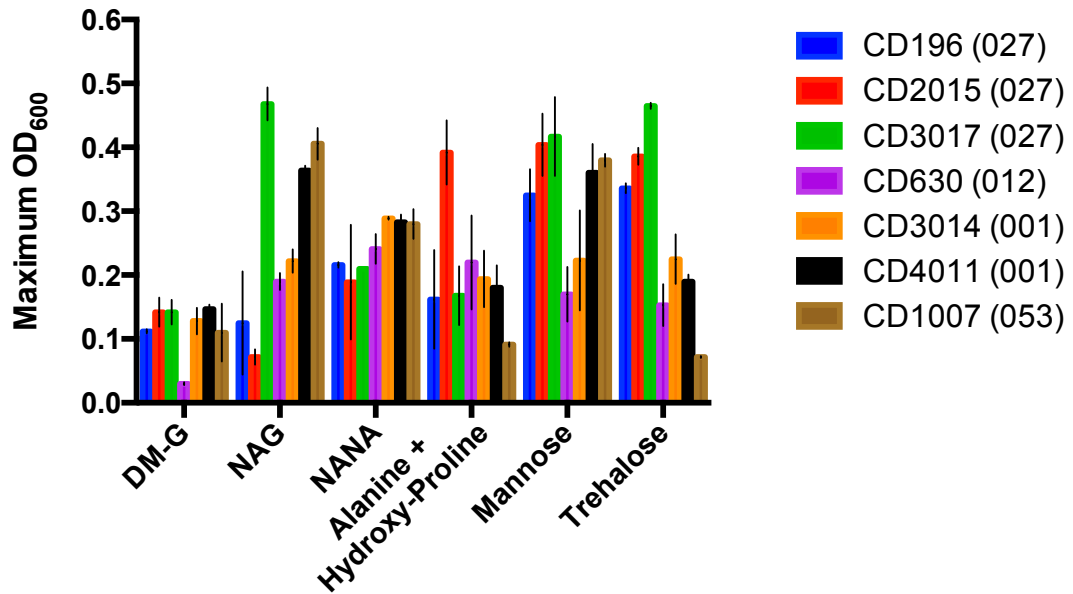


Figure 4.1. Results of growth yield experiments using compounds selected from Phenotype MicroArray plates. Results are reported as the average of three independent growth curves with associated standard deviations. (DM-G= defined medium without glucose, NAG= N-acetyl-glucosamine, NANA= N-acetyl-neuraminic acid)

Characterization of growth phenotypes of *C. difficile* strains grown on

trehalose. With the observation that RT 027 strains had higher fold-increases than RT non-027 strains in the presence of trehalose in the follow-up studies presented above, we further investigated the growth dynamics of these strains in the presence of this sugar. Four strains were selected (two RT 027 and two RT non-027) and grown on a range of trehalose concentrations to determine if the differences in growth yield were concentration-dependent. The results are presented in Figure 4.2. It was observed that the RT 027 strain cell densities began to increase at lower levels of trehalose than the RT non-027 strains, showing significant differences as low as 750uM (p-value<0.05, student's t-test), while the RT non-027 strains did not

have significant differences in cell densities even at 50mM trehalose, although they were trending higher. The variation in culture final OD's is high at these higher concentrations, however, and so repetition of growth experiments would likely result in significant differences. Nonetheless, it is clear that RT 027 strains increase growth yield in the presence of trehalose at much lower concentrations.

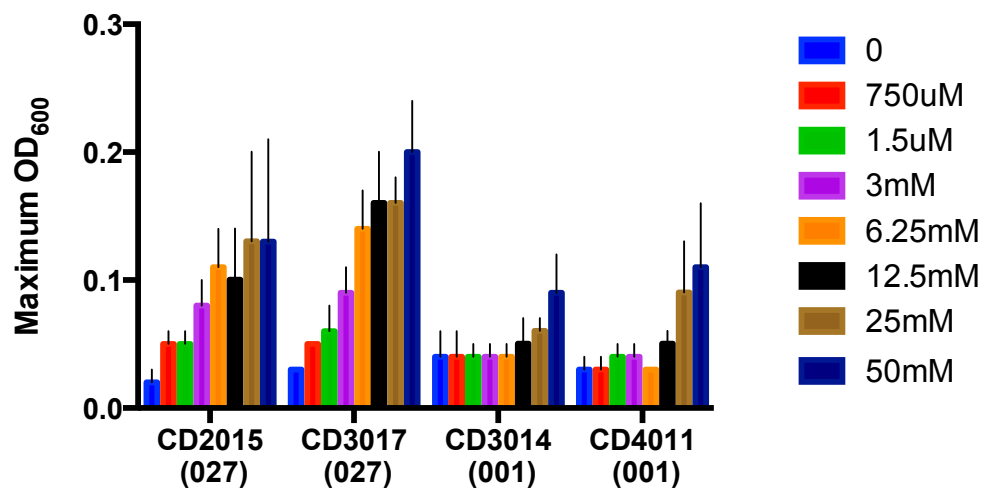


Figure 4.2. Maximum growth yield of *C. difficile* strains grown in the presence of a range of trehalose concentrations in defined medium. Ribotype 027 strains increase growth yield at lower trehalose concentrations. Results are reported as the average of three independent growth curves with associated standard deviations.

Using a concentration where there were significant differences between the growth yields of RT 027 and non-027 strains, the growth of several more *C. difficile* strains of other ribotypes was assessed. The results are presented in figure 4.3, showing growth yields of *C. difficile* strains grown in DM with and without supplementation with 10mM trehalose. All five RT 027 strains used had significantly higher maximum OD's in trehalose-supplemented DM (p-value <0.05,

student's t-test), while all six RT non-027 strains did not. We also tested three RT 078 strains (another epidemic-associated RT of high prevalence), and observed that they also had significantly higher growth yields in the presence of 10mM trehalose.

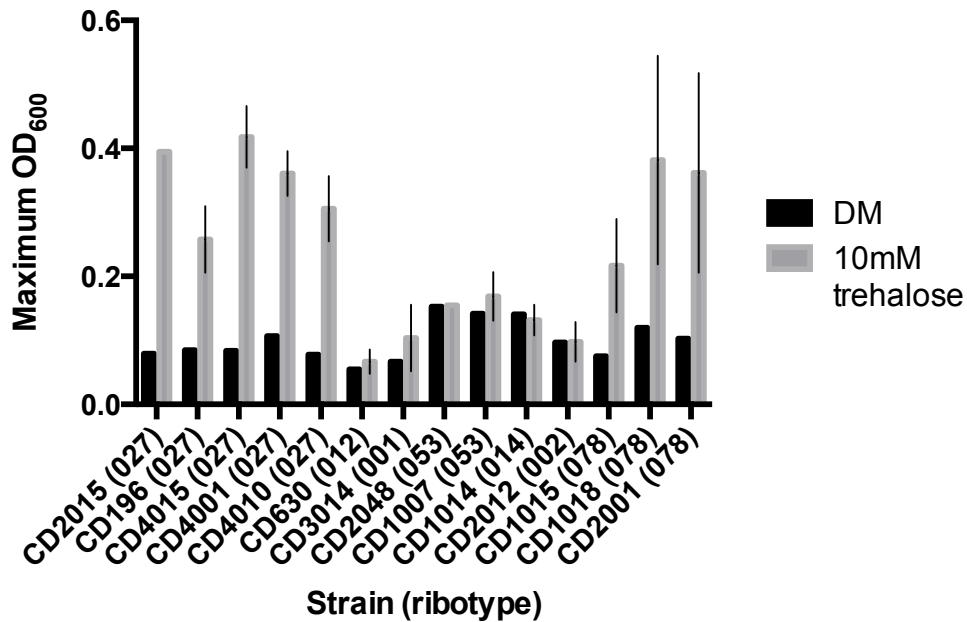


Figure 4.3. Growth yield of *C. difficile* strains belonging to several ribotype groups. Strains were grown in defined medium (DM) +/- 10mM trehalose. RT027 and RT078 strains grow to higher cell densities on 10mM trehalose. Results are reported as the average of independent replicates with associated standard deviations.

Construction of a *treA* mutant and analysis of the growth phenotype. The ability to utilize trehalose as a carbon source is dependent on a cell's ability to break the disaccharide bond, generating two molecules of glucose that can then be shuttled into the glycolytic pathway of central metabolism. In *C. difficile*, a trehalose-6-phosphate hydrolase enzyme, TreA, fulfills this function. Using a group-

II intron based gene knockout system, a *treA* knockout mutant was constructed in the CD630 Δ *erm* background. The *treA* mutant and CD630 parent were then grown in DM supplemented with glucose, trehalose, and the other glucose disaccharide sugars, cellobiose and maltose (figure 4.4). The growth experiments confirmed that the mutant is unable to metabolize trehalose; there was no increase in growth yield in DM supplemented with 25mM trehalose compared to unsupplemented DM, while the WT strain had a 4-fold increase. It is worth noting that while CD630 is not a RT 027 strain, it does grow better than other non-027 RT strains on trehalose, presumably due to its lab adaption to rich media (BHIS), which contains trehalose because of the addition of yeast extract. This supports that *treA* encodes a protein required for trehalose metabolism. Moreover, knockout of *treA* does not affect metabolism of glucose, cellobiose, or maltose, since the growth yields of the WT and mutant strains were essentially the same in media supplemented with these different sugars. This observation is evidence that the glucosidase activity of TreA is specific to trehalose and not other glucose disaccharides. Moreover, the phenotype of this mutant is specific to its ability to utilize trehalose and therefore can be used for *in vivo* or *in vitro* experiments to study the importance of trehalose metabolism to *C. difficile* colonization and virulence.

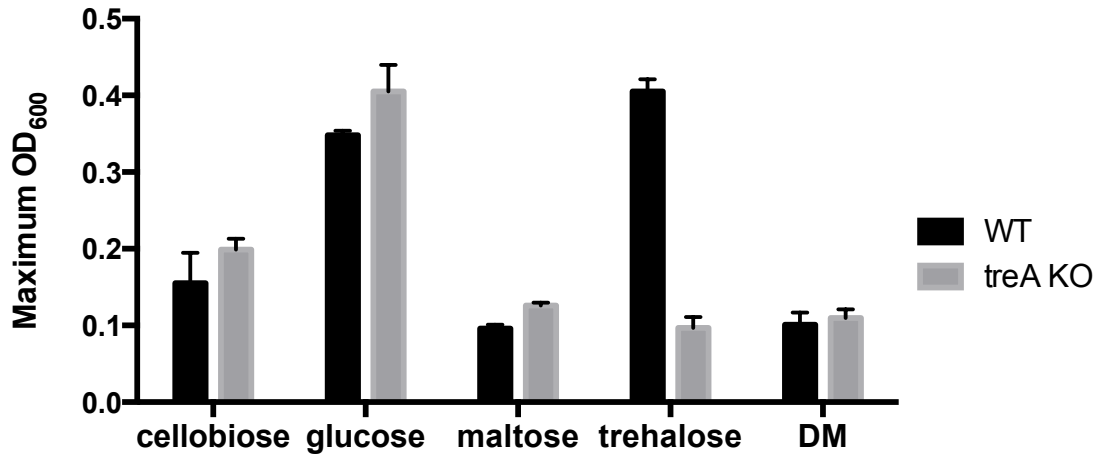


Figure 4.4. Growth yields of CD630 wild-type (WT) and *treA* knock-out mutant in defined medium (DM) supplemented with glucose and glucose disaccharide sugars (25mM).

Alignments of *treR*, the repressor of trehalase (*treA*), reveal a conserved leucine residue that is substituted with isoleucine in RT 027 strains.

The *treA* (locus tag CD3091) gene is located on the chromosome immediately downstream of a gene that codes for its cognate transcriptional repressor, TreR (locus tag CD3090) (Figure 4.5).



Figure 4.5. Trehalose utilization genes located on the *C. difficile* chromosome. The trehalase gene, *treA*, is located directly down stream of *treR*, the trehalase transcriptional repressor.

We hypothesized that the ability of RT 027 and 078 strains to grow better on trehalose was due to a genetic difference in this trehalose-utilization locus. Whole genome sequencing of several of the clinical isolates used in the trehalose growth studies above was conducted. By aligning the gene sequences pulled out of those genome sequence files, we identified a conserved amino acid substitution in TreR of the RT 027 strains that is not present in the other RT strains (figure 4.6). This substitution corresponds to a cytidine to adenine mutation in the gene sequence at bp 514, resulting in a leucine to isoleucine substitution at AA172.



Figure 4.6. Alignments of TreR amino acid sequences for several *C. difficile* strains of various ribotypes. RT027 strains have a conserved L172I amino acid substitution (circled in red) not present in the non-RT027 strains or the RT078 strain.

In order to investigate the conservation of this residue in TreR proteins of other organisms, we aligned the TreR amino acid sequences from 10 other Gram-

positive bacteria (figure 4.7). Indeed, this leucine residue was conserved across all of the organisms included in our alignments, suggesting it has structural or functional importance.

Clostridium_difficile	GFKVGSEVYYLHRLRYIDNIPKILDINYFLCSIVKDLVSVIAQGSIIYKYIEECLGTKIVS
Streptococcus_pneumonia	GFPEFRMVWQVVRQVVDLVSVDLTDYLDMEIIPNLTRQIAEQSIYSYIENGLLLIDY
Lactococcus_lactis	GFAIGDQALSILRRRKVDGKFSILDWDLFLEKYADGLTPAHAQNSTYDYLEGALGLDIAY
Lactobacillus_plantarum	TELTEAPVTAIKRVRVIDGEPAIIDKDYILKSIVPKVPKQAAEDSLYAYFENOLGLTIGY
Bacillus_cereus	NVKEKTDIDHIKVRNIDGKVIDLDINHFVSEYIPGLTSEIAAQSIYKYIEKELGLHISY
Bacillus_anthraxis	NVKEKTEIDHIKVRNIDGKVIDLDINHFVSEHIPGLTSEIAAGSIYKYIEKELGLHISY
Bacillus_thuringiensis	NVKEKTEIDHIKVRNIDGKVIDLDINHFVSEHIPGLTSEIAAGSIYKYIEKELGLHISY
Clostridium_botulinum	NLSKNDVWVKVIRVREIDNKKIILDKDFFNKKYVPLLTQKICENSIYEYLENELGLKISF
Clostridium_perfringens	EVSPNKYVWVVRNIDGKVIDLDKDYLNSEFVPRLTTEEICKDSLYKYIEGELGLKIAY
Bacillus_halodurans	GCDAAEPLWAVVRARKISGESIILDKDYFLEEYVPNLTKEICQDSIYEVVEKTLGLTISF
Bacillus_subtilis	RANLDDDIWEVIRSRKIDGHEVILDKDYFFRKHVPHLTKEICENSIYEYIEGELGLSISY
	: * * : . : * * : : . : . * * * . * *

Figure 4.7. Alignments of TreR amino acid sequences from several Gram-positive bacterial organisms showing conservation of the leucine residue.

The only available crystal structure of a TreR protein homologous to that in *C. difficile* was published by Rezacove *et al.* who studied the C-terminal (effector-binding) domain of TreR in *Bacillus subtilis* (33). This conserved leucine (AA169) is located in Helix H3 of the structure (Figure 4.8).

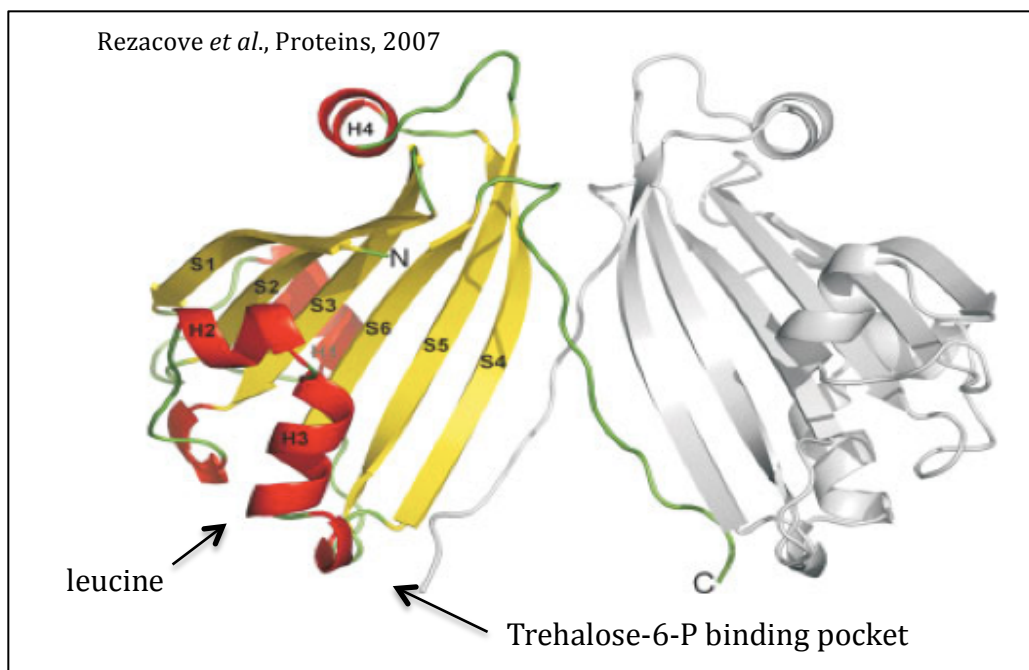


Figure 4.8. Ribbon diagram of the C-terminal (effector-binding domain) of TreR from *Bacillus subtilis* showing the locations of the predicted trehalose-6-phosphate binding pocket and conserved leucine residue (Leu-169). Structure was determined and published by Rezacova *et al.* (33).

TreR functions as a dimer of dimers, and this helix (H3) was shown to be important for interaction between subunits of the two dimers. When trehalose is absent, the dimers form a tetramer and bind to two operator sequences on the chromosome, upstream of the trehalose operon. These 14 bp inverted repeats are located 32 bp apart within the promoter sequence of the trehalose operon in *B. subtilis* (34). When trehalose is present in the medium, it gets phosphorylated to trehalose-6-phosphate during uptake into the cell by way of a trehalose-specific phosphotransferase transporter system. Trehalose-6-phosphate then binds to TreR, causing a conformational change that dissociates TreR from the DNA, allowing expression of *treA*. Additionally, the location of the leucine in the structure lies very

close (just a few amino acids away) from the predicted effector-binding pocket, more specifically, where the phosphoryl group of trehalose-6-phosphate (the effector) is predicted to interact with key amino acid residues (33). Both leucine and isoleucine are hydrophobic amino acids containing branched, non-polar side chains. While the chemistry of these two amino acids is similar, the slight differences in their structures may allow for a change in structure or function of the protein. Since this amino acid is highly conserved, it is likely that a substitution to an amino acid with significantly different chemistry would result in a structural or functional change that could be deleterious, potentially even resulting in complete loss of function. Based on the location of this substitution, we predict that the RT 027 TreR could have a change in function, which allows increased induction of *treA* expression. This could occur by destabilization of the TreR tetramer, since AA172 is located in helix H3, which is important for dimer-dimer interactions. This would allow for the dimers of TreR to more readily dissociate upon binding trehalose-6-phosphate. Alternatively, TreR could have a higher affinity for trehalose-6-phosphate, because of AA172's close proximity to the effector-binding pocket, which would also allow for TreR to more readily dissociate from the operator region. Therefore, we hypothesize that RT 027 strains are able to grow to higher cell densities on lower levels of trehalose due to increased expression of *treA*.

Since the RT 078 strains do not have this amino acid substitution, the basis for their increased growth on trehalose must be the result of some other genetic difference. Through personal correspondence with Wilco Knetsch (lab of Dr. Ed Kuijper, Leiden University Medical Center), they have shared that they recently

identified a genetic insertion in RT 078 strains, which contains genes annotated as trehalose-utilization genes (unpublished data). These genes may be the genetic basis for the trehalose growth phenotype of RT 078 strains; however, it is possible that other genetic characteristics are playing a role. Regardless, the observation of two independent lineages of epidemic-associated *C. difficile* acquiring the ability to grow better on trehalose supports that this metabolic ability may play a role in *C. difficile* colonization and disease.

RT 027 strains have increased *treA* expression. In order to test the hypothesis that RT 027 strains have increased *treA* expression, we grew four RT 027 strains, and four strains belonging to different RT groups, in DM supplemented with 25mM trehalose and compared the levels of *treA* mRNA present during mid-log phase of growth using RT q-PCR. The C_T values of each replicate were all normalized to an average baseline C_T value of replicates grown in medium without trehalose. The results are presented in figure 4.9. The mean values of the four RT 027 strains are 2599, 3339, 3451, and 3752. The mean values of the four RT non-027 strains are 392, 780, 1395, and 603. The difference *treA* expression in RT 027 strains compared to RT the non-027 strains in these conditions is significant; the p-value (student's t-test) calculated from groups of mean values from the RT 027 and non-027 groups is 0.00026. There is a large amount of variability between replicates within some strains, and this may be due to the concentration of trehalose used in these experiments. This concentration is potentially close to a threshold concentration where *treA* expression is induced, since there is a slight increase in

growth yield at this concentration in the RT non-027 strains shown in Figure 4.2. A lower concentration of trehalose ($\leq 10\text{mM}$) might yield more consistent results, however, the lower cell densities of the cultures would make obtaining adequate amounts of RNA more challenging. Regardless, there is still a strong correlation between strains that have increased growth on trehalose and increased expression of *treA*. One exception is the RT 078 strain, CD1015, which has significantly increased growth on 10mM trehalose yet I did not observe increased *treA* expression in this strain. It would be interesting to test other RT 078 strains to determine if they also do not have increased *treA* levels. If not, this might provide insight into the genetic basis for their growth phenotype. For example, it might indicate that the trehalase enzyme they carry has increased catalytic efficiency or affinity for trehalose-6-phosphate. Alternatively, it might provide evidence for the presence of an additional trehalase gene, which is suggested in the unique insertion in these strains that is discussed above.

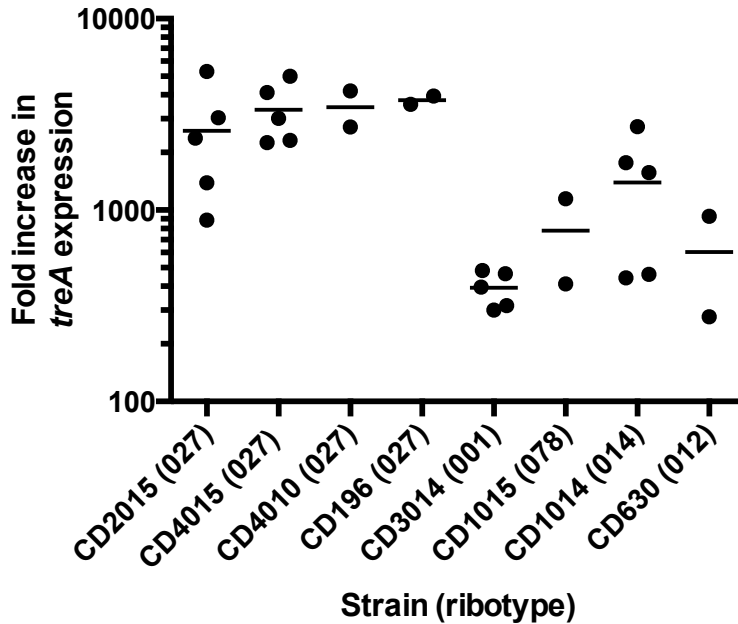


Figure 4.9. Expression of *treA* in several *C. difficile* strains grown in DM+25mM trehalose as determined by RT-qPCR. Plotted points represent the fold-increase of each replicate, normalized to an average baseline expression in medium without trehalose. Replicates of each strain are combined data from 2 or 3 independent experiments; black bars represent the means. The RT 027 strains (four on left side of graph) expressed *treA* to higher levels under the conditions tested. The p-value (student's t-test) between groups of RT 027 and RT non-027 strain averages is 0.00026.

A *treA* knockout mutant of *C. difficile* displays a decrease in colonization levels in a mouse model of *C. difficile* infection and a decrease in competitive fitness compared to the wild type strain. In order to investigate if the ability to utilize trehalose plays a role in *C. difficile* colonization *in vivo*, we infected groups of mice with either the wild-type CD630 Δ *erm*, a *treA* knockout mutant of CD630 Δ *erm*, or a mixture of the two strains. Mice were treated with an antibiotic, cefoperazone, for several days in order to induce susceptibility to *C. difficile* infection, then gavaged

with 10^4 spores of the desired strain/s. Fecal samples were collected daily and *C. difficile* was enumerated by either plating (wild-type, mutant, and competition groups) or qPCR (competition group). The CFU/g feces as determined by plating on *C. difficile* selective media of the mice infected with either the wild-type or mutant strains is plotted in figure 4.10. The fecal levels ranged from 1.2×10^7 to 1.8×10^8 CFU/g feces across all five days for the mice infected with wild-type strain, and the range for the mutant-infected mice is from 1.0×10^7 to 8.6×10^7 CFU/g feces. Interestingly, there is a significant difference between the CFU/g feces in the wild-type and mutant groups on days 1 and 2 ($p=0.02$ and 0.03 , respectively) and close to significant difference on day 3 ($p=0.08$), with the mutant colonizing the mice to lower levels on those days (~2-fold difference between means on all three days).

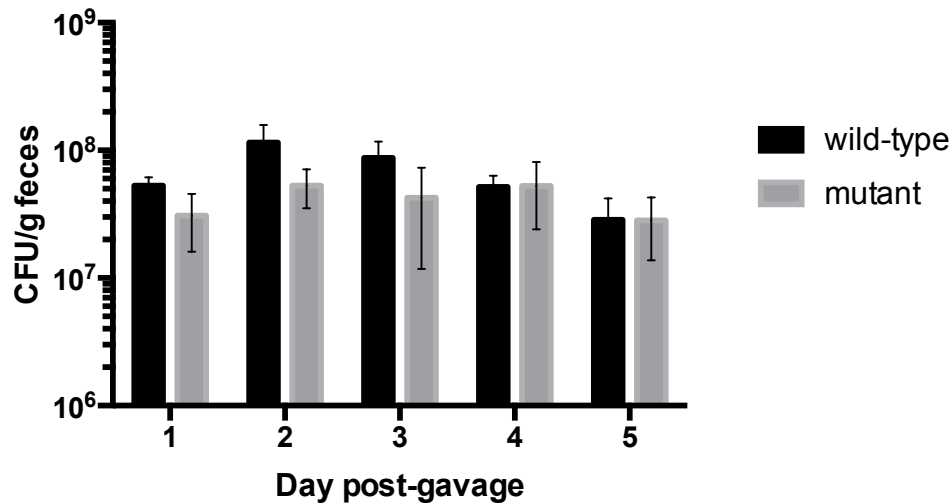


Figure 4.10. CFU/g feces of wild-type and *treA* mutant *C. difficile* infected mice. Two groups of five mice were gavaged with spores of either wild-type CD630 Δ *erm* or a *treA* knockout mutant. Fecal pellets were collected daily and *C. difficile* quantified by plating on *C. difficile* selective media. Results are plotted as the mean and standard deviation of the data points from each group on the indicated days. *p-value <0.05

In the mice infected with a mixture of wild-type and mutant spores, a competitive index was calculated to assess the advantage of having a functional *treA* gene. Competitive indices (CI's) were determined by dividing the wild-type:mutant ratio within individual mice at days 1, 2, 3, and 5, and dividing by the ratio in the gavaged spore mixture (ratio = 0.29). Quantitative PCR using primers specific to either strain was used to determine the strain ratios. The CI's are plotted in figure 4.11. Each data point represents the CI of the wild-type strain in an individual mouse on the indicated day; lines connect the CI's within each mouse across time. A CI of one would indicate no change in ratio, while a CI greater than 1 indicates an increase in ratio and therefore a competitive advantage of the wild-type strain. When tracking the CI's across time in the individual mice, four of the five mice had

CI's of >1 on or before day 3. Mouse 3 had a consistent increase in CI from days 2 to 5, indicating a clear competitive advantage for the wild-type strain. Mouse 1 had CI's >1 from days 2 to 5 as well, however, they were decreasing as the experiment progressed. Mice 2 and 4 had CI's >1 on days 2 and 3, respectively, however, they dropped below 1 by day 5. Mouse 5 CI's were below 1 throughout the experiment with the lowest CI on day 5 (0.6). In general, there was a trend of decreasing CI's toward the end of the experiment.

One observation from the plating data was that the total number of *C. difficile* in all mice had a significant decrease in CFU/g feces after day 5 (figure 4.12). There was larger drop (up to over 2 logs) in levels of *C. difficile* in the wild-type and competition mouse groups, while the drop in levels in the mutant-infected mouse group was lower, yet still significant (up to 13-fold decrease). This observation indicates that the intestinal microbiota of the mice are likely recovering from the antibiotic-induced perturbation and resistance to *C. difficile* is being restored, therefore resulting in *C. difficile* washout. Changes in the intestinal environment, including nutrient availability, are likely in this situation and would affect the outcome of these experiments, particularly the competition dynamics of the wild-type and mutant strains. Therefore, it is reasonable to draw conclusions from our data based on the earlier time points in the experiment.

In summary, there were significant differences in the wild-type and mutant levels of *C. difficile* in the individually-infected mice on days 1 and 2. In addition, CI's in the competition mice within the first 3 days of infection indicated a competitive

advantage of the wild-type strain. Combined, these data support the hypothesis that trehalose plays a role in colonization and competitive fitness *in vivo*.

In consideration of the variability in wild-type CI's among mice in the competition group, and the washout of total *C. difficile* levels in all mouse groups beyond day 5 of the experiment, the data are not as robust as desired and warrant a repeat of the experiment. Nonetheless, a recent study published by Ng *et al.* reported similar differences in colonization levels of wild-type *C. difficile* and a mutant deficient in sialic acid consumption in a mouse model, with the mutant colonizing at levels 2.3-fold lower than the wild-type (35). Unlike sialic acid, which is a component of mucin, trehalose availability in the human gastrointestinal tract is at least partially dependent on diet composition. Therefore, administration of trehalose to mice during colonization and competition studies is reasonable and potentially more closely replicate the nutritional availability of trehalose in humans. Future mouse experiments will include groups of mice fed trehalose based on the estimated average daily consumption of trehalose reported in the literature. We expect the data from these mice to reflect an even stronger support for the importance of the ability of *C. difficile* to metabolize trehalose *in vivo*.

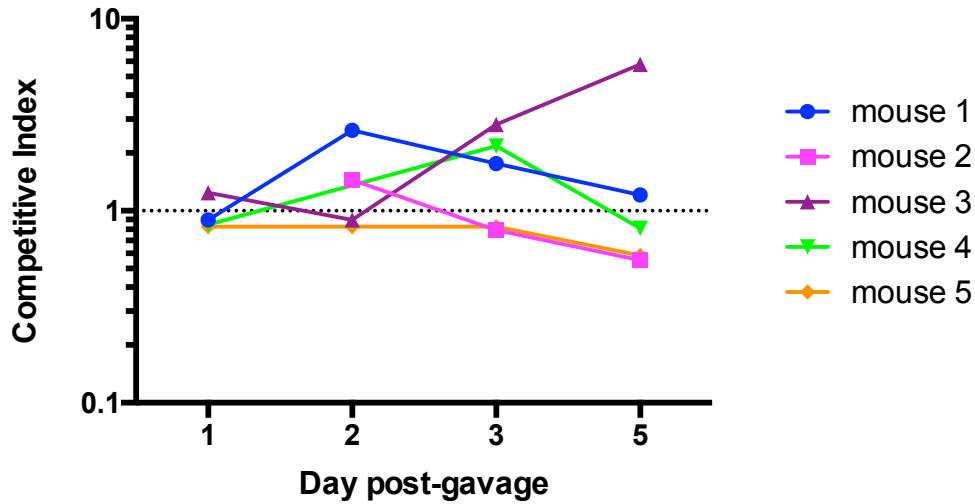


Figure 4.11. Competitive indices of wild-type CD630 Δ erm when competed against the *treA* knockout mutant in a conventional mouse model of *C. difficile* infection. Mice were gavaged with a mixture of wild-type and mutant spores, and fecal pellets were collected daily. Competitive indices were determined by qPCR using primers specific to either strain and calculated by dividing the wild-type:mutant ratio at the indicated day by the ratio of the spore mix.

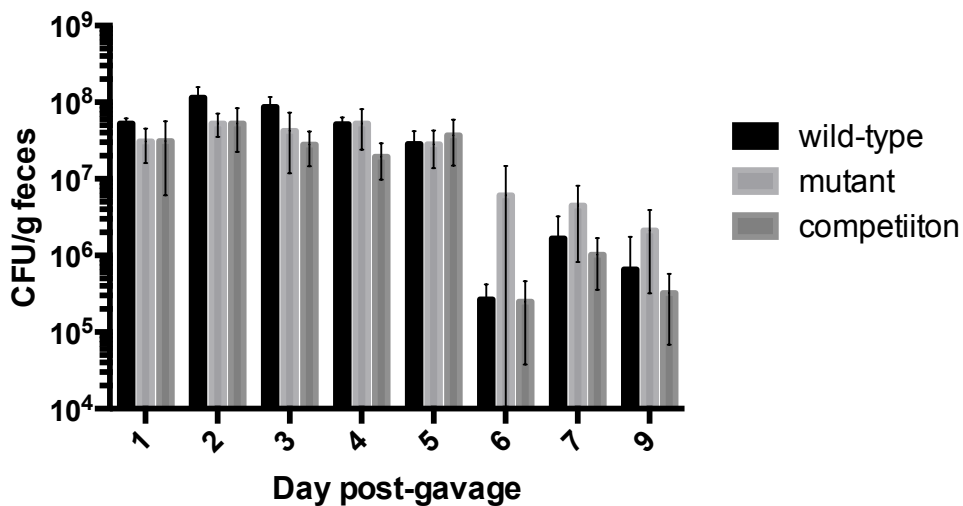


Figure 4.12. Total CFU/g feces of *C. difficile* in each group of mice. Three groups of five mice were gavaged with spores of either wild-type CD630 Δ erm, a *treA* knockout mutant, or a mixture of both strains. Fecal pellets were collected daily and *C. difficile* quantified by plating on *C. difficile* selective media. Results are plotted as the mean and standard deviation of the data points from each group on the indicated days.

Summary and Future Directions

The primary focus of the work in this chapter was to investigate carbon sources of *C. difficile*, with an emphasis on ones that RT 027 strains are able to differentially utilize, compared to other ribotypes. Using Biolog Phenotype Microarray plates, several compounds that increased growth yield of *C. difficile* were identified. Ribotype 027 strains were shown to grow to higher cell densities on one of these compounds, trehalose, as well as strains of another epidemic ribotype, RT 078. Genetic analysis identified an amino acid substitution in *treR*, the repressor of *treA* (trehalase), which is conserved among ribotype 027 clinical isolates. Moreover, increases in *treA* expression in ribotype 027 strains, presumably due to this mutation in *treR*, have been observed by RT-qPCR.

Using a *treA* knockout mutant of *C. difficile*, we tested the importance of ability to metabolize trehalose in a mouse model of *C. difficile* infection. The results of this preliminary mouse experiment suggest that trehalose utilization is important for reaching maximum levels of colonization *in vivo* and may also increase competitive fitness.

The *treA* mutant generated in this study represents the first experimental proof of the function of *treA*, the gene annotated to encode a trehalose-6-phosphate hydrolase in *C. difficile*. Not only was it shown that the mutant is unable to grow on trehalose, but that its ability to metabolize other glucose disaccharide sugars was unaffected.

Currently, the phenotypic effects of the leucine to isoleucine amino acid substitution in TreR of RT 027 strains is being investigated using a different model

organism, *Lactococcus lactis*. Genetic tools in *C. difficile* are relatively limited, however, the Britton lab has recently developed and optimized a recombineering system for making targeted mutations in lactic acid bacteria. The TreR of *L. lactis* also contains the highly conserved leucine residue, as shown in figure 4.7. Using recombineering, I have made a *treR* mutant of *L. lactis* NZ9000 that encodes the same leucine to isoleucine amino acid substitution as that in the TreR of *C. difficile* RT 027 strains. Currently, growth and expression experiments are being conducted to see if the amino acid substitution displays a phenotype. If this is demonstrated, it will provide further support that this genetic change in the RT 027 strains contributes to the trehalose growth phenotype. Moreover, additional experiments are planned to investigate if there are differences in the ability of the RT 027 TreR and the RT non-027 TreR to bind the *treR* or *treA* promoter regions using enzyme mobility shift assays. We hypothesize that the TreR of RT 027 strains will dissociate from DNA when lower levels of trehalose-6-phosphate are added compared to the TreR of RT non-027 strains. This would also provide support for the functional effect of the identified amino acid substitution.

In conclusion, the work in this chapter suggests that trehalose is one of the nutrients utilized by *C. difficile in vivo* and that epidemic-associated ribotype strains are able to utilize trehalose more efficiently. This work not only contributes to understanding the nutritional factors involved in *C. difficile* gut colonization, but also to understanding the physiology of epidemic strains. Although a potential genetic basis for the trehalose advantage of RT 078 strains was not identified, the observation that this second epidemic-associated and prevalent ribotype group

grows better on trehalose is intriguing. It further supports that the ability to utilize trehalose is important for *C. difficile* colonization and might indirectly contribute to virulence.

There are several potential applications of this insight. For example, including a trehalose-consuming organism in a prophylactic probiotic treatment during antibiotic treatment may help to reduce development of *C. difficile* infection. Additionally, altering the diet of patients at risk for *C. difficile* infection, by reducing consumption of trehalose, may also help to reduce disease development. Ultimately, the more we understand about all aspects of this complicated disease, the better we will be able to treat and prevent it.

Acknowledgments

There are several people that contributed to the work in this chapter that I would like to thank. Dr. Linc Sonnenshein, Dr. Joe Sorg, Dr. Craig Ellermeier, and Dr. Laruent Bouillaut kindly provided *C. difficile* strains, protocols, and valuable experimental advice. Sara McNamara (Michigan Department of Community Health) provided us with clinical isolate strains of *C. difficile*. Dr. Seth Walk for ribotyping many of our strains. Finally, Dr. Mark Koenigsnecht (and Dr. Vince Young) for conducting the conventional mouse experiments.

APPENDIX

Appendix

Table S4.1. Compounds that conferred at least a 1.5-fold growth yield advantage (relative to unsupplemented medium control) for either one or both strains in the Biolog PM3-8. Defined medium was used for all plates.*

	Well	Compound	CD630	CD2015
PM3:	A6	biuret	--	+-
	A7	L-alanine*	--	+-
	A8	L-Arginine	--	+-
	A11	L-cysteine	--	+-
	B5	L-leucine	++	++
	B10	L-serine	+-	+-
	B11	L-threonine	+-	++
	B12	L-tryptophan	--	++
	C12	L-ornithine	+-	++
	D9	ethanolamine	+-	+-
	D12	agmatine	++	+-
	E8	D-glucosamine	++	+-
	E9	D-galactosamine	+-	--
	E11	n-acetyl-glucosamine	+-	+-
	F6	Guanine	--	+-
	F8	Thymine	+-	+-
	F12	Inosine	+-	+-
	G2	xanthosine	--	+-
	G8	γ -amino-n-butyric acid	--	+-
	G10	D,L- α -Amino-Caprylic Acid	+-	+-
	G12	α -Amino-N-Valeric Acid	+-	+-
	H4	alanine-glycine	--	+-
	H6	alanine-leucine	--	+-
	H7	alanine-threonine	--	++
H9	Glycine-Glutamate	--	+-	
H11	Glycine-methionine	--	+-	
H12	Methionine-Alanine	--	++	
PM4:	F4	tetrathionate	--	+-
	F10	L-cysteic acid	--	+-
	G7	L-methionine	--	+-
	G8	D-methionine	--	+-
	H4	D, L- lipoamide	--	+-
PM5:	A5	L-asparagine	+-	--
	B1	L-glutamine	+-	--
	B8	L-phenylalanine	--	+-
	B11	guanosine	+-	--
	C12	deoxy-inosine	+-	+-
	F12	thymidine	+-	--

Table S4.1 (cont'd)

	G1	oxaloacetic acid	+-	+-
	G3	cyano-cobalamine	+-	--
	G4	ρ -amino-benzoic acid	+-	--
	G5	folic acid	+-	--
	H7	D, L- carnitine	+-	--
	H8	choline	+-	--
PM6:	B1	alanine-serine	--	+-
	B2	alanine-threonine	+-	--
	B6	arginine-arginine	+-	--
	B8	arginine-glycine	+-	--
	B12	arginine-lysine	+-	--
	D10	glutamate-serine	--	--
	D12	glutamate-tyrosine	--	--
	E4	glycine-cystein	+-	--
	G12	lsoleucine-serine	+-	--
	H1	isoleucine-tryptophan	--	+-
	H4	leucine-alanine	+-	--
	H6	leucine-asparagine	--	+-
	H9	leucine-isoleucine	--	+-
	H10	leucine-leucine	+-	+-
	H11	leucine-methionine	+-	+-
	H12	leucine-phenylalanine	+-	+-
PM7:	B3	lysine-threonine	+	-
	B10	methionine-glutamine	-	+
	B12	methionine-histidine	-	+
	C2	methionine-leucine	-	+
	C3	methionine-lysine	+	-
	D5	proline-asparagine	+	-
	E1	serine-alanine	+	-
	E8	serine-serine	+	-
	E12	threonine-arginine	+	-
	F1	threonine-glutamine	+	-
	F2	threonine-glycine	+	-
	F3	threonine-leucine	-	+
	F4	threonine-methionine	-	+
	F7	trpyptophan-arginine	+	-
	G10	tyrosine-leucine	+	-
	H5	valine-asparagine	+	-
	H9	valine-leucine	+	-
	H12	γ -glutamate-glycine	+	-
PM8:	E5	serine-methionine	+-	--

*Each +/- symbol represents results of an individual experiment where growth was (+) or was not (-) increased by at least 1.5-fold that of the control.

REFERENCES

REFERENCES

1. **Yassin SF, Young-Fadok TM, Zein NN, Pardi DS.** 2001. Clostridium difficile-associated diarrhea and colitis. *Mayo Clin. Proc.* **76**:725–730.
2. **Bartlett JG, Chang TW, Gurwith M, Gorbach SL, Onderdonk AB.** 1978. Antibiotic-associated pseudomembranous colitis due to toxin-producing clostridia. *N. Engl. J. Med.* **298**:531–534.
3. **Britton RA, Young VB.** 2014. Role of the intestinal microbiota in resistance to colonization by Clostridium difficile. *Gastroenterology* **146**:1547–1553.
4. **Jackson S, Calos M, Myers A, Self WT.** 2006. Analysis of Proline Reduction in the Nosocomial Pathogen Clostridium difficile. *Journal of Bacteriology* **188**:8487–8495.
5. **Nakamura S, Nakashio S, Yamakawa K, Tanabe N, Nishida S.** 2013. Carbohydrate Fermentation by Clostridium difficile. *Microbiol. Immunol.* **26**:107–111.
6. **Wilson KH, Perini F.** 1988. Role of competition for nutrients in suppression of Clostridium difficile by the colonic microflora. *Infection and Immunity* **56**:2610–2614.
7. **Wiström J, Norrby SR, Myhre EB, Eriksson S, Granström G, Lagergren L, Englund G, Nord CE, Svenungsson B.** 2001. Frequency of antibiotic-associated diarrhoea in 2462 antibiotic-treated hospitalized patients: a prospective study. *J. Antimicrob. Chemother.* **47**:43–50.
8. **Loo VG, Poirier L, Miller MA, Oughton M, Libman MD, Michaud S, Bourgault A-M, Nguyen T, Frenette C, Kelly M, Vibien A, Brassard P, Fenn S, Dewar K, Hudson TJ, Horn R, René P, Monczak Y, Dascal A.** 2005. A predominantly clonal multi-institutional outbreak of Clostridium difficile-associated diarrhea with high morbidity and mortality. *N. Engl. J. Med.* **353**:2442–2449.
9. **Ricciardi R, Rothenberger DA, Madoff RD, Baxter NN.** 2007. Increasing Prevalence and Severity of Clostridium difficile Colitis in Hospitalized Patients in the United States. *Arch Surg* **142**:624–631.
10. **He M, Miyajima F, Roberts P, Ellison L, Pickard DJ, Martin MJ, Connor TR, Harris SR, Fairley D, Bamford KB, D'Arc S, Brazier J, Brown D, Coia JE, Douce G, Gerding D, Kim HJ, Koh TH, Kato H, Senoh M, Louie T, Michell S, Butt E, Peacock SJ, Brown NM, Riley T, Songer G, Wilcox M, Pirmohamed M, Kuijper E, Hawkey P, Wren BW, Dougan G, Parkhill J, Lawley TD.** 2013.

- Emergence and global spread of epidemic healthcare-associated *Clostridium difficile*. *Nat Genet* **45**:109–113.
11. **Elbein AD**. 2003. New insights on trehalose: a multifunctional molecule. *Glycobiology* **13**:17R–27.
 12. **Arg x000FC elles JC**. 2000. Physiological roles of trehalose in bacteria and yeasts: a comparative analysis. *Archives of Microbiology* **174**:217–224.
 13. **Richards AB, Krakowka S, Dexter LB, Schmid H, Wolterbeek APM, Waalkens-Berendsen DH, Shigoyuki A, Kurimoto M**. 2002. Trehalose: a review of properties, history of use and human tolerance, and results of multiple safety studies. *Food Chem. Toxicol.* **40**:871–898.
 14. **Benaroudj N**. 2001. Trehalose Accumulation during Cellular Stress Protects Cells and Cellular Proteins from Damage by Oxygen Radicals. *Journal of Biological Chemistry* **276**:24261–24267.
 15. **Kandror O, DeLeon A, Goldberg AL**. 2002. Trehalose synthesis is induced upon exposure of *Escherichia coli* to cold and is essential for viability at low temperatures. *Proc. Natl. Acad. Sci. U.S.A.* **99**:9727–9732.
 16. **Strøm AR, Kaasen I**. 1993. Trehalose metabolism in *Escherichia coli*: stress protection and stress regulation of gene expression. *Molecular Microbiology* **8**:205–210.
 17. **Iturriaga G, Suárez R, Nova-Franco B**. 2009. Trehalose Metabolism: From Osmoprotection to Signaling. *IJMS* **10**:3793–3810.
 18. **Lebenthal A, Lebenthal E**. 1999. The ontogeny of the small intestinal epithelium. *JPEN J Parenter Enteral Nutr* **23**:S3–6.
 19. **Arola H, Koivula T, Karvonen AL, Jokela H, Ahola T, Isokoski M**. 1999. Low trehalase activity is associated with abdominal symptoms caused by edible mushrooms. *Scand J Gastroenterol* **34**:898–903.
 20. **Murray IA, Coupland K, Smith JA, Ansell ID, Long RG**. 2000. Intestinal trehalase activity in a UK population: establishing a normal range and the effect of disease. *Br. J. Nutr.* **83**:241–245.
 21. **Janvilisri T, Scaria J, Teng C-H, McDonough SP, Gleed RD, Fubini SL, Zhang S, Akey B, Chang Y-F**. 2012. Temporal differential proteomes of *Clostridium difficile* in the pig ileal-ligated loop model. *PLoS ONE* **7**:e45608.
 22. **Staib L, Fuchs TM**. 2014. From food to cell: nutrient exploitation strategies of enteropathogens. *Microbiology*. **160**:1020-1039.

23. **Martindale J, Stroud D, Moxon ER, Tang CM.** 2000. Genetic analysis of *Escherichia coli* K1 gastrointestinal colonization. *Molecular Microbiology* **37**:1293–1305.
24. **Antunes A, Camiade E, Monot M, Courtois E, Barbut F, Sernova NV, Rodionov DA, Martin-Verstraete I, Dupuy B.** 2012. Global transcriptional control by glucose and carbon regulator CcpA in *Clostridium difficile*. *Nucleic Acids Research* **40**:10701–10718.
25. **KARASAWA T, Ikoma S, Yamakawa K, Nakamura S.** 1995. A defined growth medium for *Clostridium difficile*. *Microbiology (Reading, Engl.)* **141**:371–375.
26. **Wilson KH, Kennedy MJ, Fekety FR.** 1982. Use of sodium taurocholate to enhance spore recovery on a medium selective for *Clostridium difficile*. *Journal of Clinical Microbiology* **15**:443–446.
27. **Sorg JA, Dineen SS.** 2005. *Laboratory Maintenance of Clostridium difficile*. John Wiley & Sons, Inc., Hoboken, NJ, USA.
28. **Pfaffl MW.** 2001. A new mathematical model for relative quantification in real-time RT-PCR. *Nucleic Acids Research* **29**:e45.
29. **Bouillaut L, McBride SM, Sorg JA.** 2011. Genetic manipulation of *Clostridium difficile*. *Curr Protoc Microbiol* **Chapter 9**:Unit 9A.2.
30. **Bouillaut L, Self WT, Sonenshein AL.** 2013. Proline-Dependent Regulation of *Clostridium difficile* Stickland Metabolism. *Journal of Bacteriology* **195**:844–854.
31. **Theriot CM, Koumpouras CC, Carlson PE, Bergin II, Aronoff DM, Young VB.** 2011. Cefoperazone-treated mice as an experimental platform to assess differential virulence of *Clostridium difficile* strains. *gutmicrobes* **2**:326–334.
32. **Antonopoulos DA, Huse SM, Morrison HG, Schmidt TM, Sogin ML, Young VB.** 2009. Reproducible Community Dynamics of the Gastrointestinal Microbiota following Antibiotic Perturbation. *Infection and Immunity* **77**:2367–2375.
33. **Rezácová P, Krejčíříková V, Borek D, Moy SF, Joachimiak A, Otwinowski Z.** 2007. The crystal structure of the effector-binding domain of the trehalose repressor TreR from *Bacillus subtilis* 168 reveals a unique quaternary assembly. *Proteins* **69**:679–682.
34. **Bürklen L, Schöck F, Dahl MK.** 1998. Molecular analysis of the interaction between the *Bacillus subtilis* trehalose repressor TreR and the tre operator. *Mol. Gen. Genet.* **260**:48–55.

35. **Ng KM, Ferreyra JA, Higginbottom SK, Lynch JB, Kashyap PC, Gopinath S, Naidu N, Choudhury B, Weimer BC, Monack DM, Sonnenburg JL.** 2013. Microbiota-liberated host sugars facilitate post-antibiotic expansion of enteric pathogens. *Nature* **502**:96–99.

CHAPTER 5

Discussion and Conclusions

Discussion

The intestinal microbiota plays a fundamental role in preventing disease caused by *C. difficile*, illustrated by the fact that disease generally only occurs after antibiotic treatment. However, these interactions are inherently complex due to the variation in microbiota across individuals, diversity among infecting strains, and underlying complexities of the intestinal environment. Therefore, much work is still needed to understand all of the intricacies related to the development of CDI. In addition, there is a lack of understanding about why recently emerged epidemic strains of *C. difficile* have spread globally and become prevalent in such a short time frame. The work presented in this thesis aims to address some of these questions. In chapter two, we developed a novel gut microbiota mini-bioreactor system in which we can establish continuously cultured complex fecal communities, and adapted this system as an *in vitro* *C. difficile* infection model in chapter 3. We then investigated the competitive dynamics of epidemic and non-epidemic *C. difficile* strains in the presence of complex communities in both the bioreactors and a mouse infection model, showing that these newly emerged epidemic strains have a competitive advantage. A potential physiological basis for this competitive advantage is identified in chapter 4, where I demonstrate that epidemic strains grow better on

trehalose, and that this ability may be conferred by a single amino acid substitution in a regulatory gene involved in metabolism of this sugar.

This work contributes to the field of *C. difficile* in three ways. First, we have developed a novel *C. difficile* infection model that could be used to study many different aspects of *C. difficile* physiology and interactions with intestinal microbiota. These include but certainly aren't limited to vegetative growth, sporulation and germination dynamics, gene expression including toxin production, and the effects of different community assemblages on these processes. Second, the work in chapter 4 broadens our understanding of *C. difficile* metabolism and the nutrients that potentially play a role in intestinal colonization. Lastly, identification of the trehalose growth advantage and *treR* mutation in epidemic strains provides insight into physiological attributes that potentially explain not only why these strains are so prevalent and cause more disease, but also insight into the evolution of this unique pathogen.

Since competitive interactions between the microbiota and *C. difficile* are so integral to disease development, evolutionary adaptations affecting nutrient competition are likely contributing to the evolution of this organism. In the case of RT 027 strains, the ability to grow better on trehalose may have contributed to its recent emergence; however, it is likely that there are other contributing factors. Genetic mutations affecting nutrient utilization could provide a fitness advantage, resulting in several outcomes. Firstly, a mutation might allow for more efficient growth on a particular nutrient by affecting either nutrient uptake or metabolism, such as I have demonstrated here for trehalose utilization. In this example, the new

strain is more fit than the other *C. difficile* strains, yet still less fit than the competing member/s of the microbiota. The competitive dynamics observed in chapter 3 exemplify this scenario since the colonization levels and invasion of individual strains in the *in vitro* and *in vivo* models were similar. Alternatively, there may be mutations that allow the new strain to more readily invade the intestinal environment, not only outcompeting the other *C. difficile* strains but also members of the microbiota that previously competed for a similar niche. In this situation, the evolved strain is more fit than the other *C. difficile* strains and also the competing microbiota members, therefore affecting the background community structure. In the case of epidemic *C. difficile*, some evidence of this may be demonstrated by the observation that mice infected with epidemic (RT 027) strains had persistent dysbiosis of the intestinal microbiota, different from the non-epidemic strain infected mice (1). While the authors speculate that dysbiosis is due to the epidemic strain's impact on the inflammatory response of the host which in turn affects the microbiota, it is possible that these strains directly induce changes to the microbiota through competition. Even though it does not appear that this is occurring in our humanized mouse infection model, it would be interesting to look more closely at the communities of epidemic and non-epidemic *C. difficile* infected mice and see if they are also different. In a third scenario, the new strain could acquire mutations that allow it to fill a new intestinal niche, for example, by being able to metabolize a carbon source not utilized by other *C. difficile* strains. In this scenario, it would be possible for both strains to co-colonize since they would no longer be competing for the same niche. In addition, this could affect the background community as

described in the second example above, as the new strain could now be out-competing different microbiota members for this other nutrient. The Biolog experiments reported in chapter 4 identified several compounds whose utilization may be unique to RT 027 strains, however, much more work would need to be done to support these findings by screening additional strains and growth conditions.

Several comparative genomic analysis studies have been conducted in an effort to understand *C. difficile* strain evolution and also identify genetic factors that potentially contribute to the epidemic phenotype of newly emerged strains (2-6). Stabler et al. used whole genome sequence analysis of three *C. difficile* strains; a historic non-epidemic RT 012 isolate (CD630), and historic non-epidemic RT 027 isolate (CD196), and a recent epidemic RT 027 isolate (R20291) (2). They identified 234 genes unique to the RT 027 strains, many of which are associated with motility, antibiotic resistance, and toxicity, and an additional 5 genetic regions unique to just the recent RT 027 isolate. While the impacts of some of these traits on virulence or colonization have been investigated, such as motility, for the most part most have not. Moreover, inclusion of recent clinical isolates of other RT's would have been beneficial, as some of these genes may not be unique to just RT 027 strains.

Knetcsh et al. reported several genes linked to epidemic lineages of *C. difficile*, which may have physiological implications (7). These include an antibiotic synthesis gene set in RT 078 strains, and an insertion in RT 027 strains containing genes involved in generation of thymidine. We also observed this genetic insertion in RT 027 strains, as reported in chapter 3. Their analysis, however, showed that these genetic elements are not unique to the RT 078 and 027 strains, but are found

in other closely related ribotype strains. Thus, these might not play a significant role in their epidemic phenotype, although it would be interesting to test this hypothesis.

Fluoroquinolone resistance is implicated to be an important factor in the emergence of RT 027 strains, as it was shown to have independently evolved in two separate clades of post-epidemic RT 027 isolates (6). In the same study, comparison of pre- and post-epidemic RT 027 isolates identified several SNPs unique to the post-epidemic strains, none of which suggested any obvious phenotypic function (6). This study only focused on genetic comparisons of strains within the RT 027 clade, and so would not be able to identify genetic elements novel to the RT 027 lineage as a whole, which may also be important. Again, comparison of several recent clinical isolates of different RT groups with a focus on identifying genes or SNPs unique to just RT 027 or other epidemic RT's is warranted.

Many challenges exist when interpreting the results of these genomic comparison studies. Many identified genetic elements, which are conserved among a specific strain set, are hypothetical proteins or otherwise functionally uncharacterized. Moreover, our understanding of the functions of specific genes, mutations within these genes, or regulatory networks as whole is largely not sufficient to predict the phenotypic effects of these mutations, especially for *C. difficile*. Ultimately, much work will need to be done to directly test if any of these genes or mutations play a role in *C. difficile* colonization or virulence.

Conclusions

We have only begun to scratch the surface when it comes to understanding the complexities of *C. difficile* disease. However, recent increases in the incidence and severity of CDI have fueled the need to address this issue in order to develop better ways of preventing and treating this infection. As a result, research in the areas of *C. difficile* physiology, infection model development, and generation of *C. difficile* genetic tools are advancing at an ever-increasing pace. Indeed, the work presented in this thesis is no exception. Combined with the contributions from research investigating the human microbiome structure and function, new insights into the dynamics of CDI are being made all the time. Undoubtedly, we are moving closer to discovering novel, more effective ways of preventing and treating infection caused by *C. difficile*.

REFERENCES

REFERENCES

1. **Lawley TD, Clare S, Walker AW, Stares MD, Connor TR, Raisen C, Goulding D, Rad R, Schreiber F, Brandt C, Deakin LJ, Pickard DJ, Duncan SH, Flint HJ, Clark TG, Parkhill J, Dougan G.** 2012. Targeted Restoration of the Intestinal Microbiota with a Simple, Defined Bacteriotherapy Resolves Relapsing *Clostridium difficile* Disease in Mice. *PLoS Pathog* **8**:e1002995.
2. **Stabler RA, He M, Dawson L, Martin M, Valiente E, Corton C, Lawley TD, Sebahia M, Quail MA, Rose G, Gerding DN, Gibert M, Popoff MR, Parkhill J, Dougan G, Wren BW.** 2009. Comparative genome and phenotypic analysis of *Clostridium difficile* 027 strains provides insight into the evolution of a hypervirulent bacterium. *Genome Biol* **10**:R102.
3. **He M, Sebahia M, Lawley TD, Stabler RA, Dawson LF, Martin MJ, Holt KE, Seth-Smith HMB, Quail MA, Rance R, Brooks K, Churcher C, Harris D, Bentley SD, Burrows C, Clark L, Corton C, Murray V, Rose G, Thurston S, van Tonder A, Walker D, Wren BW, Dougan G, Parkhill J.** 2010. Evolutionary dynamics of *Clostridium difficile* over short and long time scales. *Proceedings of the National Academy of Sciences* **107**:7527–7532.
4. **Stabler RA, Dawson LF, Valiente E, Cairns MD, Martin MJ, Donahue EH, Riley TV, Songer JG, Kuijper EJ, Dingle KE, Wren BW.** 2012. Macro and Micro Diversity of *Clostridium difficile* Isolates from Diverse Sources and Geographical Locations. *PLoS ONE* **7**:e31559.
5. **Knetsch CW, Terveer EM, Lauber C, Gorbalenya AE, Harmanus C, Kuijper EJ, Corver J, van Leeuwen HC.** 2012. Comparative analysis of an expanded *Clostridium difficile* reference strain collection reveals genetic diversity and evolution through six lineages. *Infection, Genetics and Evolution* **12**:1577–1585.
6. **He M, Miyajima F, Roberts P, Ellison L, Pickard DJ, Martin MJ, Connor TR, Harris SR, Fairley D, Bamford KB, D'Arc S, Brazier J, Brown D, Coia JE, Douce G, Gerding D, Kim HJ, Koh TH, Kato H, Senoh M, Louie T, Michell S, Butt E, Peacock SJ, Brown NM, Riley T, Songer G, Wilcox M, Pirmohamed M, Kuijper E, Hawkey P, Wren BW, Dougan G, Parkhill J, Lawley TD.** 2013. Emergence and global spread of epidemic healthcare-associated *Clostridium difficile*. *Nat Genet* **45**:109–113.
7. **Knetsch CW, Hensgens MPM, Harmanus C, van der Bijl MW, Savelkoul PHM, Kuijper EJ, Corver J, van Leeuwen HC.** 2011. Genetic markers for *Clostridium difficile* lineages linked to hypervirulence. *Microbiology* **157**:3113–3123.